POWER SYSTEM OPERATION WITH HIGH PENETRATION OF ELECTRIC VEHICLES AND RENEWABLE ENERGY

By Jose David Alvarez Guerrero

A Dissertation

Submitted in Partial Fulfillment

of the Requirements for the Degree of

Doctor of Philosophy

in Earth Sciences and Environmental Sustainability

Northern Arizona University

May 2022

Approved:

Thomas L. Acker, Ph.D., Chair

John T. Tester, Ph.D.

Venkata Yaramasu, Ph.D.

Rafael Castro, Ph.D.

Lefeng Shi, Ph.D.

ABSTRACT

POWER SYSTEM OPERATION WITH HIGH PENETRATION OF ELECTRIC VEHICLES AND RENEWABLE ENERGY

JOSE DAVID ALVAREZ GUERRERO

This dissertation document explores the potential impacts of integrating electric vehicles (EVs) and variable renewable energies (VRE) on power system operation. EV penetration scenarios of the light-duty vehicle fleet of 10%, 20%, and 30% are considered in the RTS-GMLC test system. RTS-GMLC is an updated version of the IEEE RTS-96 test system, allowing for modern inter-hour or real-time market modeling; it has a generation fleet with characteristics comparable to current power systems used in the western United States, and VRE penetration equal to 34% of annual energy consumption. The impacts of EVs are investigated during the annual peak in the summer and during four weeks of the year in which high VRE combined with low loads lead to overgeneration. Uncoordinated and coordinated EV charging scenarios are considered. In the uncoordinated scenario, charging is undertaken at the convenience of the EV owners, and this is modeled using data from the Idaho National Laboratory's EV Project. To create an uncoordinated charging load profile, the parameters of importance are the number of vehicles, charger type, battery capacity, availability for charging, and battery beginning and ending states of charge. Beta distributions were found to be the most appropriate distribution for statistically modeling the initial and final state of charge (SoC) of vehicles in an EV fleet. A Monte Carlo technique was implemented by sampling the charging parameters of importance to create an uncoordinated charging load time series. Coordinated charging is modeled as a controllable load using an "aggregator" model, wherein EV charging is scheduled to minimize operating costs while meeting the daily charging requirements subject to EV availability and charging constraints. To capture the impacts, the production cost model (PCM) Power

System Optimizer (PSO), created by Polaris, is employed. The model uses load and VRE forecasts as part of a multiple-planning cycle rolling horizon approach to commit realistic generating units based on their start-up characteristics, while preserving the flexibility of units with short start-up times and EV charging. At each EV penetration level, the uncoordinated charging costs were higher than the coordinated ones. At 10% EV penetration, the uncoordinated charging cost per vehicle was four times higher than with coordinated charging during a low load week in February. During a high-VRE, low-load week in April, with uncoordinated EV charging at 30% penetration (3% energy penetration), the peak load increased as much as 27%. Using coordinated EV charging, the EV load shifts to hours with low prices, coincident with either low load, high VRE, or both. Furthermore, coordinated charging reduces the curtailment of PV by as much as nine times during the winter operation season, and the curtailment of wind generation by more than half during the summer operation season, compared to the scenarios with no EVs and uncoordinated EV charging. Using multiple planning cycles, load and VRE forecasts, and a “look ahead” period during scheduling and dispatching, units were judged to be important in creating and utilizing the flexibility of coordinated EV charging.

Acknowledgments

I would like to thank Tom Acker for all his support and guidance in my career. It has been a privilege to be part of his research group. I also want to thank my committee members for their feedback and support, Drs. Rafael Castro, Venkata Yaramasu, John T. Tester, and Lefeng Shi. They have been a great resource and inspiration in my professional journey.

This dissertation would not have been possible without an academic license of PSO by Polaris. Special remarks to Russ Philbrick for his direct support and guidance.

Also, thank you to Bikash Bhattarai and Rajendra Shrestha, both colleagues and coauthors of my first journal publication.

My family has been a crucial part of my journey, and my wife Gisela is the best partner I could ever have. My success is linked to her support, I would never thank Gisela enough especially for our children Abril and Julian.

Table of Contents

ABSTRACT ii
Acknowledgments iv
Table of Contents v
List of tables ix
List of figures xi
Acronyms xiii
Chapter Introduction 1
1.1 Objective 1
1.2 Background 1
1.2.1 Charging technology 1
1.2.2 Electricity Distribution System 3
1.2.3 Transmission System and Power System Operation 4
1.2.4 Power System Load Shape 6
1.2.5 Reliability and Demand Side Management (DSM) with EV 9
1.2.6 Status of DSM in the U.S. Power Markets 14
1.3 Research Questions 16
1.4 Literature Review Power System Modeling 18
1.4.1 Power system modeling 18
1.4.2 Capacity Expansion Models 18
1.4.3 Production Cost Models 19
1.4.4 Capacity Expansion Model for EV 21
1.4.5 Production Cost Model and EV 24
1.4.6 Production Cost Model and VRE 27
1.4.7 Production Cost Model and DSM 30
1.4.8 Methodology in PCM for VRE 31
1.5 Approach and structure of the dissertation 35
Chapter three: Integrating Electric Vehicles into Power System Operation Production Cost Models 36
Preface 36
Abstract 36
1.6 Introduction 37
1.6.1 Batteries and their effect on EV costs 39

1.6.2 Production Cost Model 40
1.7 Methods 41
1.7.1 Battery and Charging Level 41
1.7.2 Battery State-of-Charge 42
1.7.3 Availability - Arrival and Departure time 44
1.7.4 Modeling the Charging of Electric Vehicles 46
1.7.5 *NAU 5-BUS SYSTEM* 50
1.7.6 Production Cost Model 53
1.8 Results 56
1.8.1 System Operation without EVs 56
1.8.2 System Operation with Uncoordinated EV Charging 57
1.8.3 System operation with Coordinated EV Charging 58
1.8.4 Comparing the EV Cost of Charging 61
1.9 Discussion 62
1.10 Conclusions 64
Chapter Four: Power System Impacts of Electric Vehicle Charging Strategies 67
Preface 67
Abstract 67
1.11 Introduction 68
1.12 Penetration levels of EVs 72
1.13 Production Cost Model 73
1.14 Description of RTS-GMLC Power System 74
1.14.1 Commitment Decisions and Multicycle Rolling Planning Horizons 76
1.14.2 EV modeling 80
1.14.3 Weeks of Analysis 83
1.15 PCM Results and Metrics 85
1.16 Cases Examined 86
1.17 Results 87
1.17.1 RTS-GMLC model results without EVs 87
1.17.2 VRE Curtailments 95
1.18 Results for Cases with EVs 96
1.18.1 System Operation Cost 96
1.18.2 Cost to Charge EVs 98

1.18.3 Locational Marginal Price (LMP) 99
1.18.4 Generation Stack 100
1.18.5 VRE Curtailments 104
1.19 Discussion 106
1.20 Conclusion 108
Conclusions 111
Research questions 112
References 116
Appendix I 128
Cost Curves NAU-5 Bus System 128
Appendix II 131
PSO inputs 131
Model Setup (MS) 132
Model Definition (MDL_ID) 133
Model Configuration (MC) 133
Cycle ID (CYC_ID) 133
Cycle Period ID (CYC_PRD_ID) 134
Scenario Cycle (SCN_CYC) 135
Time Series Data (TS) 136
Schedule Attributes (SCH_ATT) 136
Schedule Time-point (SCH_TMP) 136
Economic Dispatch (ED) 137
Scenario Area Load (SCN_ARA_LOD) 137
Injector ID (INJ_ID) 137
Injector in Service (INJ_INS) 138
Scenario Injector Dispatch (SCN_INJ_DSP) 138
Scenario Injector Max-MW (SCN_INJ_MAX) 139
Unit Commitment (UC) 139
Injector Commit (INJ_CMT) 139
Cycle System Commitment (CYC_SYS_CMT) 140
Power Network (PN) 140
Branch ID (BRN_ID) 140
Electrical Node ID (NDE_ID) 141

Injector Network (INJ_NET) 141
Power Flow States (PF) 142
State Electrical Node MW (STE_NDE) 142
Power Constraints (PC) 142
Heat Dispatch (HD) 143
Injector Heat (INJ_HEA) 143
Heat Curve Attribute (HCV_ATT) 143
Heat Curve Points (HCV_PNT) 144
Injector Heat Curve (INJ_HCV) 146
Fuel Dispatch (FD) 146
Fuel ID (FUE_ID) 146
Fuel Thermal Unit (FUE_UTH) 146
Specialized Injector Energy Limited (EL) 147
Injector Energy Limits (INJ_ELM) 147
Scenario Injector Min-Energy (SCN_INJ_EMN) 148
Scenario Injector Max-MW (SCN_INJ_MAX) 148
Appendix III 149
Generator Data 149

List of tables

Table 1 Overview of the ancillary services offered by each ISO/RTO [18] 12

Table 2 Brief description of Capacity Expansion Modeling methodology [31] [38] 19

Table 3 Brief description of Production Cost Modeling methodology [31] 20

Table 4 Summary of the best practices related to inputs and processes for VRE integration studies [52]. 29

Table 5 Summary of methodology presented in the most relevant integration studies in North America [56],[57],[58],[59],[60]. 33

Table 6. Generation capacity per technology and penetration percentage presented in the NAU 5-bus system. 52

Table 7. Load distribution presented in the NAU 5-bus system. 53

Table 8. Summary of dispatchable generators in the NAU 5-bus system. 53

Table 9. EV penetration in thousands of vehicles as a percent of LDVs and of the annual system load, and the number of vehicles assumed in each region. 80

Table 10. EV nodal distribution at 10% penetration of LDV in RTS-GMLC Region 1 based on the nodal peak load participation. 81

Table 11 Enumeration of the cases considered in the analysis of the effects of EV Charging in the RTS-GMLC. 87

Table 12. Summary of production costs and reliability metrics for the RTS-GMLC base case with no EVs. 88

Table 13. Load-Weighted Average LMP (USD/MWh) over all nodes in the RTS-GMLC without EVs. 93

Table 14. VRE curtailments expressed as a percentage of total weekly VRE production for each of the weeks analyzed for the base case with no EVs. 96

Table 15. Weekly average LMP (USD/MWh) occurring over the entire system (RTS-GMLC). 100

Table 16 Model Setup (MS) input parameters provide a quick list of parameters that defines the PSO model. 132

Table 17 Model Definition (MDL_ID) specifies the unit of time and temporal length covered in the model 133

Table 18 Cycle ID (CYC_ID) defines the solution time of the horizons contemplated in the cycle. 134

Table 19 Cycle Period ID (CYC_PRD_ID) defines the resolution of horizons and their look ahead. 135

Table 20 Scenario Cycle (SCN_CYC) specifies the scenario of the PSO model. 136

Table 21 Schedule Attributes (SCH_ATT) provides characteristics of the model's Time Series Data (TS). 136

Table 22 Schedule Time-point (SCH_TMP) provides the time series data in the model. 136

Table 23 Scenario Area Load (SCN_ARA_LOD) specifies the data the model uses as system load. 137

Table 24 Injector ID (INJ_ID) defines the economic dispatch parameters of the injectors (generation or load resources) in the model. 137

Table 25 Injector in Service (INJ_INS) specifies the injectors disabled in the base model. 138

Table 26 Scenario Injector Dispatch (SCN_INJ_DSP) defines fixed schedules for a given set of injectors. 139

Table 27 Scenario Injector Max-MW (SCN_INJ_MAX) specifies the maximum power limits of a set of injectors passed as a time series..... 139

Table 28 Injector Commit (INJ_CMT) provides the commitment constraints for the model's injectors. 140

Table 29 Cycle System Commitment (CYC_SYS_CMT) specifies to solve the commitment in a given cycle. 140

Table 30 Branch ID (BRN_ID) defines the parameters of the transmission lines in the model. 140

Table 31 Electrical Node ID (NDE_ID) specifies the nodes (substations) in the power network. 141

Table 32 Injector Network (INJ_NET) identifies the nodal location of each injector. 141

Table 33 State Electrical Node MW (STE_NDE) provides the load distribution factors for the model. ... 142

Table 34 Injector Heat (INJ_HEA) provides a simplified heat representation for modeling the baseload nuclear generator. 143

Table 35 Heat Curve Attribute (HCV_ATT) provides the Base Heat for the model's dispatchable generators. 144

Table 36 Heat Curve Points (HCV_PNT) provides the incremental heat rate curve for the model's dispatchable generators. 145

Table 37 Injector Heat Curve (INJ_HCV) associates the heat curves with the model's injectors 146

Table 38 Fuel ID (FUE_ID) defines the thermal units and cost of the generator's fuels. 146

Table 39 Fuel Thermal Unit (FUE_UTH) associates the fuel with the injectors. 147

Table 40 Injector Energy Limits (INJ_ELM) provides the time window for accomplishing the coordinated EV charging. 147

Table 41 Scenario Injector Min-Energy (SCN_INJ_EMN) defines the schedule for determining the EV charging requirement. 148

Table 42 Variant of the Scenario Injector Max-MW (SCN_INJ_MAX) defines the maximum charging availability for the coordinated EV charging. 148

List of figures

Figure 1 An illustration of the power system: in the left are high voltage transmission and generators; in the center is shown a substation that converts electricity from high voltage to low voltage and a system operator in a control room; and in the right is the distribution side with commercial and residential users [12]. 5

Figure 2 Typical load shape for one day during peak load season, generation dispatch, and installed capacity. The shaded portion refers to the "valley filing" approach of charging EVs [14]. 7

Figure 3 The Duck-Chart, steep ramping needs and over generation risk portrayed in the net load of CAISO during a typical day of spring [15]. 8

Figure 4 Historical and projected annual electricity consumption. Electrification of the transportation sector represents the most sensitive variable in the model [16]. 9

Figure 5 Operating Reserve categories and their relation to each other. [19] 11

Figure 6 Geographical distributions of the ISO/RTO in North America. 15

Figure 7 Aggregated load profile for EVs in the REFS and their transition from 2010 to 2050 [44] 25

Figure 8. Charging level proportion (%) modeled in the electric vehicle (EV) fleet. 42

Figure 9. A plot of the beta distribution model of the initial state-of-charge (SoC) values fitted to the source data 43

Figure 10. Beta distributions fitted to the target state-of-charge source data. 44

Figure 11. Weekday charging availability covering all types of chargers of the EV Project 2013 [97]. 45

Figure 12. EV availability in the EV Project data during weekdays as (**a**) departures and (**b**) arrivals [97]. 46

Figure 13. Flowchart of EVs uncoordinated load modeling. 48

Figure 14. Flowchart of the modeled aggregator. 49

Figure 15. Projected maximum power (P) in MW for 1000 EVs on a weekday based on charging availability and charging capacity. 50

Figure 16. Northern Arizona University (NAU) 5-bus system layout that portrays buses (bold vertical lines), transmission lines (connecting the buses), loads (inverted triangles), and generators (circles and rectangles). 51

Figure 17. Proportion ratio (%) for the types of generators considered in the NAU 5-bus system (CC = combined cycle; CT = combustion turbine; PV = photovoltaics; RTPV = rooftop PV). 52

Figure 18. Power generation (Pg) stack MW (left axis) and locational marginal price (LMP) USD/MWh (right axis) in the NAU 5-bus system occurring without EVs. 57

Figure 19. Uncoordinated EV charging power (P) profile in MW developed for 1000 EVs. 58

Figure 20. Coordinated EV charging power (P) profile in MW developed for 1000 EVs. 59

Figure 21. Power generation (Pg) stack MW (left axis) and LMP USD/MWh (right axis) in the NAU 5-bus system occurring with coordinated EV charging. 60

Figure 22 Comparison of the EV coordinated and EV uncoordinated charging profile power (P) in MW (left axis) and their corresponding system LMPs in USD/MWh (right axis). 60

Figure 23. Comparison between the coordinated and uncoordinated cost in USD of EV charging for 1000 EVs 61

Figure 24. Comparison of the system load (L) in MW (left axis) against the EV coordinated and EV uncoordinated charging power (P) profiles (right axis) of 1000 EVs. 62

Figure 25. Summary of the system operation cost and LMP change with the introduction of EV charging, gross comparison against the system with no EVs. 64

Figure 26. Installed capacity in MW per region in the RTS-GMLC. The peak load per region is the same at 2,850 MW and is shown by the lower dashed line, with a total peak load of 8.2 GW shown by the upper dashed line, with at total installed capacity of 14.3 GW. 76

Figure 27. Multicycle rolling horizon modeling implemented in this study. 79

Figure 28. Net load distribution per month in the RTS-GMLC. 83

Figure 29. Average net load per day of the year occurring in the RTS-GMLC. 84

Figure 30. The load, net load, and minimum dispatch of nuclear power generation occurring in the RTS-GMLC during Duck week. 85

Figure 31. The generation stack for Duck week in April, assuming no EV charging. 90

Figure 32. The generation stack for the peak weeks in July, assuming no EV charging. 91

Figure 33. Net load after VRE curtailment and LMP for one day during Duck week (April) for the RTS-GMLC model without EVs. 94

Figure 34. Zoomed-in view of the generation stack on April 11 (Duck curve) with no EVs. 95

Figure 35. Average daily system operation cost for all the scenarios considered 98

Figure 36. The average daily cost to charge an EV per scenario 99

Figure 37. The generation stack for Duck week in April, assuming 30% EV penetration and uncoordinated EV charging. 101

Figure 38. The generation stack for Duck week in April, assuming 30% EV penetration and coordinated EV charging. 102

Figure 39. The generation stack for peak weeks in July, assuming 30% EV penetration and uncoordinated EV charging. 103

Figure 40. The generation stack for peak weeks in July, assuming 30% EV penetration and coordinated EV charging. 104

Figure 41 VRE curtailments during the Duck week in April for all scenarios and charging strategies. 105

Figure 42. The percent curtailments during peak weeks in July for all EV penetration scenarios and charging strategies 106

Figure 43. EV load and LMP results for one day during Duck week, including 30% EVs implemented with uncoordinated charging. 107

Figure 44. LMP and EV load profiles when employing coordinated EV charging, on a day during Duck week. 108

Acronyms

$/MWh	Electricity Price
AC	Alternating Current
AEO	Annual Energy Outlook
AGC	Automatic Generation Control
BA	Balancing Authority
CAISO	California Independent System Operator
CEM	A Capacity Expansion Model
CHP	Combined Heat And Power
DC	Direct Current
DCFC	Dc Fast Chargers
DOE	The Department Of Energy
DSM	Demand Side Management
ED	Economic Dispatch
EIA	Energy Information Agency
EPRI	The Electric Power Research Institute
ERCOT	Electric Reliability Council of Texas
EV	Electric Vehicles
EVSE	Electric Vehicle Supply Equipment
FERC	The Federal Energy Regulatory Commission
HPC	High-Performance Computing
HVAC	Heat Ventilation and Air Conditioning
ICEV	Internal Combustion Engine Vehicles
IEEE	Institute of Electrical And Electronics Engineers
INL	Idaho National Lab
IRENA	International Renewable Energy Association
ISO	Independent System Operator
ISO-NE	New England Independent System Operator
LBNL	Lawrence Berkeley National Lab
LCOD	Levelized Cost of Driving
LCOE	Levelized Cost of Energy
LDV	Light Duty Vehicle
Li-ion	Lithium-Ion
LMP	Locational Marginal Price
LMP	Locational Marginal Prices
MISO	Midcontinent Independent System Operator
NG-CC	Natural Gas Combined Cycle
NG-CT	Natural Gas Combustion Turbines
NREL	National Renewable Energy Lab
NYISO	New York Independent System Operator
PCM	A Production Cost Model
PJM	Pennsylvania-New Jersey-Maryland Interconnection
REEDS	Regional Energy Deployment System
REFS	The Renewable Electricity Futures Study

RTO	Regional Transmission Organization
RTS	Reliability Test System
RTS-79	Original RTS Of the IEEE Introduced in 1979
RTS-86	Modified RTS Of the IEEE in 1986
RTS-96	Modified RTS Of the IEEE in 1996
RTS-GMLC	The Reliability Test System of The Grid Modernization Laboratory Consortium
SPP	Southwest Power Pool
SW	Southwest
TOU	Time-of-Use
U.S.	United States
UC	Unit Commitment
V	Voltage
V2G	Vehicle to Grid
VRE	Variable Renewable Energy
WinDS	Wind Deployment System
WWSIS-II	Western Wind And Solar Integration Study Phase 2
ZEV	Zero-Emission Vehicle
ZEVR	Zero Emission Vehicle Regulation

Chapter Introduction

The purpose of this work therefore is to explore the opportunities and challenges posed by a high penetration of electric vehicles from the perspective of operating the transmission system.

1.1 Objective

The main objective of this research is to determine the impacts of electric vehicles on power system operation and costs under conditions of high penetration of EVs and VRE (wind and solar power). In particular, this research will determine the effects of possible uncoordinated and coordinated EV charging strategies. It will also identify the benefits and detriments of those strategies for future generation scenarios with and without high penetration of VRE.

1.2 Background

1.2.1 Charging technology

Availability of the Charging infrastructure is essential to ensure high levels of EV penetration.

Charging stations or Electric Vehicle Supply Equipment (EVSE) deliver energy to charge EV batteries. One classification of the charging stations is by their ownership, public or private. DOE considers as public charging stations that are accessible to any driver, such as shopping malls, parks, or other public facilities [1]. Private charging stations are those located in private parking locations of homes, apartment buildings, or businesses. The next classification of charging stations is by the rate that it delivers energy to the EV. Referring to light-duty vehicles, level 1 and level 2 chargers are considered to charge at a slow rate: level 1 provides enough charge for up to 5 miles of range per hour of charge, and level 2 up to 20 miles per hour of charge [1]. The difference in the rate of charging between level 1 and level 2 lies in the voltage level of the EVSE: Level 1 charging employs 120 V outlets, and level 2 uses 240 V or 208 V outlets. In addition to Level 1 and 2 chargers, there are faster chargers able to provide charge for up to 80 miles of

range in about 20 minutes. These are called DC Fast Chargers (DCFC), and these require heavy-duty or industrial electric installation, 480 V AC [1]. The EVSE cost depends on the charging rate. For level 1 the costs range from 300 to 1,500 USD, Level 2 from 400 to 6,500 USD, and for DCFC between 10,000 to 40,000 USD. The range in prices for each type of charger depends in the type of the charger mounting (wall or pedestal), communication capabilities (user, host, utility, and internet), access control (log in), paying functionalities, energy monitoring (energy consumption), energy management (demand respond), display screen, and retractable cord [2].

Public charging stations are important because they allow travel beyond the range capacity of a single charge of EV batteries. Currently, the EV driver is able to locate public charging stations on the Internet or on phone apps like the Alternative Fueling Station Locator, which is sponsored by DOE [3]. Referring to global EV charging infrastructure, China is the country with the largest deployment. This country has twice as many DCFCs than Japan, and about three times more than the U.S. [4]. Regarding the infrastructure in the U.S., DOE concludes that for covering the traveling and commuting needs of 81% of the U.S. population between cities and towns, it is necessary to install a DCFC on average every 70 miles along interstate highways, and in metropolitan areas in a radius of every 3 miles [5]. The DOE used a tool named EVI-Pro, which includes the geographical distribution of the population to compute the distance between charging stations [5]. DCFC fits better along corridors with heavy traffic, like freeways highways and interstate highways than level 1 or 2 EVSE, because drivers can recharge enough energy in 20 minutes to drive for 80 miles. All EVs are configured for all three types of charge levels; however, there is no standard for the connectors or plugs that vehicle manufacturers employ [6]. Regarding the connectors, the options available for consumers in the U.S. are as follows: most EVs use the SAE J1772 charge port for level 1 and level 2; European and American cars use the J1772 combo connector for DCFC, which differs from the SAE J1772 by having located in the bottom of the standard connector two more pins; Asiatic automakers

employ the CHAdeMO connector in their models for DCFC; Tesla has their own charge port that works for all level of charging; and adapters are sold to accommodate the different ports [7]. According to a recent study led by Lawrence Berkeley National Lab (LBNL), this lack of charging standard is considered a risk for consumer adoption since it locks the interoperability of EV through a certain type of charger technology [8][9]. Thus an imperative is the development of an open standard for connectors that facilitate the integration of EV for all the key sectors, utilities, aggregators, charger manufacturers, EV manufacturers, and overall consumers [9].

1.2.2 Electricity Distribution System

High penetration of EVs in the transportation system will require upgrades as well, or replacement of the distribution system transformers in residential areas. This problem results from many people charging their EVs at the same time, which causes residential distribution transformers designed to deliver power to households to handle the increased load due to the EVs. This additional load will push distribution line transformers over their limits. No matter if EV charging uses level 2 chargers (240V -6.6kW) or level 1 chargers (120V-1.9kW), both reduce the lifetime of the transformers [10]. This means, for the average household, adding a charger on their residential circuit increases the peak power demand, because it draws power steadily for a time interval to charge the battery. However, the residential load varies through the day since household appliances are not on all the time. Thus, the problem of overloading the transformers is exacerbated if high power demand household appliances, (HVAC and Kitchen) coincide with the EV charging, especially during peak hours of energy service. If this effect is multiplied for the whole neighborhood, then the peak power increases in the whole area and can easily overload the distribution transformer. One can extrapolate this problem of an overloaded distribution line/transformer to the high voltage transmission system. At high penetration of EVs on many distribution lines, there can also be impacts on electric system operation, transmission congestion, locational prices, and reserves.

Though the problems in the distribution side are interesting and important, this dissertation will focus on high penetration of EVs and the associated challenges faced on the high voltage transmission system in electric system operation.

1.2.3 Transmission System and Power System Operation

The Power System has two main divisions: high voltage transmission lines, and lower voltage distribution lines. Large central generators, like utility-owned nuclear, coal, gas-fired, storage, wind, and solar, after the step-up transformers, interact with the high voltage side, 69kV and greater [11] (see the left side of Figure 1 [12]). The energy users -residential, commercial, and industrial consumers- are on the distribution side, typically 12 kV and lower, though ranging from 2.3 kV to 34.5 kV [11] (right side of Figure 1 [12]). Power system operation involves the economic operation of the power system, committing and dispatching power generators while maintaining system reliability; these actions keep the balance between power generators (generation-supply) and consumers (load-demand); the control room (system operator) appears in the center of Figure 1. Also shown in the center of Figure 1 is a sub-station, where the voltage level of electricity on the high-voltage side of the transmission system is stepped-down and transferred to the lower voltage distribution side. Committing of the generators by the system operator is usually referred to as Unit Commitment (UC): system planners and operators need to make sure that enough power generators are committed or online and ready to dispatch power to meet the anticipated load. These actions are often planned and taken at different time intervals, like for the next day or few days, or the whole week, or shorter periods such as for the next few to several hours. Once system operators have committed their generators, they have to decide the amount of power coming from each generator: here the goal is to dispatch the lowest-cost generators first and make sure that the next MW of power comes from the least expensive generator available. This is called Economic Dispatch (ED) [13]. Usually low cost generators such as wind and solar power are dispatched first along with natural gas

combined cycle generation; and then more expensive fossil-fueled generators, like combustion turbines, are dispatched as necessary. Conventional baseload generators such as nuclear and coal power are committed and run at a load level that does not change (as in the case for nuclear), or is not dispatched to different levels very often (such as for coal). For example, natural gas combustion turbines are usually the most expensive resource, and therefore these generators are committed and dispatched for relatively short periods, and they are usually referred to as peaking units because they serve only peak loads. The generator that is able to provide the next incremental unit of power is the one that fixes the price in the system, which is referred to as locational marginal price (LMP) [11]. Therefore, system operators choose a unit commitment schedule and economic dispatch that minimizes the operation cost of the electric system while adhering to reliability and risk guidelines.

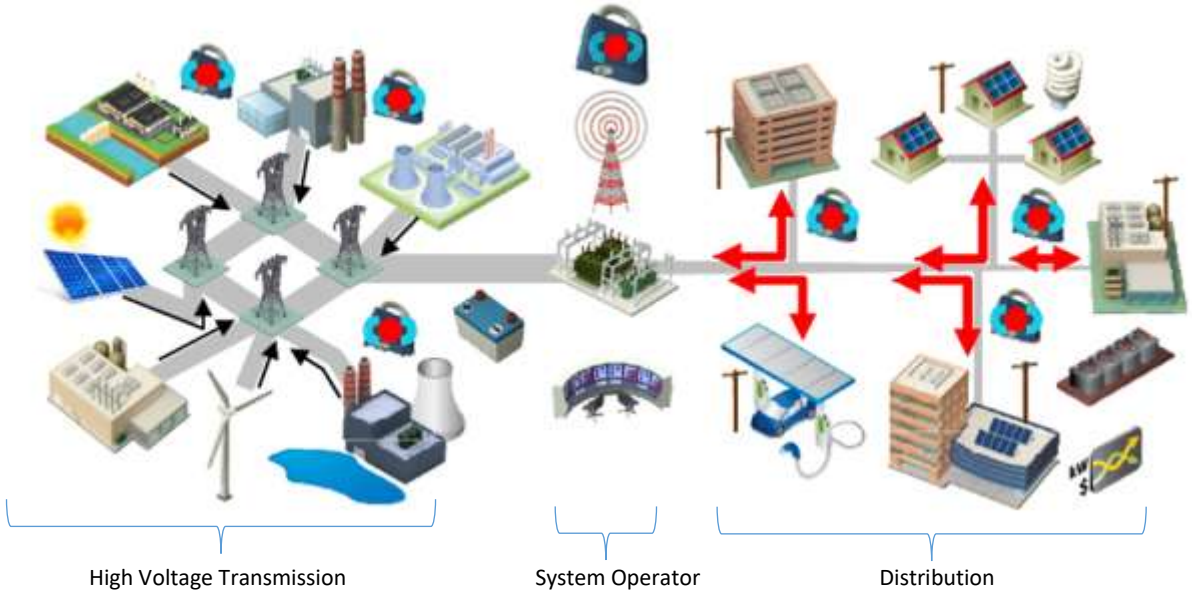

Figure 1 An illustration of the power system: in the left are high voltage transmission and generators; in the center is shown a substation that converts electricity from high voltage to low voltage and a system operator in a control room; and in the right is the distribution side with commercial and residential users [12].

In addition to generation resources, some system operators also have the availability to commit and dispatch another type of resource called demand response, in which certain commercial loads, usually lighting and cooling, are turned down or reduced. Furthermore, there are small generators located on the

distribution side of the grid, i.e. on the distribution system. These small generators on the distribution system, also called distributed energy resources, are often composed of renewable energies, photovoltaics and wind; conventional generators, backup generators and Combined Heat and Power (CHP); and storage, like lead acid or Li-ion batteries. For instance, in cities like Los Angeles, California, there is a large and growing penetration of solar photovoltaics and this distributed resource is usually not in control of the system operator. The concept of a "smart grid" involves both demand response and distributed generators that are able to be committed and dispatched by the system operator or respond automatically by sensing the electrical system conditions [12]. This is pictured using bidirectional red lines in Figure 1.

1.2.4 Power System Load Shape

Some of the tools employed by electric system operators and planners to shape the load include dynamic pricing and "valley-filling" technologies, like demand response and storage. This work will explore dynamic pricing and EVs as demand response or flexible load.

Kintner-Meyer et al. report that the electric infrastructure (electric generators and the high-voltage transmission system) in the U.S. is currently capable of supplying energy to more than 70% of the light duty fleet for a daily drive of 33 miles on average, which equates to more than 50% the U.S. petroleum imports [14]. In making this prediction, these investigators assumed a "valley-filling" approach to the daily load shape, which means EVs are charged with the same resources we use to operate the electrical system on a daily basis, but during times of low electricity consumption (Figure 2). Thus, this assumes charging of electric vehicles is done during off-peak periods to avoid creating a higher peak load in the system or taxing generation resources when already being utilized.

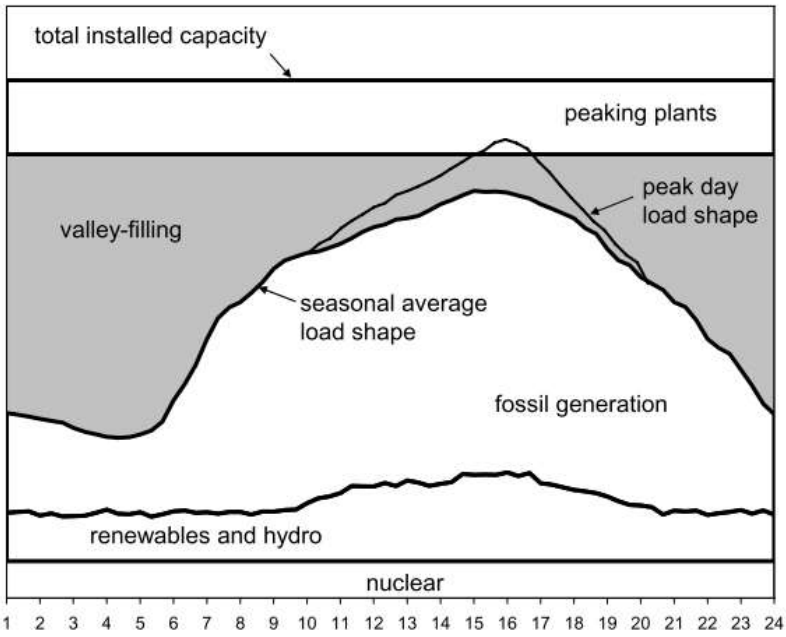

Figure 2 Typical load shape for one day during peak load season, generation dispatch, and installed capacity. The shaded portion refers to the "valley filing" approach of charging EVs [14].

With regard to renewable energy in the southwest (SW) U.S., the California Independent System Operator (CAISO) experiences a challenge balancing supply (generation) and demand (load) during some spring and fall weeks when the load is relatively low and when solar energy generation is high. Net load is defined as the load minus the generation from solar and wind resources, and it represents the power demand that dispatchable generators, like fossil generation or storage, have to cover. In California, during periods when cooling is not necessary (winter and spring) the net load curve in the midafternoon becomes skewed down, which imposes a steep ramp up in the dispatchable generators as soon as the solar power starts decreasing, and thus resembles the shape of a duck (Figure 3) [15]. The concept of "valley-filling" using EVs is even more interesting for CAISO during the "duck curve" season, since it can increase the power demand by switching some of the transportation to electricity. In addition, during the middle of the day and while in the belly bottom of the duck curve, increasing the demand can alleviate the risk of over-generation. Every time that over-generation appears, it requires curtailment of solar energy or the selling

of power at very low or negative prices because dispatchable generators are not able to reduce the power further.

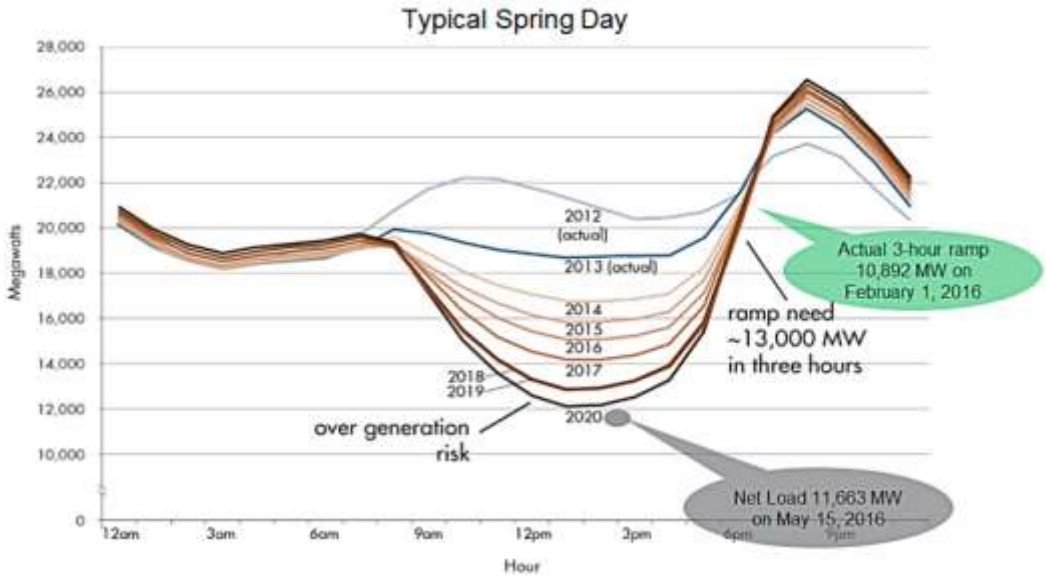

Figure 3 The Duck-Chart, steep ramping needs and over generation risk portrayed in the net load of CAISO during a typical day of spring [15].

There is no doubt that EVs will increase the electric energy consumption in the years to come. In specific, NREL projects that in the U.S. the transportation sector may dominate the incremental growth of the future electric consumption, refer to Figure 4. In this study, NREL assumes that high policy support and consumer adoption of EVs leads to an increase in energy consumption from 2016 levels of about 30%, arising only from the transportation sector. This corresponds to about 84% of the light-duty transportation fleet being electrified [16]. Thus, with these predictions of high EV penetration and consequently load increase, it is important to study impacts of EV on the operation of the power system and production costs.

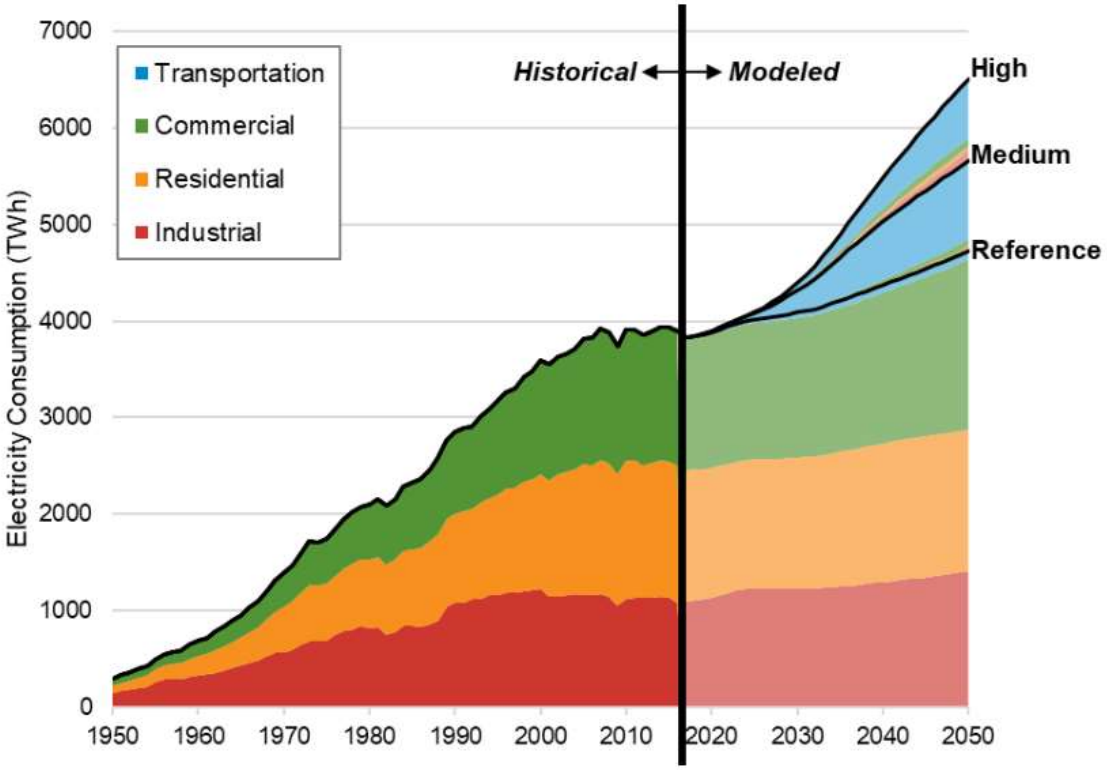

Figure 4 Historical and projected annual electricity consumption. Electrification of the transportation sector represents the most sensitive variable in the model [16].

1.2.5 Reliability and Demand Side Management (DSM) with EV

To maintain reliability of the power system (voltage and frequency in their limits), the system operator needs to balance instantaneously generators (supply) and loads (demand), which it is not an easy task since there are fluctuations in both supply and demand [17]. The demand fluctuation or variability in the power system load is a consequence of the random turning on and off many electric devices. On the other hand, the supply variability is a result of unexpected failures and errors from the dispatchable generators in following their schedules. VRE generators introduce supply fluctuation as a consequence of the natural variation of the wind and solar resource [17]. System operators counteract all these fluctuations in both supply and demand through the provision of ancillary services.

1.2.5.1 Ancillary services

Ancillary services are defined as the actions taken to keep the reliability of the power system, and commonly are differentiated by their reaction time [18]. Operating reserves are ancillary services that add extra generation capacity able to respond to unexpected reductions of supply, and it responds in a range of seconds to 30 minutes [18]. These operating reserves are divided into two categories based on the nature of their response to changes in net load as “event” and “non-event”, see Figure 5 [19].

“Non-event” refers to adjustments of generation and supply under normal power system operation, and it is divided into regulation and load following [19]. Regulation is an operating reserve that balances the supply and demand, and it responds automatically to changes in either generation or load within the timeframe of the shortest market optimal dispatch. Via automatic sensing of imbalances in power and load, the system operator delivers adjusting signals to the generation resources that provide regulation through what is called automatic generation control (AGC). Load following is an operating reserve that balances supply and demand, it is scheduled as part of the intervals of the market economic dispatch, and it is the action of following the general load pattern. Thus, Regulation and load following counteract the inevitable errors in forecasting the load under normal power system operation.

“Event” refers to adjustments of generation and supply under an unexpected imbalance, like a trip off a generator or a transmission line, and it is divided into contingency reserve and ramping reserve, see Figure 5 [19]. Contingency reserve responds to near instantaneous events for arresting the frequency excursion. Ramping reserve responds to non-instantaneous and infrequent events that are difficult to predict. Thus, ramping reserve are designed to cover the infrequent and large in magnitude events from unpredictable VRE.

Contingency reserve is divided by their reaction response time as primary, secondary and tertiary reserve, see Figure 5. Primary reserve, responds immediately after the event and avoids extreme frequency deviations. Once frequency is stabilized by the primary reserve, secondary reserves restore the frequency back to the scheduled setting. Tertiary reserve is deployed only after a subsequent event, it restores the primary and secondary reserve of the balancing area. It is important to note that ancillary services are defined differently in each electricity market. Table 1 provides an overview of the names employed by each Independent System Operator (ISO) or Regional Transmission Organization (RTO) for their reserves.

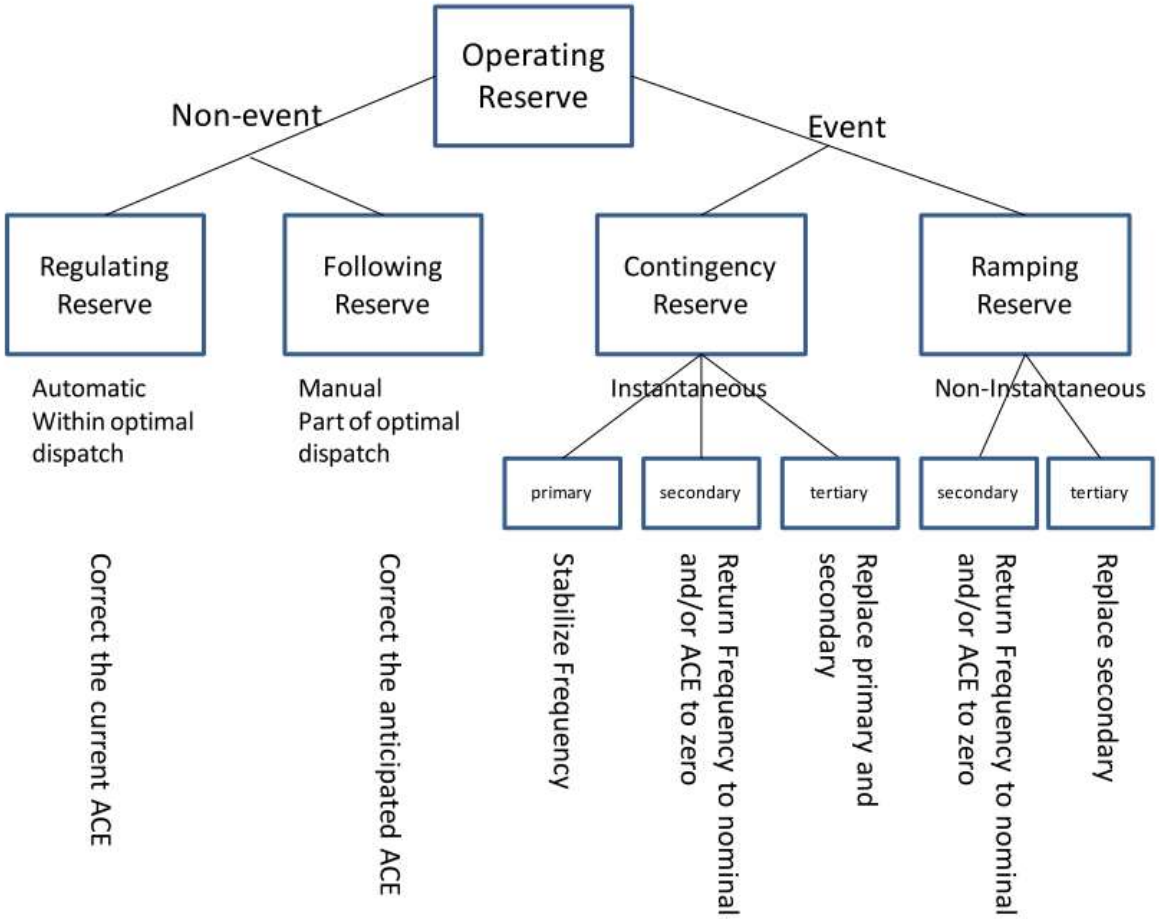

Figure 5 Operating Reserve categories and their relation to each other. [19]

Thus, supply-side (generation) or demand-side (load) resources provide ancillary services. In general, demand-side resources (demand response) are faster than a dispatchable generator, because there is no machine inertia or thermal constraints. The Federal Energy Regulatory Commission (FERC) estimates that DSM can reduce up to 20% of the national peak power consumption [20]. Subsequently, the focus of this research is related to the DSM that can be provided through the interaction of EVs. In order to understand the potential of using EVs as a DSM tool, it is important to know the status of and potential for EVs as DSM in the U.S.

Table 1 Overview of the ancillary services offered by each ISO/RTO [18]

ISO/RTO[1]	Spinning reserves	Non-spinning reserves	Regulation
CAISO[2]	Spinning	Non-spinning	Regulation-up Regulation-down Regulation mileage-up Regulation mileage-down
ERCOT[3]	Responsive	Non-spinning	Regulation-up Regulation-down
ISO-NE[4]	Ten-minute synchronized	Ten-minute non-synchronized Thirty-minute operating	Regulation
MISO[5]	Spinning	Supplemental	Regulation
NYISO[6]	Ten-minute spinning Thirty-minute spinning	Ten-minute non-synchronized Thirty-minute non-synchronized	Regulation
PJM[7]	Synchronized	Primary	Regulation
SPP[8]	Spinning	Supplemental	Regulation-up Regulation-down

[1] ISO: independent system operator, RTO: regional transmission organization

[2] CAISO: California independent system operator

[3] ERCOT: electric reliability council of Texas

[4] ISO-NE: New England independent system operator

[5] MISO: midcontinent independent system operator

[6] NYISO: New York independent system operator

[7] PJM: Pennsylvania-New Jersey-Maryland interconnection

[8] SPP: Southwest Power Pool

1.2.5.2 DSM and EVs

In every electricity market there are DSM programs. One simple approach of implementing DSM is through time-of-use (TOU) electrical rates, which impose a higher tariff (cost) of electricity during peak hours and thus encourage electricity consumers to modify their energy consumption based on the tariff scheme. Another approach is the direct control of the energy consumption of consumers by the power company. For example, in the residential sector, power companies could control (turn on or off) air conditioners, water heaters, or pool pumps, etc. In both approaches, the benefit for the consumer is a reduction in their electric bill, and for the power company it is a reduction in the peak load, and consequently a reduction in the operating cost of their system [21]. Subsequently, "uncoordinated" charging refers to the interaction of EVs with the electric grid in which the charging process is in control of the electricity customer and in which the consumers act as individuals for their benefit only. In this case the charging process starts as soon the EV is parked and plugged in (mainly at home), or it starts as soon as the TOU rate begins with its cheaper rate for charging. "Coordinated" charging, on the other hand, refers to the interaction of EVs with the electric grid in which the charging process is in control of the utility, the market operator, or through an aggregator, such that the benefit to the customer and the utility is increased.

1.2.5.3 Coordinated Charging

Coordinating the charge of EVs is advantageous to avoid troubles at the distribution line and at the transmission level, as well as in the operation of the power system. There are two main ideas to discuss: the first one is related to the charging behavior on a single EVSE, and the second one to the aggregation of many EVSEs. The first approach requires monitoring the distribution line voltage and reducing the power withdrawn by an EVSE so that the charging load does not cause a voltage drop and overload of the distribution side transformers [22]. It is possible to design a micro-grid on the distribution system that

includes battery storage and distributed generators that handle the charging of the EVs; this approach is likely to minimize power losses and total annual cost [23].

The second approach requires the oversight and aggregation of many EVSEs in the operation of the electric grid and considers the EVs load as a demand response resource or distributed storage [24]. The EV charging will be traded in the electric market, for example by the aggregator, as a demand response resource or as an ancillary service [25]. In specific, this type of service can stabilize the voltage and frequency of the electric grid [26]. In addition, coordination of the charge of the EVs can mitigate a steep ramp in power demand, and the grid power is changed smoothly [27]. This coordinated charging should be part of an optimization scheme that also considers the changes of the load by season, time of day, and in a particular region or grid. There is a good example of this technique in a Metropolitan area in China, in which peak load shaving of the electric system has been projected via the use of EVs [28]. Another example of coordinated charging was an analysis of the load in Belgium, which demonstrated that coordinated charging reduces power losses and avoids overloading of the distribution grid transformers [29].

1.2.6 Status of DSM in the U.S. Power Markets

According to the Energy Information Agency (EIA), electricity markets (ISO/RTO) covered about 60% of the country's power supply in 2009[9], and nowadays this number has increased to cover as much as 67% of the entire customers in the U.S.[10] (Figure 6). In addition, according to EIA in 2014[11], most of the demand

[9] See: https://www.eia.gov/todayinenergy/detail.php?id=790

[10] See: https://isorto.org/

[11] See: https://www.eia.gov/todayinenergy/detail.php?id=24872

respond enrolled customers were in the residential sector (93%), however most of the peak demand savings came from the industrial (61%) plus the commercial (21%) sector. In average, the participation incentives for the customers were higher in the industrial sector, which were more than 9,000 USD, following by an average of 600 USD in the commercial sector. In the residential sector, the average customer saved 100 kWh in energy and earned $40 for their participation. Having these as a context, the state with the highest contribution in peak demand savings is California (20%) which is also the state with the most customers enrolled in demand response programs (20%). Consequently, the addition of EVs in DSM programs can increase the peak savings from both the residential and commercial sectors in the areas covered by an ISO/RTO.

Figure 6 Geographical distributions of the ISO/RTO in North America.

1.3 Research Questions

The charging of these electric vehicles can increase the peak demand (uncoordinated charging) or provide the opportunity to be part of the demand response program (coordinated charging) for the system operators. Consequently, it is important to further study the impact in the power system operation of this new load coming from high penetration of EVs under both coordinated charging and coordinated charging. Furthermore, it will be imperative to understand the challenges and opportunities that face the system operator with the increase in penetration of VRE. Finally, it will be important to evaluate the effect imposed by electrification of part of the transportation sector concurrent with increasing levels of VRE.

Beyond just matching generation and demand, it is necessary to address these questions using a model complex enough that includes transmission and accounts for congestion. Such a model will naturally develop different locational marginal prices (LMP) by regions or areas as happens in real power systems. In addition, it is appropriate to use a reference test system in testing the effects of EVs. The reference test system to be used here is the IEEE[12] Reliability Test System (RTS) [30]. Thus, this dissertation will pick an appropriate RTS to test the research objectives. Using the RTS-GMLC[13] electrical system model as the candidate power system, the specific research questions to be addressed in this dissertation are:

- What are impacts of uncoordinated and coordinated EV charging strategies in power system operation, peak loads, and cost?
- What are the combined impacts of a high-penetration EVs and VRE on power system loads, operation, and cost, when considering both uncoordinated and coordinated EV charging models?

[12] Institute of Electrical and Electronics Engineers

[13] The Reliability Test System of the Grid Modernization Laboratory Consortium RTS-GMLC [99]

How do the two models of EV charging influence the integration of high-penetration solar and wind power, for example as related to curtailment of VRE?

1.4 Literature Review Power System Modeling

1.4.1 Power system modeling

There are different methods for modeling the electric power system, which includes Capacity Expansion Modeling, Production Cost Modeling, and Reliability Modeling. Each approach is designed to answer a scope of questions, therefore it is imperative to pick the approach according to the research interest [31]. This literature survey will focus on the questions suitable for Capacity Expansion Modeling and Production Cost Modeling. In addition, this literature review identifies the previous studies that answered questions related to electric vehicles (EVs) and variable renewable energy (VRE). Moreover, this survey will set the background for designing a detailed research plan, and answering the research questions, in this proposal.

1.4.2 Capacity Expansion Models

What is a capacity expansion model? A capacity expansion model (CEM) determines the cheapest energy sources (generation mix), levelized cost of energy (LCOE), to serve the load in the future. A capacity expansion allocates enough generation and transmission capacity to match the future load and reserves. The temporal scope of a CEM is many years in the future. Thus, a CEM has a coarse temporal resolution of every year. In addition, the spatial resolution in a CEM can cover a region, like a utility or balancing authority (BA), or even a whole country. For example, the CEM Regional Energy Deployment System (REEDS) explores more than 40 years for the U.S., in which every year is simplified by considering one representative day per season, where each day is divided into four sections (16 time slices) plus an extra section during the peak load day for a total of 17 time slices [32]. In short, in a region for a given timespan a CEM makes sure that there is enough generation, transmission, and reserves.

Furthermore, to answer the question “What type of generation and transmission should be built to meet the demand?”, a CEM also explores how the optimal system change (sensitivity analysis) under different policies like RPS [33], emission constraints [34], environmental constraints like water [35], and fuels like

natural gas [36]. In addition, CEMs help in assessing the benefits and detriments of policies like RPS [37]. Moreover, CEMs are intended to inform on possible trajectories of the power system, based on both policy and technical constraints, and CEMs are not intended to predict the future [38]. Table 2 presents a brief description of the CEM process, which includes inputs, outputs, and limitations.

Table 2 Brief description of Capacity Expansion Modeling methodology [31] [38]

Inputs	Output	Limitations
• Future electricity demand • Fuel prices • Renewable energy resources (Datasets) • Technology cost, capital (fixed) and operational (variable). • Policy and regulation	• Annual generation • Generation and transmission capacity builds and retirements • Emissions • Fuel consumptions • Electricity prices (LCOE) • Credit/allowances prices	• No chronological unit commitment • A simplified model for generator dispatch • Limited representation of DC power flow

1.4.3 Production Cost Models

A production cost model (PCM) makes sure to serve the demand by committing and dispatching the generators in a feasible approach by adhering to reliability.

A PCM determines the lowest cost to operate the system while keeping the reliability and operational constraints for a given system, transmission and generation fleet [31]. Thus, the outputs of a CEM, generator fleet and transmission, serve as inputs for PCM [39]. In addition, a PCM requires high temporal data resolution inputs, from every hour to every 10 minutes, in order to model market operation and security constrained unit commitment. Moreover, to simulate the uncertainty from load and VRE it is

necessary to include their forecasts into the modeling analysis. Table 3 presents a summary description of the PCM process, which includes inputs, outputs, and limitations.

Table 3 Brief description of Production Cost Modeling methodology [31]

Inputs	Output	Limitations
• Load and forecasted load • Renewable resources and forecasted resource • The variable cost of the generator fleet • Fuel cost for traditional generators • Model of transmission system • Constraints on generation resources • Reserve requirements	• Operation cost of the system • Sub-hourly unit level generation • LMP ($/MWh) • Operation cost of the generators and revenue • Fuel consumption per generator • Emissions per generator • Price of ancillary services • VRE curtailments • DC Power flow	• Limited timespan analysis • Limited geographical analysis • Simplified model of the transmission system • Requires estimates of future O&M costs • Requires estimates of generation and transmission changes

Regarding the PCM limitations, the limited timespan analysis, usually a couple of days or weeks up to a couple of years, is based on high computational requirements for modeling the power system under such detailed temporal resolution. In addition, due to computational restrictions, most PCMs are intended for regions, BA or utilities. However, the computational restrictions of typical workstations can be partly addressed with parallel programming and high-performance computing (HPC) systems. For example,

NREL has the HPC Peregrine[14], which it runs the PCM PLEXOS. Another approach for solving these limitations is with cloud-based computing, which refers to HPC and parallel programming through the internet. For example, the cloud service ENELETYX[15] runs the PSO PCM. Thus, these computational solutions allow running bigger regions like the whole U.S. and for multiple years. In addition, time partitioning is a procedure of the parallel solving for the SCUC [40],[41], here the yearly data is broken down in parts in order to be run in parallel into the HPC. Once the solution of each individual partition is complete, then it is necessary to put all parts together. This approach saves a lot of computational time. For example, an analysis for the whole U.S. eastern interconnection can be run in more than 2 months with a single partition or in less than three days with 52 partitions and using 2 days overlapping.

1.4.4 Capacity Expansion Model for EV

This section covers these questions: What will be the cheapest way to serve the new demand that electric vehicles will impose? What capacity expansion model includes EVs? What did they find?

There is a preliminary assessment of the interaction of EVs and Wind energy [42], which proposes the use of EVs as a dispatchable load to address the variability of wind energy. In addition, the modeling tool Wind Deployment System (WinDS), originally designed to evaluate the wind energy generation potential in the U.S. covering the period from 2000 through 2050. Moreover, reserves in WinDS are accounted for as a margin of the peak demand. Thus, EVs are intended to become spinning reserves. Furthermore, the EV reserve capacity is estimated from assuming that 50% of the EV fleet is plugged-in at any time during every year of the analyzed period; the EV fleet is assumed from an adoption curve or S curve. In addition, this

[14] NREL Peregrine HPC: https://www.nrel.gov/hpc/peregrine-system.html

[15] ENELYTIX: http://www.enelytix.com/

study assumes that all EVs are able to charge and discharge, known as Vehicle to Grid (V2G). The sensitivity parameters in this CEM are the size of the battery and charging availability of the EV fleet. The results show that EV integration can increase the penetration of wind energy in the system, and based on the assumptions, electricity generation of wind can be as much as 16% by 2050. From here WinDS evolved to become REEDS and include EVs as a controllable or flexible load.

The Renewable Electricity Futures Study (REFS) assumes that only 40% of the EV fleet is plugged-in and controllable by the system operator at any time [43]. Moreover, this controllable EV charging reduces the curtailment of VRE. Thus, the EV charging was a main demand-side management option in the analysis. The load curve for EV came from driving profile vehicle simulations [44]. The core scenarios explored in this study are for supplying 80% of the electricity with renewable energies, in which VRE penetration is as high as 50% (about 38% wind and 12% solar). The cost and performance assumptions for technology in the CEM REEDS are based on projections from early 2010, which prioritizes the energy generation of wind energy over solar energy and coal over natural gas. Moreover, this study prioritizes technical issues over policies; therefore, it only includes the RPS and federal credits in the baseline scenario.

The annual energy outlook (AEO) is a yearly report conducted by the Energy Information Agency (EIA), which cover projections for energy use and supply for the U.S. towards 2050 [45]. EIA uses the National Energy Modeling System (NEMS) for the creation of the AEO. Related to electricity, AEO covers generation and consumption of electricity, covering the sources of generation and the electricity end-use. One of these end-uses is transportation. AEO reports of the total amount of electricity that goes into all forms of transportation, in the future the electricity consumption increases because of the increase of EVs. In the AEO the policy assumption is the Zero-emission Vehicle regulation (ZEVR) of California and nine additional

states[16]. Regarding new electricity capacity additions, combined-cycle and solar photovoltaic are the most attractive type to build. This is based on projected low prices of natural gas, and the continuation of the renewable tax credit for solar photovoltaics.

The Annual Standard Scenarios Report tracks the evolution of the electric power sector under different alternative pathways towards 2050. For the 2015 edition of this series [46], in one from a total of 19 scenarios, it is considered vehicle electrification following the approach proposed in the REFS, in which 45 % of the EV load is a utility controlled (DSM). The same assumption for EVs is kept for the following yearly reports [47]. For example, the last version of this series explores up to 42 scenarios that are focused on operational impacts of VRE, the potential for other types of renewables, natural gas deployment, and the reduction of tax credits for renewable energies. Moreover, the scenarios include a reference case (mid-case) with the policies in place by early 2018 and the rest of scenarios (sensitivity cases) explore fuel prices, technology cost, demand growth, retirements, transmission restrictions, and policy changes. Regarding the VRE penetration, in the mid-case, the VRE penetration is 43% by 2050, in which PV has the highest capacity. In addition, the natural gas combined-cycle (NG-CC) generation fleet provides the flexibility necessary to deal with VRE. Therefore, the capacity installation in mid-case is mainly VRE and NG-CC.

The Electrification Futures Study (EFS) explores electricity consumption in the United States towards 2050 [16]. This report covers the following sectors: transportation, residential and commercial building, and industry. In addition, this report includes technologies that can switch to electricity in the years to come, for example, EVs in the transportation sector. Each sector will increase their electricity consumption;

[16] Nine states considered for ZEVR: Connecticut, Massachusetts, Maryland, Maine, New Jersey, New York, Oregon, Rhode Island, and Vermont.

however, the transportation sector will have the highest increase. According to this report, EVs can have penetration in the range from 11% to 84%. In the high end of the EV penetration in the U.S by the year 2050, researchers estimate 240 million light-duty, 7 million medium and heavy-duty trucks, and 80,000 transit buses. As a whole, these EVs would account of more than 3 out of 4 of the vehicle miles traveled in 2050. In this study, NREL assumes that high policy support and consumer adoption of EVs leads to an increase in energy consumption from 2016 levels of about 30%, arising only from the transportation sector. Following EFS publications will inform about the generation mix towards 2050 (CEM) and system operation (PCM).

In conclusion, the most recent capacity expansion studies inform that demand will be balanced with an increase in penetration of VRE and NG-CC if the natural gas price stays low and supportive policy for solar photovoltaic (federal tax credits) continues. Regarding the retirements, coal is the power generation type with the highest decline. Therefore, for detailed operational modeling of the power system, PCM, the generation fleet should be in accordance with a set of assumptions of future fuel prices, transmission expansion or constraints, and policies.

1.4.5 Production Cost Model and EV

This section covers the following questions: How to determine the economic value in operating the grid of a resource like electric vehicles? What are the integrations studies, most important and recent, that include EVs?

The REFS has a PCM part [43][44], in which the ABB GridView software simulates particular days of 2050. GridView performed scheduling of EVs in the day ahead market (DA) and adjustments in the real-time (RT) market. Operational challenges took place at off-peak time, seasonally in spring and diurnally at night. Moreover, curtailment was greater in the spring season due to low demand and high VRE generation. This

was the first study that addressed the potential flexibility of EVs on a regional basis. The study assumed that light-duty vehicles will be at least 40% EVs by 2030 and 60% by 2050. Energy consumption of the EV fleet by 2050 will be at least 350 TWh and will represent 9% of the electricity demand of that year. In addition, based on the fact that in the year 2050 40% of the load from the EV fleet will be controllable by the system operator, on average the peak power per vehicle will be close to 0.3 kW at 7 pm with a lower valley approaching no load around 4 am, see Figure 7.

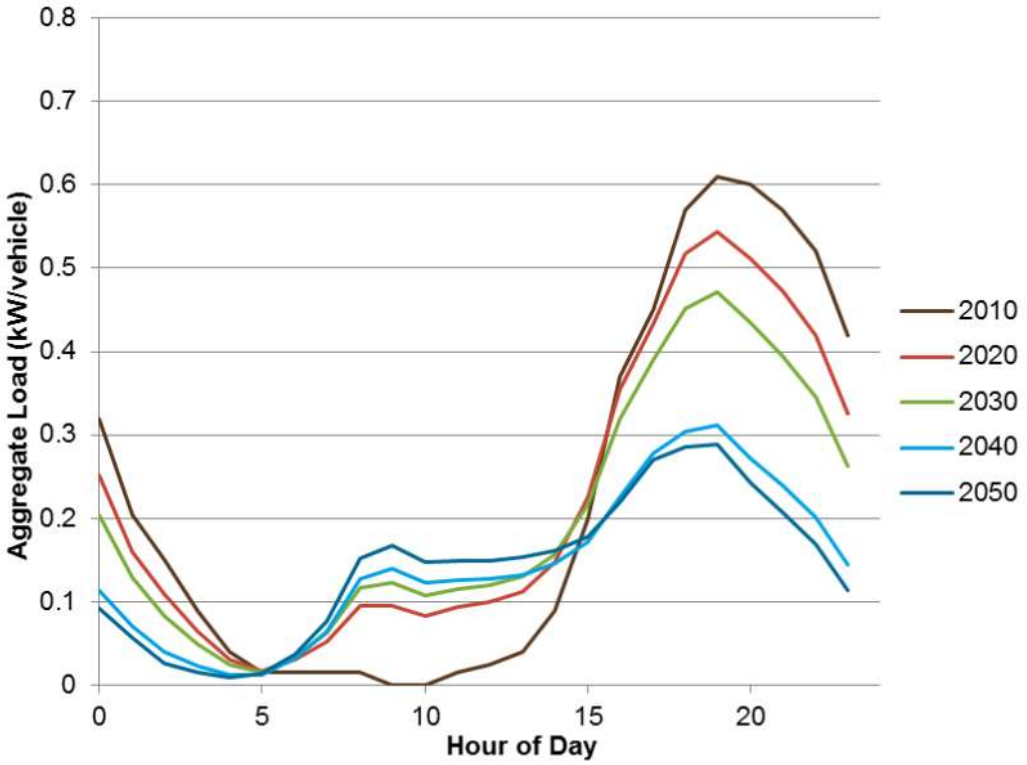

Figure 7 Aggregated load profile for EVs in the REFS and their transition from 2010 to 2050 [44]

The California 2030 Low Carbon Grid Study (LCGS) analyzes the grid impacts for achieving a 50% carbon emission reduction in the power sector operation under different scenarios [48]. These scenarios are built upon a portfolio of three cases, the baseline, the target, and the high solar. The baseline assumes the RPS

mandate of 33% by 2020. The target uses 56% renewable penetration plus storage. The high solar prioritizes PV over the rest of renewables. In this study, emissions-capping is the main constraint for the system operation. In addition, flexibility analysis of the system is tested in different scenarios that assume conventional flexibility and enhanced flexibility. The difference between these two flexibility categories are in constraints of zero-emission generation (nuclear, renewables and hydro) trade, minimum conventional generation (fossil-fueled), storage capacity, and hydro constraints. Furthermore, the enhanced flexibility reduces the curtailment of renewables in as much as 10% but increases the cycling of the natural gas generators. However, cycling of these generators is reduced with the implementation of storage and demand response. EVs charging is assumed as a source of flexibility. The number of EVs assumed in California is 3 million with an expected load of 13 TWh. Electric vehicle charging is assumed in all scenarios as demand response, in which half of the fleet is under coordinated charging. This electric vehicle fleet adds up to 3,000 MW of flexible load during the mid-day and reduces the VRE curtailment. The results are focused on the reduction of the production cost, the emissions, the capacity factors of the natural gas fleet (NG-CC), highest ramp in the year, and the percentage of VRE curtailment. The procedure is to compare the base case scenario against the sensitivity scenarios and then compute the reduction of each main result. In general, the highest ramp occurs on February 8 between 3 to 4 pm, which is a result of the decrease in PV generation, the magnitude of ramping this hour is 11 GW and is filled with imports (4.5 GW), natural gas fleet (3.2 GW), storage (3.2 GW), and demand respond (0.2 GW). In short, the focus of this study is not in EVs but it considers EVs as an important source for demand response, as high as 80% of the responsive load. In this instance, EVs charging start ramping at 2 pm and halt at 3 pm.

The state of California conducted a vehicle integration study back in 2014, The California Transportation Electrification Assessment Phase 2: Grid Impacts [49]. This study covers 4 utilities in California and uses the REFLEX methodology [50]. The SCUC in this methodology is simulated into a randomly generated

collection of days from a historical dataset. Therefore, this methodology is able to simulate the full range of system operational conditions. The largest challenge mentioned in this study for the integration of VRE is over-generation, which lead to the curtailment of VRE. In addition, this challenge is addressed with EVs as a flexible resource. Therefore, the EV fleet absorbs the overgeneration of VRE and reduces the ramping necessities of a typical spring day. In addition, the researchers determine that TOU avoids the increase of the peak load; however, TOU does not encourage the reduction of VRE curtailment. The benefits of dynamic charging (coordinated charge) are calculated by first estimating the hourly marginal price of electricity for eight typical days that represents the year, under the different combinations of VRE and load, high or low. Then, the lifespan benefits of EVs are calculated using the California Public Utilities Commission (CPUC) Total Resource Cost Test (TRC). This TRC considers gasoline savings, EVs federal tax credits, and carbon emissions costs. The lifespan costs of EVs include upgrades in the distribution system, energy delivery avoided cost, charging infrastructure cost, and vehicle incremental cost. Finally, the net benefit per EV is the difference between the benefit and the cost, this net benefit is a positive monetary quantity, which means that EVs add value in California. Consequently, this net benefit is focused on net present value (physical cost) and not in operational value (market cost) of EVs.

1.4.6 Production Cost Model and VRE

This section answers the following questions: How to determine the integration cost or the value of a grid resource? What are the integrations studies, most important and recent (state of the art), that include VRE? What should be included in an integration cost study?

The value of hydro-power [51] is determined using a PCM, in which the operation cost ($) of a base case or baseline scenario (A) is compared against the cost of running the under drought conditions resources (B) or generation scenarios. This comparison is an arithmetic subtraction (A-B). In addition, the value of the resource ($/MWh) is the comparison of the operation cost (A-B), divided by the energy produced by

the resource (MWh) with the average price of electricity (LMP). Usually, the operation cost with more hydro is lower. Therefore, under severe drought conditions, the value of the hydropower is higher.

The report “Review and Status of Wind Integration and Transmission in the United States: Key Issues and Lessons Learned” [52], explores recent studies that are the state of the art regarding integration studies, lessons from the system operators, the main organizations involved in VRE integration, and a brief discussion about transmission expansion related to VRE. Related to the wind integration studies, this report covers the questions addressed, the importance of ancillary services, best practices in the wind integration study methodology, key integration study results, and the lessons learned.

The major integration studies considered in this report [52] were the Western Wind and Solar Integration Study phase I (WWSIS-I), the Western Wind and Solar phase II (WWSIS-II), the Eastern Wind and Transmission Study (EWITS), ISONE-up to 24% wind energy penetration, ERCOT-9% wind energy penetration.

Regarding the questions addressed in the study, they are from the perspective of system operation and reserve procurement, because the power system operator deals with the uncertainty of power production of VRE [52]. The report specifically looked at the following:

- Identify the integration limits of VRE
- Identify necessary operational changes due to VRE
- Identify the change in system operation cost when incorporating VRE
- Identify the change of operating reserves due to VRE
- Identify detriments in power system reliability due to VRE

With respect to the best practices methodology for VRE integration studies, the authors cite a list of references and then focus on best practices. A summary of these best practices is in Table 4.

Table 4 Summary of the best practices related to inputs and processes for VRE integration studies [52].

Inputs	Processes
• Time-coincident time series for wind power and load. • Use representative forecast for VRE and load. • Include geographic diversity for the VRE. • Transmission modeling (transmission constraints. • Generation fleet modeling (operational constraints). • Emissions or other policy-environmental constraints if necessary.	• Realistic operation scenarios. • Balance the system net load. • Sufficient time resolution in PCM to simulate system operations and responses. • Ensure PCM captures the extreme ramping events. • Identify Reserve requirements. • Use loss-of-load probability and effective load-carrying capability to asses the capacity value of VRE • Use PCM for determining the total system operation cost. • Use the transient analysis for addressing reliability.

Therefore, the processes in Table 4 enable PCM to accurately emulate system planning and operation, e.g., via simulating the actions and timing of transactions in electric markets or vertically integrated systems.

The main lessons learned in integrating VRE are to increase the size of the Balancing authority areas and implements a sub-hourly market [52]. Moreover, responsive load has been identified as an important source of future flexibility. This responsive load should be incorporated in the sub-hourly market to balance the VRE. Furthermore, the authors describe that even large balancing authorities are facing

flexibility issues. In general, they are having troubles accommodating responsive load and allocating contingency reserves in the frame of 30 minutes for VRE.

This report states that integration studies should focus on overall system operation cost and determine the reliability, flexibility and operation impacts [52]. Therefore, an integration study should consider different power system configurations (scenarios) from a base scenario, then compare and contrast these scenarios against the baseline for determining changes in the operation cost and associated impacts. In conclusion, the value of adding VREs or another type of generator is recognized from the production cost savings.

1.4.7 Production Cost Model and DSM

This section answers the following questions: How does PCM implement DSM? How to determine the value of DSM?

The “Grid Integration of Aggregated Demand Response” report [53] identifies the potential demand response in the U.S. western interconnection. The report defines resource availability, which means the time window that a resource has for providing a load service. Then, it considers the inconvenience of changing electricity consumption, which means the service consequences that a user incurs for changing their power consumption. Third, it accounts for the temporal variation of ancillary services' market price, which is in relation to the monetary compensation that a user is expecting for changing their power consumption. The end-uses considered are residential, commercial, industrial, and municipal. Finally, a PCM determines the operational savings in a test system, which implements these demand response schedules [54]. As a conclusion, this report demonstrated a power capacity of 113 MW (an equivalent of a 2% of the system peak load), a 19% of the contingency reserve, and an 85% of flexibility reserve.

1.4.8 Methodology in PCM for VRE

The integration cost of a VRE is the increase in cost incurred to enhance the energy reserves and balancing resources (ancillary services). The integration cost includes the increase in the operation cost due to the uncertainty and variability of wind and solar energy. However, this procedure of identifying the integration cost ignores the value that VRE adds to the power system. This value of VRE is assessed by comparing overall operation costs minus the technology investment (i.e., in an "evolutionary" integration study that contemplates the full impact of VRE, both positive and negative) [55]. From the analysis of different integration studies, this report presents a list of comparable items and a summary matrix. The list provides a good reference for the parts or items that an integration study methodology should include. A brief description of these items is the following:

1. The aim of the study, identifies the consequences of wind power or finds the penetration limit of wind power.
2. The method of adding VRE in the power system model, to add VRE to an existing generation fleet into a model or VRE is part of an optimized new generation fleet for the region of study.
3. The simulation method, deterministic or stochastic.
4. The time resolution, like every minute, hour, or day.
5. The pricing, to pick between physical cost and market cost.
6. Design of the remaining system, to pick between economic optimization, operational optimization, or assume actual operation and market rules.
7. Imbalance calculation, refers to the inclusion of wind forecast and the system imbalance, the mismatch between generation and load, accounts for procuring the reserves.
8. Balancing location, refers to the reserves that are assumed in the same area or from a different region, and the reserves allocation within the generation fleet.

9. Grid limits on transmission, refers to the inclusion of the physical limits of the power transmission system.
10. Uncertainty treatment, explains the modeling of the uncertainties in the analysis. Usually, the uncertainties modeled are for transmission limits, wind and solar power, hydro availability, load, generation outages, and transmission outages.
11. Hydropower modeling, if there is consideration of environmental constraints in the use of the water resource, or the commitment and dispatch of hydropower only considers technological and physical limits.
12. Hydro capacity service, describes the existence of a special model of interaction between Hydro and VRE, like hydro storage for VRE.
13. Thermal power modeling, lists all the operational constraints included for the conventional generation fleet, like startup cost, ramping capabilities, heat rates or variable cost of operation.
14. Wind Power modeling, explains the details of the modeling of the VRE generators.

Due to the low cost of solar photovoltaics, it is appropriate to add, “Solar Power modeling” to item 14 in the list.

In relation to the previous list, Table 5 presents a methodology summary for the most relevant integration studies of North America.

Table 5 Summary of methodology presented in the most relevant integration studies in North America [56],[57],[58],[59],[60].

Study	WWSIS-I[17]	EWITS[18]	ISONE[19]	ERCOT[20]	ERGIS[21]
Aim					
Penetration limit					
VRE impacts	x	x	x	x	x
Adding VRE					
Add to existing fleet	x	x	x	x	
New optimal fleet					x
Simulation					
Deterministic	x	x	x	x	x
Stochastic					
time resolution	10 minutes	10 minutes	10 minutes	1 minute	5 minutes
Pricing					
Physical cost					
Market cost	x	x	x	x	x
System design					
Economic Optimization	x	x	x		x
Operational Optimization	x	x	x		x
Actual market rules			x	x	x
Imbalance calculation					
Wind forecast	x	x	x	x	x
Reserve procurements	x	x	x	x	x
Balancing location					
Local reserves	x	x	x	x	x
Import reserves	x	x			x
Transmission					
Copper sheet					
Physical limits	x	x	x	x	x
Uncertainty					
Thermal fleet modeling	x	x	x	x	x
VRE modeling	x	x	x	x	x

[17] WWSIS-1: Western Wind and Solar Study phase I

[18] EWITS: Eastern Wind Integration and Transmission Study

[19] ISONE: Independent System Operator New England up to 24% wind energy penetration

[20] ERCOT: Electric Reliability Council of Texas 9% wind energy penetration

[21] ERGIS: Eastern Renewable Generation Integration Study

The major integration studies presented in Table 5 targeted the impact of VRE and used a deterministic simulation approach, which is the standard [52]. In addition, the integration studies for ISONE and ERCOT considered only local reserves for balancing purposes. Moreover, these integration studies with exception of ERGIS, employed hourly PCM but included statistical analysis in the range of minutes to identify ramping events and procure reserves, i.e. statistical analysis complemented the PCM [61]. Therefore, only the most recent integration study, ERGIS, employs in the PCM a five minutes resolution, which enables the direct exploration of net load impacts in system operations, i.e. no need for statistical analysis. Consequently, the high temporal resolution in the PCM for ERGIS employed parallel computing in an HPC (time partitioning) [60]. Furthermore, ERGIS instead of just adding renewables is the only integration study in Table 5 that included a CEM (REEDS), which determined the new optimal generation fleet for each explored scenario [60].

The authors of this report [55] focused on the integration of Hydro and Wind in power system operation. However, the modification of the previous list, especially items 11 and 12, will enable the analysis of any other type of technology interaction, like EVs and VRE. Therefore, it will be necessary to consider EV modeling and a set of EV capacity or grid services, e.g. consider EVs as a responsive load.

1.5 Approach and structure of the dissertation

The dissertation covers two main parts. The first develops the methodology to model and integrate EVs into power system operation (PCM). Thus, to focus only on integrating EVs into the power system, the modeling of EV takes place in a smaller scale system (RTS). The second topic explains the integration of EV into different planning stages or markets, from days before the trading day, like the day week ahead (WA), to the trading hour or real-time (RT), Also, the second part is the exploration of the high penetration of VREs and EVs. Therefore, EV integration is projected into a larger scale and different seasons (off-peak season and on-peak) using the RTS-GMLC and modeling multicycle rolling horizons.

Thus, the dissertation consists of four chapters, the introduction chapter, two "content" chapters, and a conclusion chapter. Chapter 2 is a journal manuscript that addresses the integration of uncoordinated and coordinated EV charging in a PCM. The second manuscript, in chapter 3, addresses the main results and conclusions obtained in this dissertation. A conclusion chapter follows, along with references and appendices.

Chapter three: Integrating Electric Vehicles into Power System Operation Production Cost Models

Preface

This chapter is a published article in the World Electric Vehicle Journal for publication as a stand-alone manuscript.

Abstract

The electrification of the transportation sector will increase the demand for electric power, potentially impacting the peak load and power system operations. A change such as this will be multifaceted. A power system production cost model (PCM) is a useful tool with which to analyze one of these facets, the operation of the power system. A PCM is a computer simulation that mimics power system operation, i.e., unit commitment, economic dispatch, reserves, etc. To understand how electric vehicles (EVs) will affect power system operation, it is necessary to create models that describe how EVs interact with power system operations that are suitable for use in a PCM. In this work, EV charging data from the EV Project, reported by the Idaho National Laboratory, were used to create scalable, statistical models of EV charging load profiles suitable for incorporation into a PCM. Models of EV loads were created for uncoordinated and coordinated charging. Uncoordinated charging load represents the load resulting from EV owners that charge at times of their choosing. To create an uncoordinated charging load profile, the parameters of importance are the number of vehicles, charger type, battery capacity, availability for charging, and battery beginning and ending states of charge. Coordinated charging is where EVs are charged via an "aggregator" that interacts with a power system operator to schedule EV charging at times that either minimize system operating costs, decrease EV charging costs, or both, while meeting the daily EV charging requirements subject to the EV owners' charging constraints. Beta distributions were found to be the most appropriate distribution for statistically modeling the initial and final state of charge (SoC) of vehicles

in an EV fleet. A Monte Carlo technique was implemented by sampling the charging parameters of importance to create an uncoordinated charging load time series. Coordinated charging was modeled as a controllable load within the PCM to represent the influence of the EV fleet on the system's electricity price. The charging models were integrated as EV loads in a simple 5-bus system to demonstrate their usefulness. Polaris Systems Optimization's PCM power system optimizer (PSO) was employed to show the effect of the EVs on one day of operation in the 5-bus power system, yielding interesting and valid results and showing the effectiveness of the charging models.

1.6 Introduction

Currently, electric vehicles represent a small fraction of the transportation sector. Nevertheless, different market analysts predict a high penetration of electric cars, which will increase up to 33% by 2040 [62] and 50% by 2050 [63]. The advancement propelling the increase in the penetration of electric vehicles is the battery, via both an increase in the energy density (kWh/kg) and a reduction in the cost per energy (USD/kWh). In 2018, costs were in the range of 209 USD/kWh [64]. In 2020, the battery pack achieved a price of 137 USD/kWh [65]. The International Renewable Energy Association (IRENA) anticipates a cost of 150 USD/kWh in the 2020s, which will make EVs a competitive transportation option [4].

An electric vehicle needs to hold enough energy for the everyday commute and extra energy for extended travel. Charging technology is also relevant, since it is necessary to supply energy at a reasonable rate for the next day's commute by charging at home and traveling beyond the battery charge capacity at public charging stations [5]. The electrification of the transportation sector will lead to a reduction in primary fuel consumption and an increase in the power output of the electric sector [66]. This increased amount of power in the electrical system requires analysis from different perspectives, such as the impacts on the low-voltage distribution system [10] and the high-voltage transmission system [14]. Furthermore, it is important to consider the operation of the electric system as a whole to minimize the increase in the peak

load and ensure the lowest cost of electricity [27]. The charging of electric vehicles, if done intelligently and in a coordinated fashion, can enhance the penetration of variable renewable energy (VRE) sources such as wind and solar power. As an example, the research from Tuffner and Kintner-Meyer demonstrated that controlling the rate of charge of EVs can compensate for abrupt or step changes in power production from wind farms [67]. The charging of EVs, if done in an uncoordinated fashion, could increase the peak energy demand.

The EV Project from Idaho National Lab (INL), explores the uncoordinated charging of electric vehicles in different cities, including San Francisco, CA and Nashville, TN [68]. Charging availability (charger connected to a car) is similar in both regions, low during the day and increasing during the evening. Nevertheless, there is a difference in the charging demand: In Nashville, the demand peaks at 8 PM, and in San Francisco, it peaks at 1 AM due to utility time-of-use (TOU) rates offering reduced rates at off-peak hours [68]. In this latter case, the uncoordinated response to TOU rates created a new spike in demand during off-peak hours. In other words, the charging of EVs poses both opportunities and challenges. The purpose of this work is to devise models of EV charging behavior, both coordinated and uncoordinated, suitable for incorporation in a PCM and thus facilitating investigation of their impact on power system operation and costs.

Recently, the methods for modeling EV load have mainly used bottom-up behavioral techniques such as Markov chain [16,66,69], Markov chain Monte Carlo [70-72], machine learning [73-74], and agent-based [75-83] (aggregator) simulations. Moreover, some authors have used travel survey data to construct the EV load, using either a Monte Carlo simulation approach [84] or stochastic modeling [85]. The focus of the modeling in the reviewed literature is on the distribution grid (voltage and line loading), hub management (transactions on the distribution side), and grid infrastructure planning (capacity expansion country or

microgrid). This paper's contribution is to link EV modeling with power system operation, detailed point by point as follows:

- The paper focuses on the bulk power system rather than the distribution side, which usually involves AC power flow simulations.

- This paper is the first to describe the incorporation of EV modeling of coordinated charging directly into a production cost model (PCM). Uncoordinated and coordinated EV charging models have been devised to bookend the positive and negative impacts of charging strategies.

- This work successfully demonstrates the implementation of both uncoordinated and coordinated charging models in a PCM for a simple power system.

1.6.1 Batteries and their effect on EV costs

A reduction in the cost of batteries for electric vehicles decreases the cost of new electric cars. Battery packs account for about half the cost of modern EVs. Recently, the cost of batteries for EVs has been decreasing year by year, reducing 73% from 2010 to 2016 [4] . The price reduction from 2010 to 2020 is estimated at 89% [65]. The price drivers for EV lithium-ion (Li-ion) batteries are the chemistry, manufacturing capacity, battery size, and charging speed [13] . Battery cells for fast charging are more complex and thus more expensive to produce. As there has been an increase in the production and size of Li-ion batteries, the manufacturing cost has decreased. The chemistry of the battery is one key to their price reduction. Reducing the percentage of cobalt in the battery cathode reduces their cost.

The reduction in the price of EVs is also due to the cost of batteries. In this regard, the Vehicle and Technology Office at the U.S. Department of Energy (DOE) set a goal to reach 100 USD/kWh by 2033, and 80 USD/kWh by 2038 [86]. Regarding the capital cost of new vehicles, the U.S. National Renewable Energy

Laboratory (NREL) projects substantial, yet achievable, reductions in battery costs that would lead to the capital cost of EVs matching the capital cost of equivalent conventional vehicles before the year 2030 [13].

It is essential to consider the operating cost of new vehicles, as this compensates for a higher capital cost. The Electric Power Research Institute (EPRI) showed that the total cost of ownership is lower for EVs than for conventional vehicles and hybrids [87]. In this comparison, EPRI used 2014 cost data (manufacturer, taxes, credits, destination charges, and EV chargers for Palo Alto, CA) and assumed 12 years or 150,000 miles of ownership. Concerning the lower cost of driving EVs, NREL anticipates that the levelized cost of driving (LCOD) [86] (without tax credits or other incentives) will be in parity with conventional vehicles as soon as 2021. For example, using the vehicle cost calculator from the DOE's alternative fuel data center, the Tesla Model 3 Standard Range has an equivalent cost of driving to the Toyota Camry XLE after eight years of ownership [88]. With cost parity between EVs and standard vehicles, there is a high chance that EVs will become a substantial portion of the car fleet in the years to come; as much as 75% of the sales of light-duty vehicles will be electric in 2050 [89].

1.6.2 Production Cost Model

A power system PCM is a software tool that mimics the operation of the power system by minimizing operation costs while adhering to operational constraints, ultimately yielding operational costs and locational marginal prices (LMPs), as well as other useful information. PCM software solves the unit commitment (UC) and economic dispatch (ED) optimization problems to minimize power system operational costs. ED is an optimization problem in which the objective function is to minimize the total operation cost of the system from a predetermined set of online resources to meet the load in the system. ED considers min/max power dispatch, transmission, ramping, and fuel constraints. Linear programming optimization is a common method to solve this type of problem. UC is also an optimization problem, where the goal is to determine the electrical generators that must be available for use, i.e., be committed,

to meet the forecasted power demand at the minimum operation cost in a system. Mathematically, the state of a particular generation unit is either off (not committed) or on (committed) in a time step (i.e., the decision variable is binary). A solution technique appropriate for solving both UC and ED is mixed-integer linear programming (MILP), which adds integer multipliers in the objective function to account for the state of each generator as on or off. The MILP formulation of UC includes more integer variables (constraints) than ED, also called "security-constrained unit commitment" (SCUC) [90]. For example, it includes start-up costs, start-up time, minimum up/downtime, reserve requirements, transmission, ramping, and fuel constraints. In this research, statistical models of EV charging appropriate for incorporation into a PCM are presented. The specific PCM employed to demonstrate the method is Polaris Systems Optimization's power system optimizer (PSO), which uses MILP to solve the optimization problems [91].

1.7 Methods

This section presents statistical models for EV charging that are adaptable to any regional mobility pattern, based on data from the EV Project. The EV Project data came from over 10,000 public and residential charging stations over three years (2011 to 2013), covering 4 million charging events in 18 different metropolitan areas across the U.S., with more than 4200 Nissan Leaf (24 kWh) and 1800 Chevrolet Volt (16 kWh) vehicles. In addition to describing the charging characteristics, a model of a simple 5-bus grid for use in testing the statistical models, the "NAU 5-bus system", is also presented. Further details on the methods described below are reported in two M.S. theses [92,93]

1.7.1 Battery and Charging Level

This study assumed a battery capacity of 24 kWh (Nissan Leaf 2013) as an average representative of all EVs. For statistical modeling, the EV and its charging characteristics are arbitrary. Regarding the type of charger, a survey study performed in the Salt River Project service area (in Arizona, U.S.) by the EPRI

showed that 66.7% of charging events occur using Level 2 chargers [94]. Level 1 and DC fast-charging event occurrences were 32.5% and 0.9%, respectively. Therefore, we assumed that the EV fleet will employ the percentage of each charger portrayed in Figure 8. For the statistical models being created, the battery capacity and distribution of charger types were definable variables (i.e., they are not constrained to the numbers mentioned above).

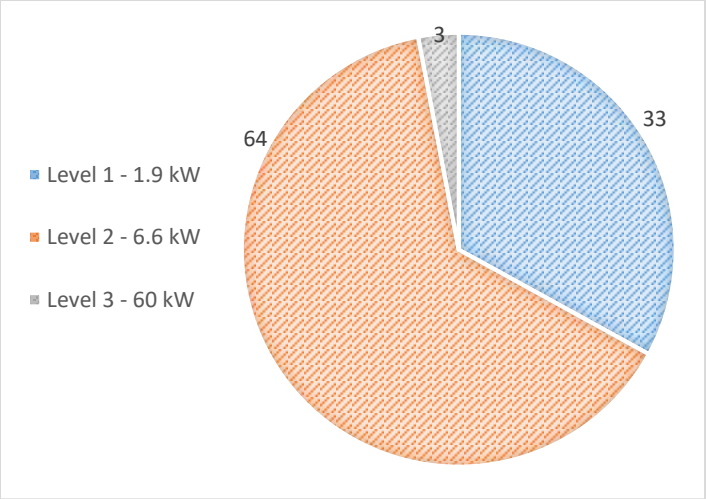

Figure 8. Charging level proportion (%) modeled in the electric vehicle (EV) fleet.

1.7.2 Battery State-of-Charge

This research assumed that the charging behavior of the EV owners in the EV Project data can be modeled statistically and scaled to be representative of any number of EV owners. Four statistical distributions of the state-of-charge (SoC) data were tested: normal (Gaussian) distribution, binomial distribution, Poisson distribution, and beta distribution. The chi-square goodness-of-fit test was applied to each distribution for the fitted data. For both the initial and final SoC data, the best fit was found using the beta distribution. At a 95% confidence in the differences between the observed value and the predicted value from a probability distribution, the best fit is the distribution with the smallest chi-square test value. For the initial SoC, the beta distribution with a chi-square test value of 357.76 ranked the lowest.

The beta distribution is a general type of continuous probability distribution. This distribution is defined on the interval (0, 1) parametrized by two positive shape parameters α and β. The probability density function of a random variable "x" that follows the beta distribution is determined as follows [95]:

$$y = \frac{1}{B(\alpha,\beta)} x^{\alpha-1}(1-x)^{\beta-1}$$

Where *B* is the beta function, a normalizing constant to keep the total probability equal to 1.

A histogram of the initial SoC data from the EV Project and beta distribution is shown in Figure 9. The least-squares method for the beta distribution took values of α = 3.28 and β = 3.27.

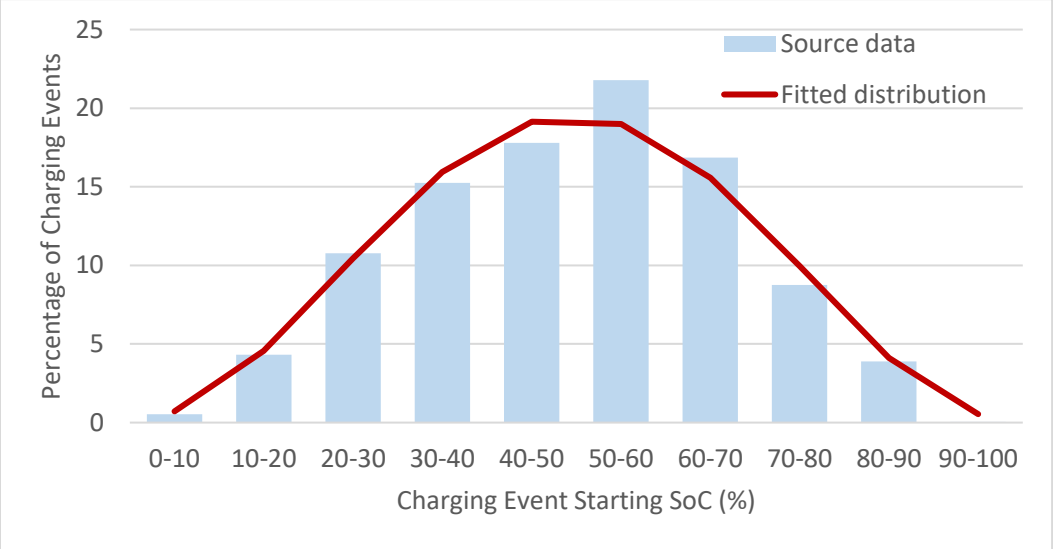

Figure 9. A plot of the beta distribution model of the initial state-of-charge (SoC) values fitted to the source data .

A histogram showing EV battery state of charge at the end of charging events (i.e., target state of charge) taken from the EV Project [96], along with a fitted beta distribution, is shown in Figure 10. Note the two peaks in the data, one at 70–80% SoC and the other at 90–100% SoC. The double peak occurs because 80% or lower was the target SoC. A faster charging rate happens below 80% for lithium-ion batteries. However, more than two-thirds of the charging ended with an SoC above 80%, and more than half above

90%. Beta distributions were once again found to fit the data best, and in this case, two beta distributions were used, one for the range 0–80% of SoC ($\alpha = 5.51$ and $\beta = 0.16$) and another for the range 80–100% of SoC ($\alpha = 14.59$ and $\beta = 0.67$). Again, at 95% confidence, the lowest difference from the observed and predicted values for the final SoC came from using two beta distributions with a chi-square test value of 371.

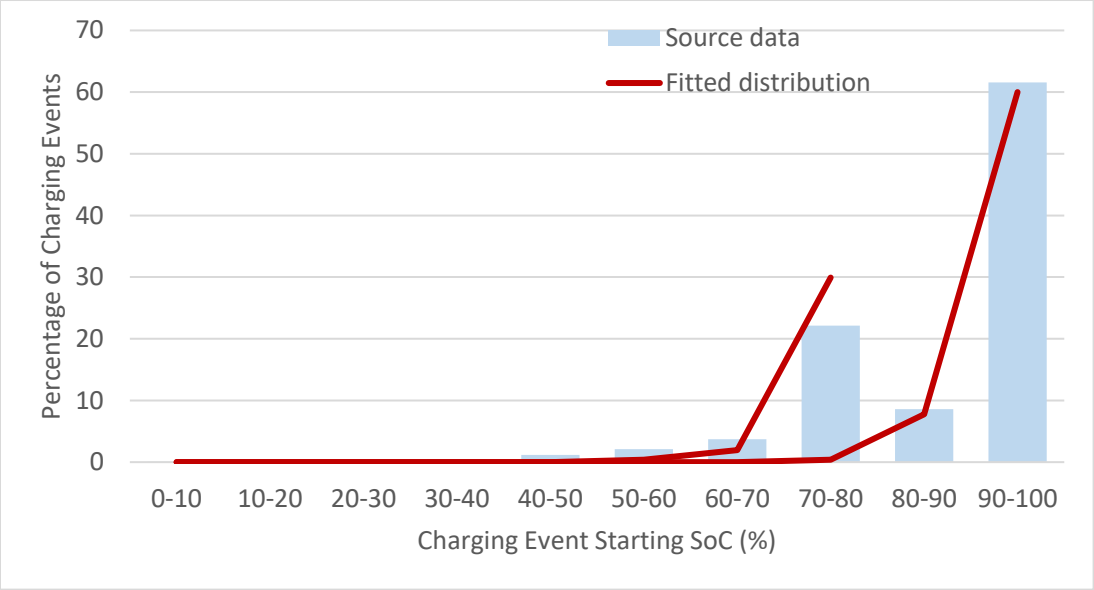

Figure 10. Beta distributions fitted to the target state-of-charge source data.

1.7.3 Availability - Arrival and Departure time

Charging "availability" is defined here as the period when the charger for an EV is connected to a vehicle and is able to charge. The EV Project data include charging availability at home, at work, and at public locations. A chart showing the charging availability data for each hour of the day on an average weekday is provided in Figure 11 [97]. Of the charging events, 85% occurred at home, with just above 40% availability during the night-time hours, and between 10% and 15% during daytime working hours. As the distribution of charging availability data can vary significantly between different regions of a country, or between different countries, it was not fitted to a statistical distribution but was directly used. In the EV

charging models implemented below, a distribution such as this is necessary to determine the charging load profile.

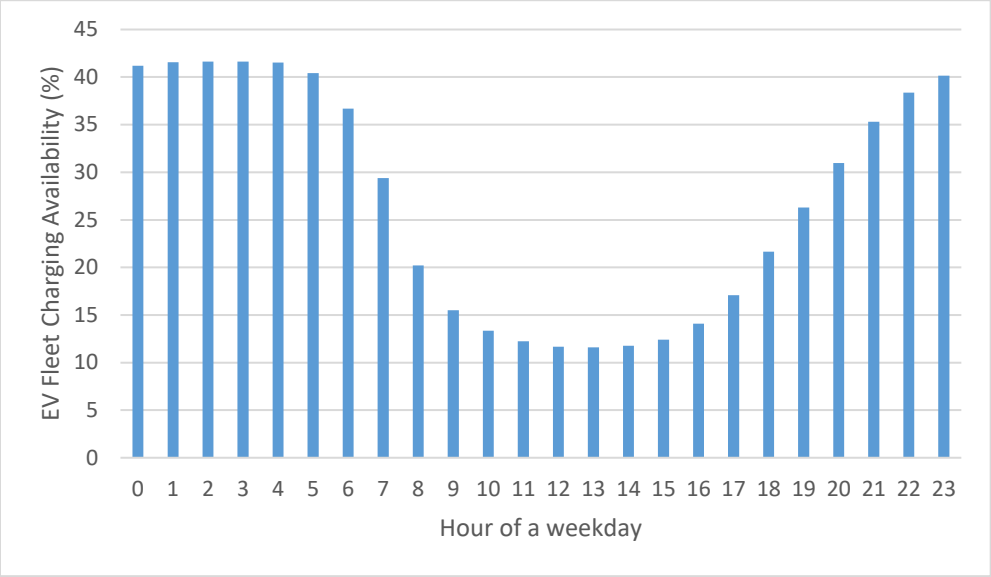

Figure 11. Weekday charging availability covering all types of chargers of the EV Project 2013 [97].

In addition to charging availability, the EV Project data included both the arrival and departure times of the EVs. Departure times, which represent an end to an EV's availability for charging, are shown in the histogram in part (a) of Figure 12. Arrival times, the times at which an EV is available for charging, are presented in part (b) of Figure 12. . Note the preponderance of departure times in the morning hours and arrival times in the evening hours, with a low and fairly constant number of arrivals and departures during the other hours of the day. The arrival data were used as the start time of charging if there was no TOU price incentive to start charging later in the day. The given distributions for the arrival and departure times were used with a Monte Carlo sampling technique to reproduce the arrival and departure data for a population of vehicles, thus allowing for easy adaptation to other regional or country profiles.

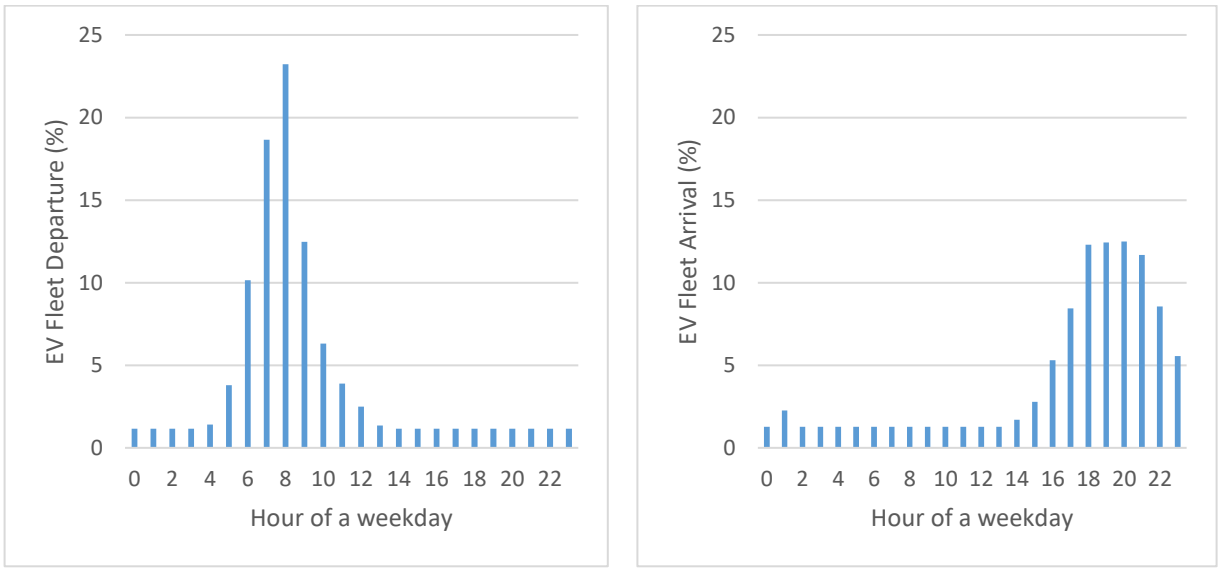

*Figure 12. EV availability in the EV Project data during weekdays as (**a**) departures and (**b**) arrivals* [97].

1.7.4 Modeling the Charging of Electric Vehicles

A survey of modeling techniques used to estimate EV load profiles showed that most researchers implemented bottom-up and agent-based simulations to generate a load profile, and that these were primarily for distribution system load studies [75-83]. Bottom-up simulation requires a transition probability at every step, which is unnecessary when creating a load profile for transmission-level studies. Consequently, this research used a Monte Carlo sampling technique, which can generate the load profile by accounting for the charging state of an EV.

1.7.4.1 Uncoordinated Charging of Electric Vehicles

The uncoordinated charging of EVs occurs when EV owners charge their vehicles according to convenience and without any information about, or communication with, other EV owners or the electric utility

supplying the electricity. This section presents a load profile model for reproducing the uncoordinated charging behavior of EV users.

The previous section demonstrated that the various deciding factors of electric vehicle charging may follow some kind of probability distribution. This application of statistical models to address our problem is helpful, as they can be scaled to create load profiles for different numbers of EVs. By definition, Monte Carlo is a method for randomly sampling from a probability distribution to create a random process for a problem [98]. For a chosen number of EVs, a random sampling of the values of the influencing factors (SoC, availability, etc.) for each EV from these distributions can be achieved. In this way, it is possible to produce a load profile from a population of vehicles that adheres to the overall shape of the distribution, scales to the number of vehicles, and gives daily load profiles that differ from day to day.

The sampled values of the influencing factors, as explained above, are processed to obtain the total charging profile of EVs. The flowchart in Figure 13 describes the step-by-step procedure for determining an uncoordinated load profile. The charging profiles for each EV in the fleet are consecutively created in the loop structure. Once all individual EV load profiles are created, they are summed to generate the overall load profile.

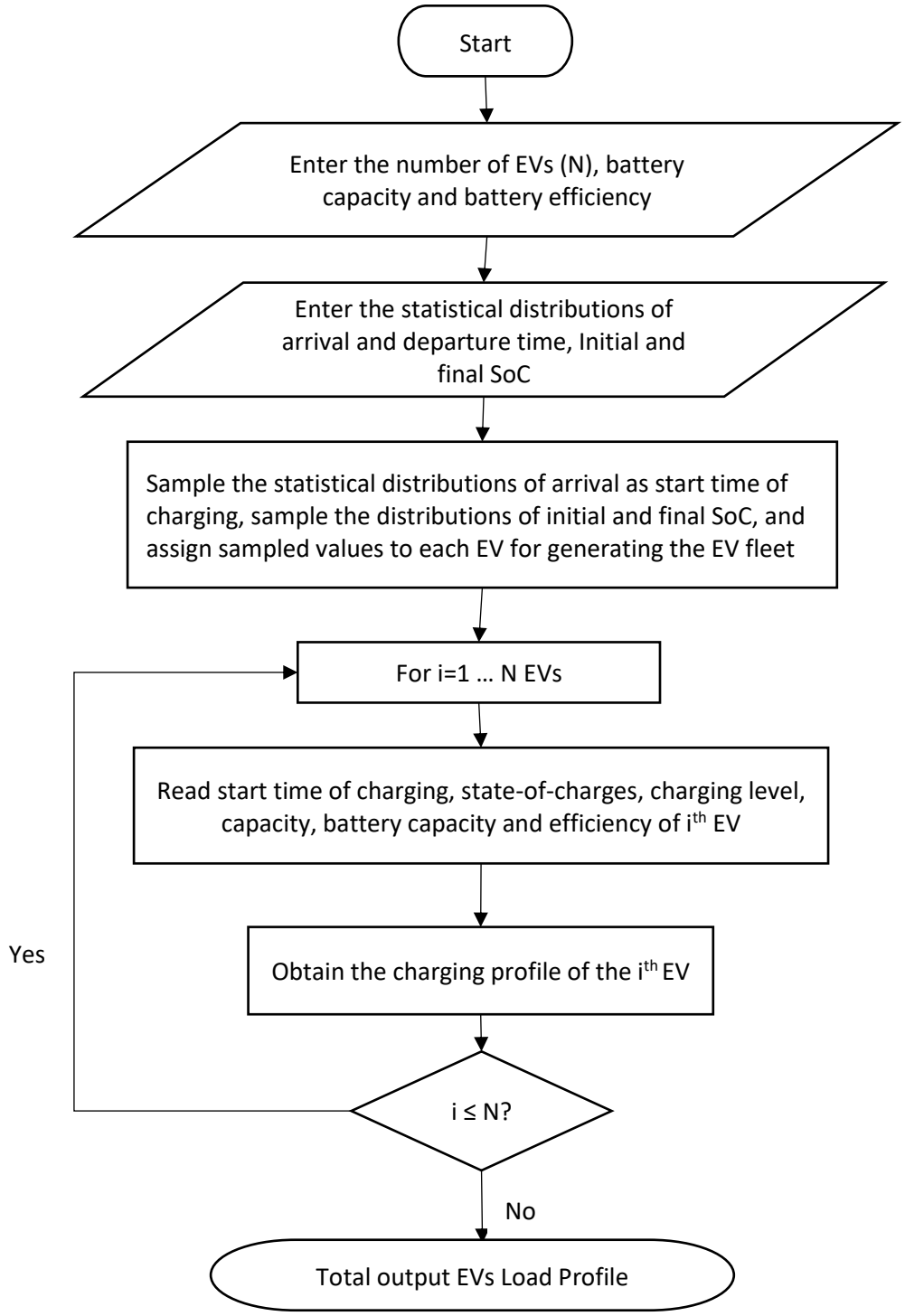

Figure 13. Flowchart of EVs uncoordinated load modeling.

1.7.4.2 Coordinated Charging of Electric Vehicles

The coordinated charging model of EVs in this research employed an aggregator scheme. An overview of the algorithm used to model the aggregator is described in the flowchart in Figure 14.

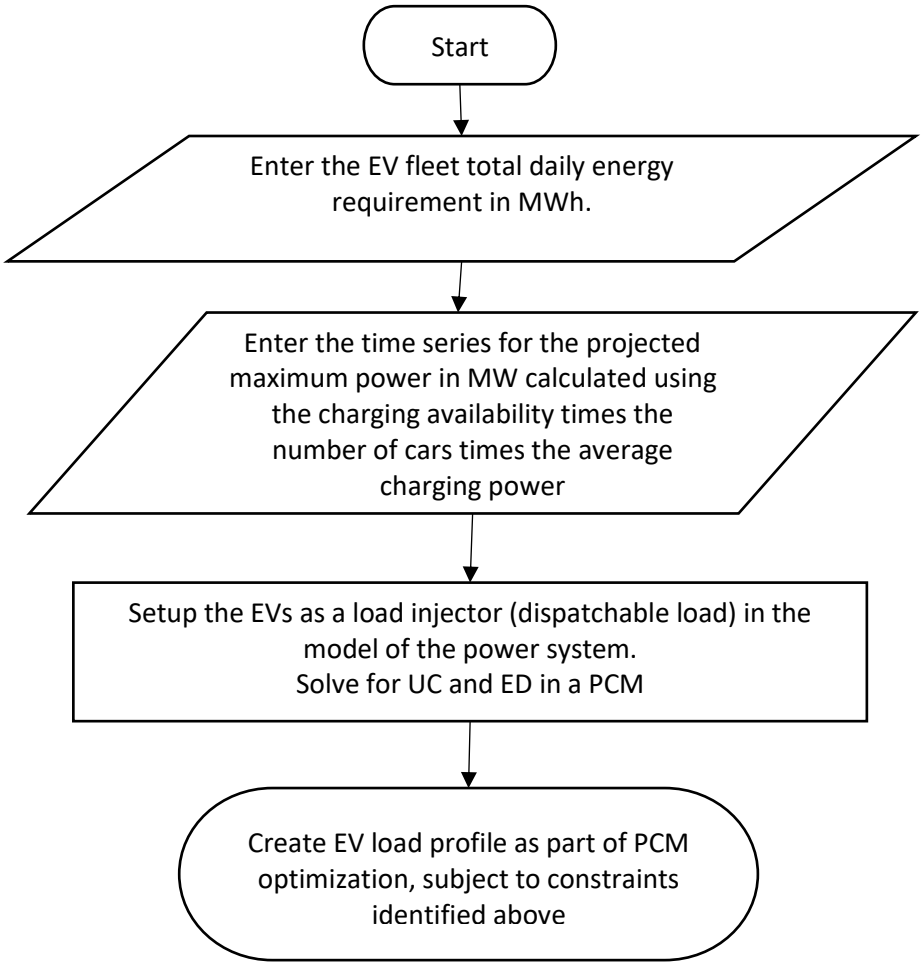

Figure 14. Flowchart of the modeled aggregator.

The first step in coordinated charging is to determine the daily energy requirement for charging the fleet of EVs. The projected maximum power draw at each time of the day comes from the charging availability distribution, the number of EVs (e.g., 1000 or 10,000, etc.), and the charging capacity, as shown in Figure 15. This profile defines a dispatchable EV load during each period of the day. The time in Figure 15 is in hours, but any time increment desired can be created, depending on the time resolution of the source

data, which in this case was 15 min. As the size of the EV fleet increases to higher penetrations, EV charging impacts both the total load profile and the correspondent local marginal pricing (LMP) of electricity. Consequently, trying to allocate a coordinated charging profile by using only the day-ahead forecast of LMP with no EVs neglects the influence of EV charging in the LMP profile. Therefore, the coordinated charging profile is determined in the PCM optimization as a dispatchable load. This is necessary so that the charging time series can respond to LMP changes as the load increases or decreases.

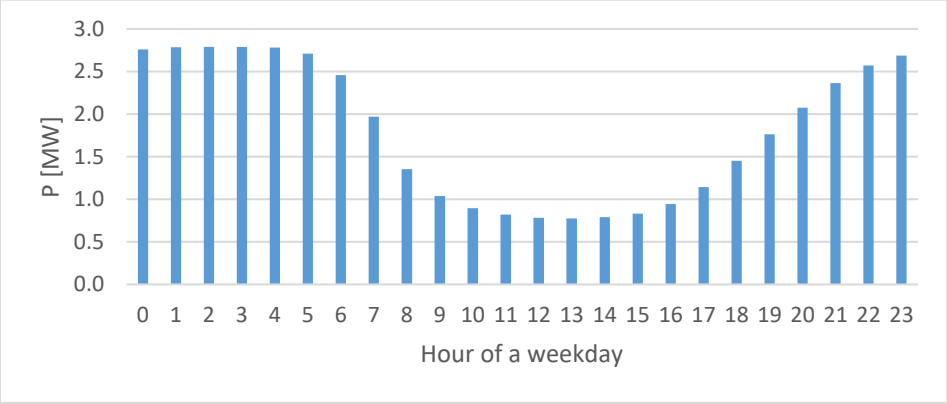

Figure 15. Projected maximum power (P) in MW for 1000 EVs on a weekday based on charging availability and charging capacity.

1.7.5 *NAU 5-BUS SYSTEM*

The goal of creating the EV load models described above was to use them in studying the effects of EVs on the operation of an actual power system (e.g., the Western Interconnect in the U.S., a regional utility power system model, etc.). However, to show the effectiveness of the models, it is only necessary to use a simple transmission system model that contains loads, generators, and transmission linkages that are representative of an actual power system. Therefore, a simple 5-bus system, namely the "NAU 5-bus system" (NAU is the acronym for Northern Arizona University), was created, and is depicted in Figure 16. The generator types and capabilities, the renewable energy generation time series, and the load time series are representative of those found in the southwestern U.S.; it includes a subset of the variable

renewable energies and generator characteristics from the Reliability Test System of the Grid Modernization Laboratory Consortium (RTS-GMLC) [99][100].

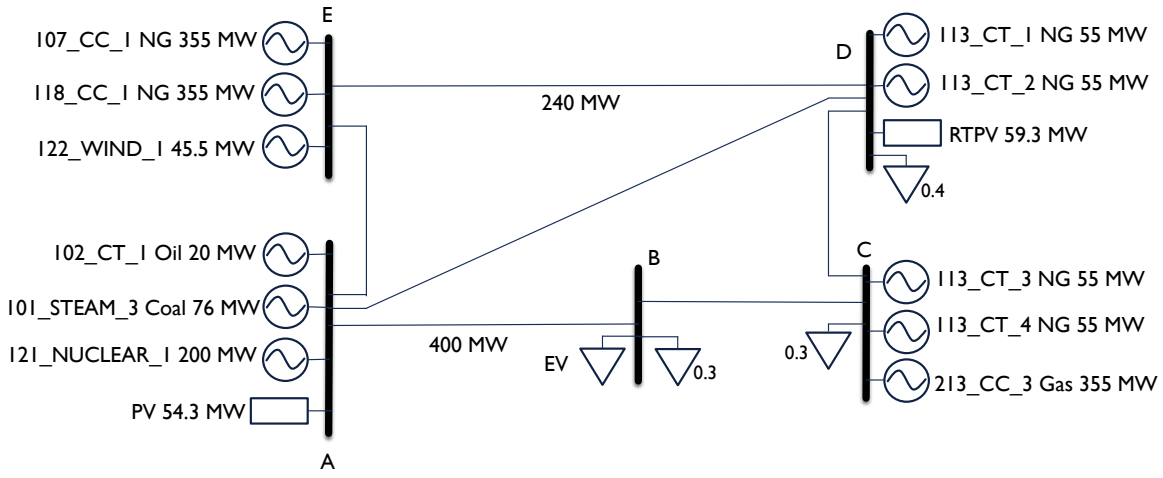

Figure 16. Northern Arizona University (NAU) 5-bus system layout that portrays buses (bold vertical lines), transmission lines (connecting the buses), loads (inverted triangles), and generators (circles and rectangles).

The NAU 5-bus system has an installed generation capacity that is representative of a utility in the southwestern U.S. (see Figure 17). The researchers scaled the load from region 1 of the RTS-GMLC down to 1580 MW and applied it to the NAU 5-bus system. This peak load of 1580 MW matches the peak load in the "Pennsylvania-New Jersey-Maryland (PJM) 5-bus system", from which the NAU 5-bus system drew its inspiration [101]. Similarly, VRE sources were also scaled down from region 1 in the RTS-GMLC to the NAU 5-bus system. The capacity of the generators used in the NAU 5-bus system is shown in Table 6. The time-series data for load and VRE are the actual real-time (RT) of a 1-hour resolution in the RTS-GMLC.

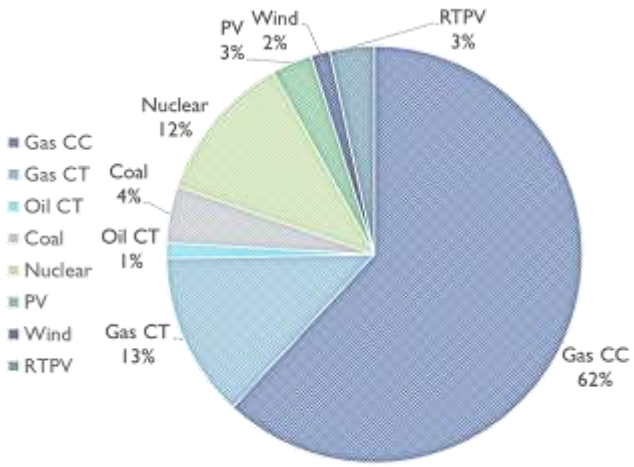

Figure 17. Proportion ratio (%) for the types of generators considered in the NAU 5-bus system (CC = combined cycle; CT = combustion turbine; PV = photovoltaics; RTPV = rooftop PV).

Refer to Table 7 for the load distribution per node in the NAU 5-bus system, which is similar to that of the PJM 5-bus system, except for the additional EV load in node C. A summary of the dispatchable generation fleet of the NAU 5-bus system is presented in Table 8. The prices of various fuels are considered for the year 2025. The transmission parameters for the NAU 5-bus system are the same as those in the PJM 5-bus system [101]

Table 6. Generation capacity per technology and penetration percentage presented in the NAU 5-bus system.

NAU 5-BUS	Capacity (MW)	Percentage (%)
Gas CC	1065	62
Gas CT	220	13
Oil CT	20	1
Coal	76	4
Nuclear	200	12
PV	54	3
Wind	28	2
RTPV	59	3
TOTAL	1722	100

Table 7. Load distribution presented in the NAU 5-bus system.

Node	System load (%)	EV load (%)
A	0%	0%
B	30%	0%
C	30%	100%
D	40%	0%
E	0%	0%

Table 8. Summary of dispatchable generators in the NAU 5-bus system.

Node	Name	Type	Fuel	Fuel[1] (USD/ MMBtu)	Max Dispatch (MW)	Min Dispatch (MW)	Cold Start (USD/ MWh)
E E C	107_CC_1 118_CC_1 213_CC_1	Combined Cycle	Natural Gas	4.2	355	170	30,303
D	102_CT_1	Combustion Turbine	Oil	23.9	20	8	120
A	101_STEAM_3	Steam Turbine	Coal	2.8	76	30	8,600
A	121_NUCLEAR_1	Steam Turbine	Nuclear	0.8	200	198	31,600
D D C C	113_CT_1 113_CT_2 113_CT_3 113_CT_4	Combustion Turbine	Natural Gas	4.2	55	22	6,121

[1]Fuel prices come from the EIA Annual Energy Outlook 2019 Nominal Cost reference year 2025.

1.7.6 Production Cost Model

As mentioned, this research aimed to create models of EV load that are suitable for studying the integration of EVs into power system operations via a power system production cost model. Thus, the time resolution in the models is 1 hour to replicate the day-ahead electricity market integration of EV charging. The objective of the PCM is to minimize the electricity generation cost, subject to a host of

power system constraints. Production costs depend on a variety of factors, including the characteristics of the load and the generation on each node, the capabilities of the interconnecting transmission elements, the reserve requirements, the accuracy of load and VRE forecasts, etc. Consequently, the electricity prices at each node, i.e., the LMPs, often differ from one another. LMPs are an important output from a PCM and are typically higher during the peak load hours and lower during the off-peak hours. Due to the variation in the LMP with the time of day, a price-based charging strategy is a good choice for minimizing operating costs and reducing charging costs.

1.7.6.1 Power System Optimizer (PSO)

An appropriate PCM tool for this research requires capabilities similar to those typical in power system planning and operations. Polaris Systems Optimization's power system optimizer (PSO) is a tool with the capabilities that are necessary for an accurate simulation of power system operations that mimics the actions and timing of power system planners and operators. PSO uses MILP, has multilevel nested time intervals (overlapping time frames), and simulates uncertainties for both load and VRE resource forecasting [91]. An appropriate PCM tool for this research requires capabilities similar to those typical in power system planning and operations. Polaris Systems Optimization's power system optimizer (PSO) is a tool with the capabilities that are necessary for an accurate simulation of power system operations that mimics the actions and timing of power system planners and operators. PSO uses MILP, has multilevel nested time intervals (overlapping time frames), and simulates uncertainties for both load and VRE resource forecasting.

For this simulation, the planning cycle for committing units was a day ahead. It had a collection of horizons consisting of 24 1-hour periods with a look-ahead of 24 h, and the time increment for dispatch (i.e., the period resolution) was hourly. The look-ahead ensures that the commitment decisions in every horizon are related to the expected conditions in the next horizon. The PCM outputs analyzed to show the effect

of the EVs include total production cost (USD), generation (energy produced in megawatt hours; MWh), revenue (USD), and electricity price (LMP, USD/MWh). The revenue (USD) is calculated as the LMP (USD/MWh) times the generation (MWh). Therefore, the EV charging cost is equivalent to the negative of the revenue for the EV load. The model simulated seven days, using RTS-GMLC data from Wednesday 31 January to Tuesday 4 February. Net loads were low at times when the VRE was relatively high. The model run started on Wednesday and finished on Tuesday to ensure that the commitment on Sunday (the day for which analyzed the results) was in accordance with the previous and future power system conditions (i.e., there was sufficient time in advance of Sunday to start the slowest starting coal units). In the NAU 5-bus system on Sunday 2 February, the VRE reached its highest hourly penetration of 18% of the load between 11 a.m. and 1 p.m.

For each time increment of the model data, the "net load" that the conventional, dispatchable generation must serve is found by subtracting the VRE from the load on each bus. During system operation, dispatchable generators are committed and dispatched to serve the net load. The heat curves (heat rates) of the dispatchable generators listed in Table 8 (taken from RTS-GMLC) are multiplied by their fuel costs to calculate the dispatch curves (cost curves), which have units of USD/MWh (refer to Appendix I).

1.7.6.2 EV penetration and modeling

Regarding the quantity of EVs, we tested 1000 EVs. Given the assumed EV characteristics and their availability profile, this represented a maximum possible EV load of 2.8 MW during the morning hours, and about 0.8 MW during the midday hours (refer to Figure 15). This was a small but realistic load penetration compared to the peak load of ~550 MW in the results to be presented in the next section. During periods of low load (e.g., night-time), fewer dispatchable generators will be online. Consequently, it is expected that any VRE or dispatchable load will be a more decisive factor influencing the system operation cost.

Within the PSO, the uncoordinated charging model was implemented as an “injector” with a discrete time series of EV load data points. These data resulted from the uncoordinated model previously described. To apply the coordinated charging model, we employed the built-in library “Energy Limited” (EL) in the PSO. The setup for this library requires an estimate of the amount of energy that needs to be served in a decision horizon (i.e., over the course of a day); this energy can be determined from the total daily energy supplied in the uncoordinated charging model, or by using the fleet’s daily energy consumption or total charging load in MWh. The dispatch constraint for the EVs is their charging availability, which represents the number of vehicles plugged into the grid; this number caps the power that can be drawn from the power network to charge the EVs in any time period (see Figure 15). The EL library ensures that the total amount of the charging load is served, while honoring the EV availability constraints. For a detailed examination of the input data in PSO format (comma-separated values format), refer to the Appendix II.

1.8 Results

This section presents the results of running the PSO production cost model for the NAU 5-bus system for the week of interest. As a representative sample, the results of the simulation are presented for one day, in this case, 22 February, as it had the largest VRE penetration. This section starts by showing the results for the NAU 5-bus system with no EVs, followed by the results when charging 1000 EVs under the uncoordinated and coordinated charging scenarios.

1.8.1 System Operation without EVs

The generation stack and system LMPs for each hour of the day are presented in Figure 18 for a typical day of operation in the period analyzed. The system LMP is represented by the dark dashed line and refers to the scale on the right side of the graph. The LMP varied between 24.6 USD/MWh at low net load, up to 35.4 USD/MWh during the peak load hours. The bars show the generation stack and refer to the scale on the left-hand side of the graph. The nuclear generation is represented by the green color on the bottom

of each column and is the base load generation, which does not vary from hour to hour. The next generator stacked on each bar is the combined cycle (CC) gas generation (light blue color). This represents the marginal generator, and its output varies from hour to hour. Between hours 5 and 17, there was substantial VRE generation, represented by the small bars (dark blue, yellow, and red, respectively) stacked on the top of each bar. Note that the LMP increased and decreased as the CC generation changed, according to its cost curve (Appendix I frame (e)). The LMP followed the expected behavior and had two peaks, one in the early morning and a higher second peak in the early evening. The LMP valley in the middle of the day was a consequence of high solar and wind power that reduced the net load. During this day, the total operation cost was calculated as 359,060 USD, the daily average system LMP was 29.65 USD, and the peak load was 551 MW at 18 h (6 p.m.).

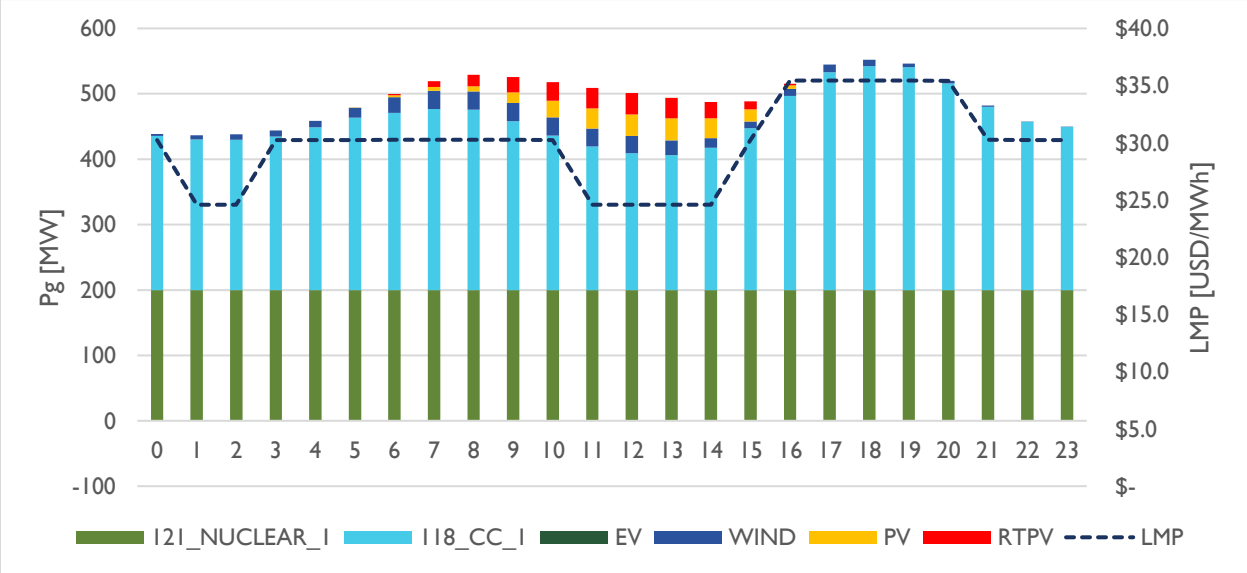

Figure 18. Power generation (Pg) stack MW (left axis) and locational marginal price (LMP) USD/MWh (right axis) in the NAU 5-bus system occurring without EVs.

1.8.2 System Operation with Uncoordinated EV Charging

Applying the uncoordinated charging model scaled to 1000 EVs resulted in the hourly EV load profile shown in Figure 19 Uncoordinated EV charging had a maximum load of just under 1 MW at 20 h (8 p.m.),

with a base load of just over 0.2 MW. The total energy consumed over the course of the day in charging the EVs was 10.75 MWh. The uncoordinated charging profile followed the trend of the EV arrivals (Figure 12 b), peaking in the early evening, as 85% of the charging happened at home

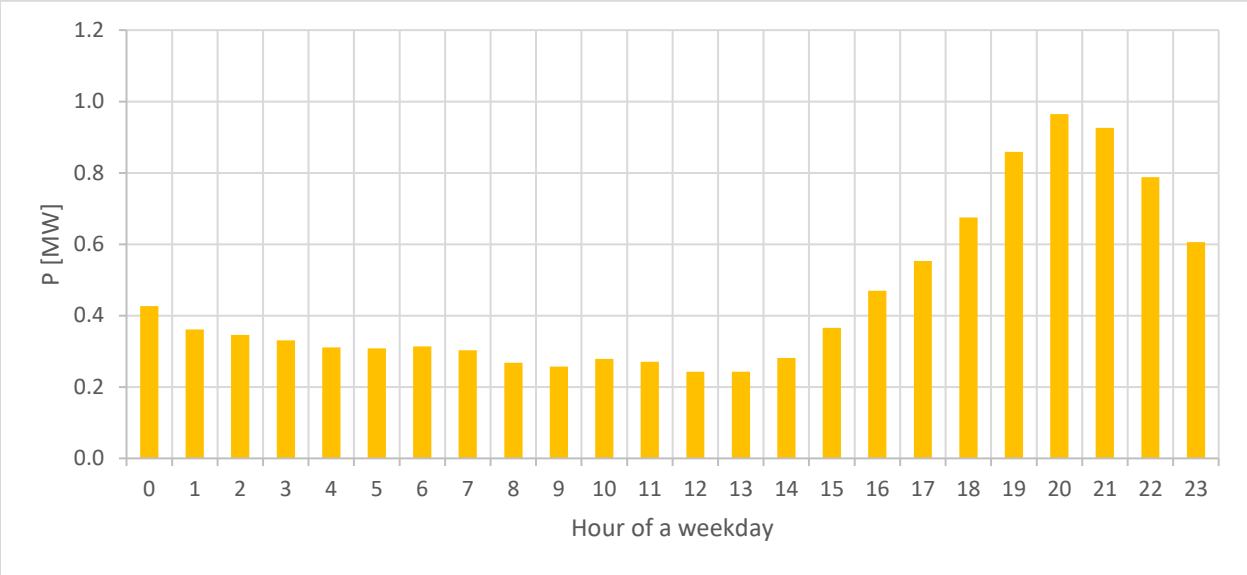

Figure 19. Uncoordinated EV charging power (P) profile in MW developed for 1000 EVs.

Running the PCM PSO for the NAU 5-bus system with the addition of the EV load resulted in an operating cost of 359,390 USD (an increase of only 330 USD). In addition, the system LMP did not change; the system dispatch stack and LMP are similar to those shown in Figure 18 because the EV charging profile was small compared with the rest of the injectors.

1.8.3 System operation with Coordinated EV Charging

Implementing the coordinated charging modeling in the PSO resulted in the daily charging profile shown in Figure 20. Recall that the coordinated charging model used the LMP in combination with EV availability and battery SoC in determining the time to charge as part of the goal to minimize operating costs over the course of a day. Compared with the uncoordinated charging profile (Figure 19), most of the EV charging was moved to the low-LMP hours of the day (hours 1, 2, and 11 to 14). The total daily energy used in

charging was the same as in the uncoordinated case (10.75 MWh), but the charging timing was shifted in a way that complied with EV charging availability, battery SoC, and daily charging requirement.

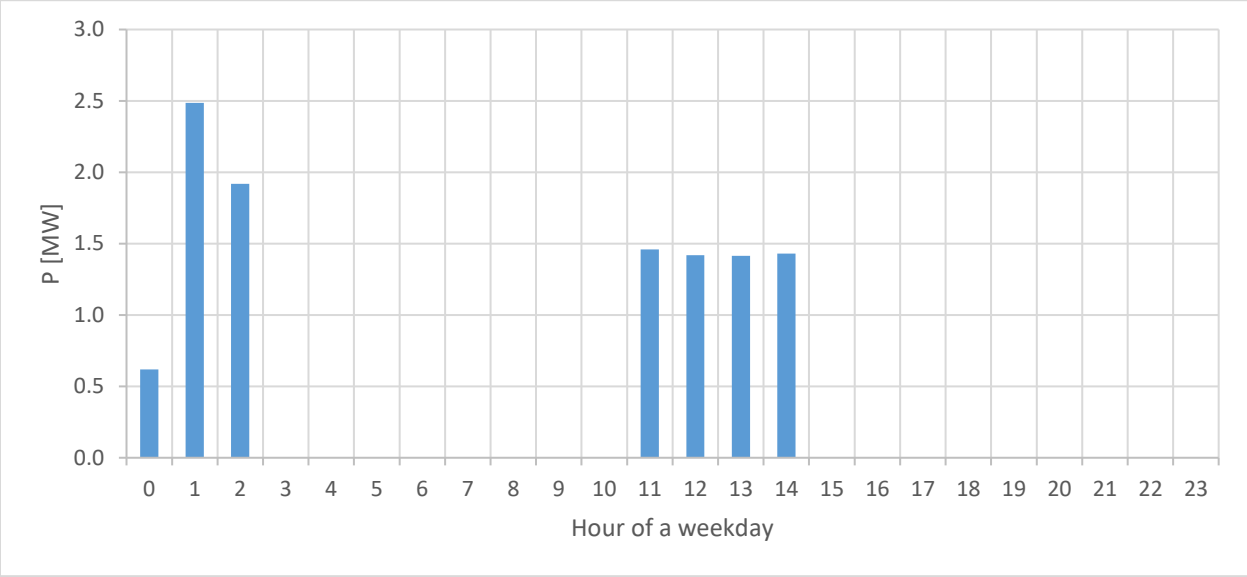

Figure 20. Coordinated EV charging power (P) profile in MW developed for 1000 EVs.

In the case of coordinated charging, Figure 21 shows the generation stack and LMPs. The system operation cost for the day was 359,330 USD. Relative to the plot shown in Figure 18 the system LMP increased between 1 a.m. and 2 a.m., which means that as the marginal generator increased its power dispatch due to the EV load, it increased a step in its cost curve. Figure 22 directly compares this point, plotting the EV charging profiles and the system LMPs. Regardless of this increase in LMP, the overall production cost was less than for the case of uncoordinated charging, as the charging occurred during the lower-cost (i.e., lower LMP) hours during the day.

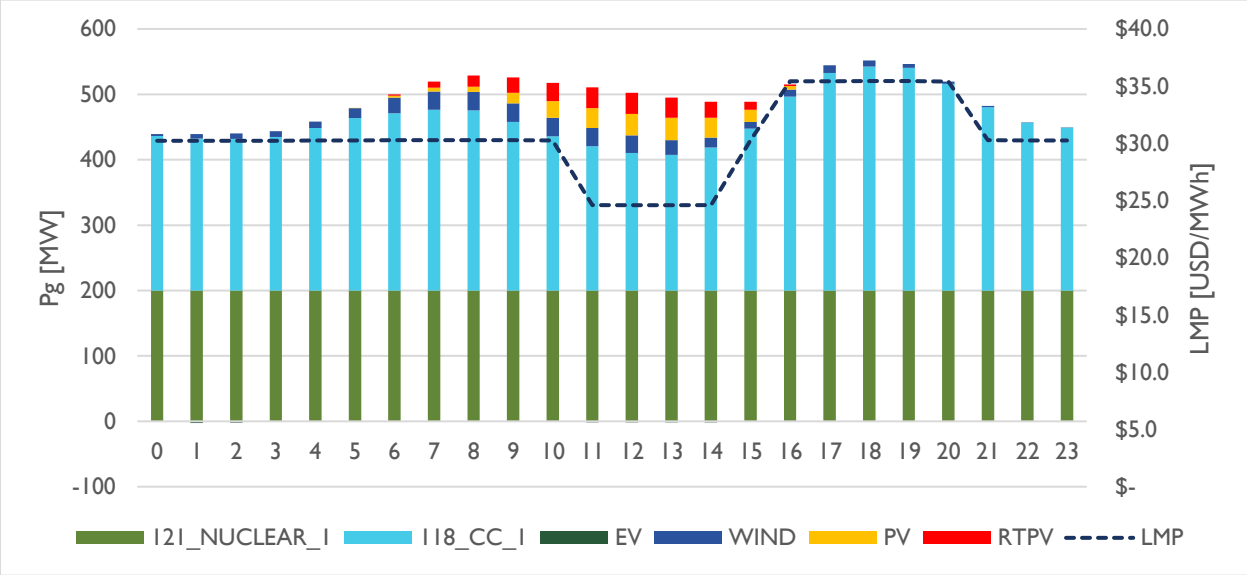

Figure 21. Power generation (Pg) stack MW (left axis) and LMP USD/MWh (right axis) in the NAU 5-bus system occurring with coordinated EV charging.

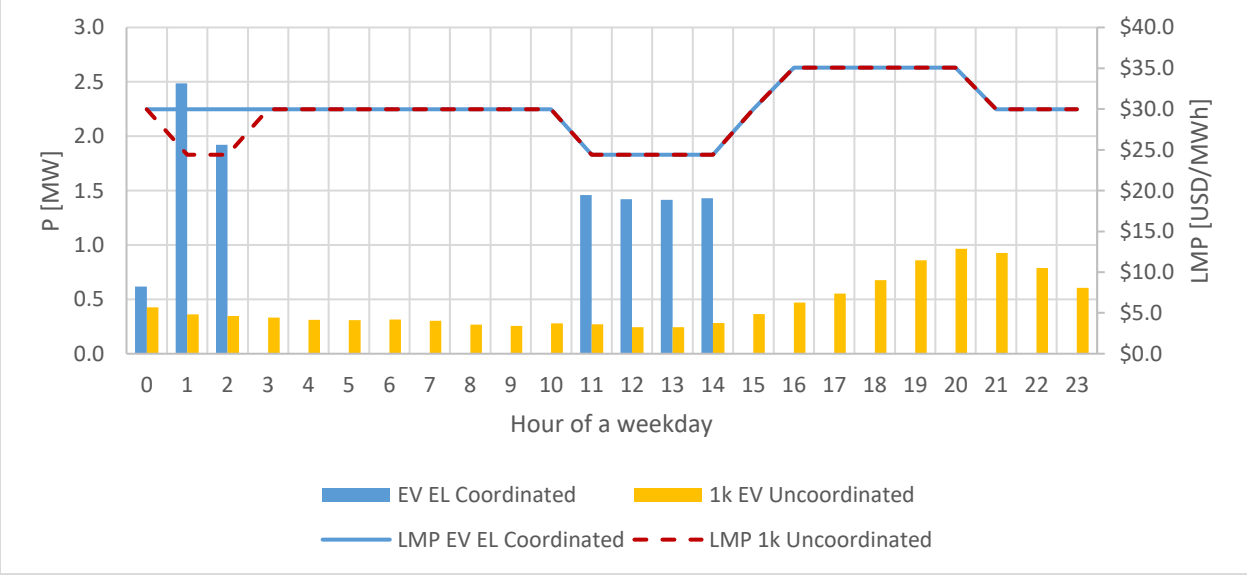

Figure 22 Comparison of the EV coordinated and EV uncoordinated charging profile power (P) in MW (left axis) and their corresponding system LMPs in USD/MWh (right axis).

1.8.4 Comparing the EV Cost of Charging

The cost to charge the EVs was determined by multiplying the magnitude of energy used to charge the EVs each hour by the LMP that hour. The total cost to charge was then computed by summing the hourly charging costs over all hours of the day. The uncoordinated charging approach led to a cost to charge of 334 USD, while the coordinated charging cost was 294 USD (see Figure 23). Using the coordinated charging approach reduced the cost of charging by 40 USD, equal to 12%. Interestingly, the system production cost decreased by 60 USD between the uncoordinated and coordinated cases, which was slightly different from the reduction in cost to a charge of 40 USD. This phenomenon is due to the coordinated EV charging profile changing the LMP in the early morning hours. Putting the charging numbers into a per vehicle context, the average EV will charge 10.75 kWh. The average uncoordinated charging cost was close to 0.33 USD per day per vehicle, and the coordinated charging cost was close to 0.29 USD, representing roughly 12% in savings. These numbers are representative of the low energy cost experienced by EV owners.

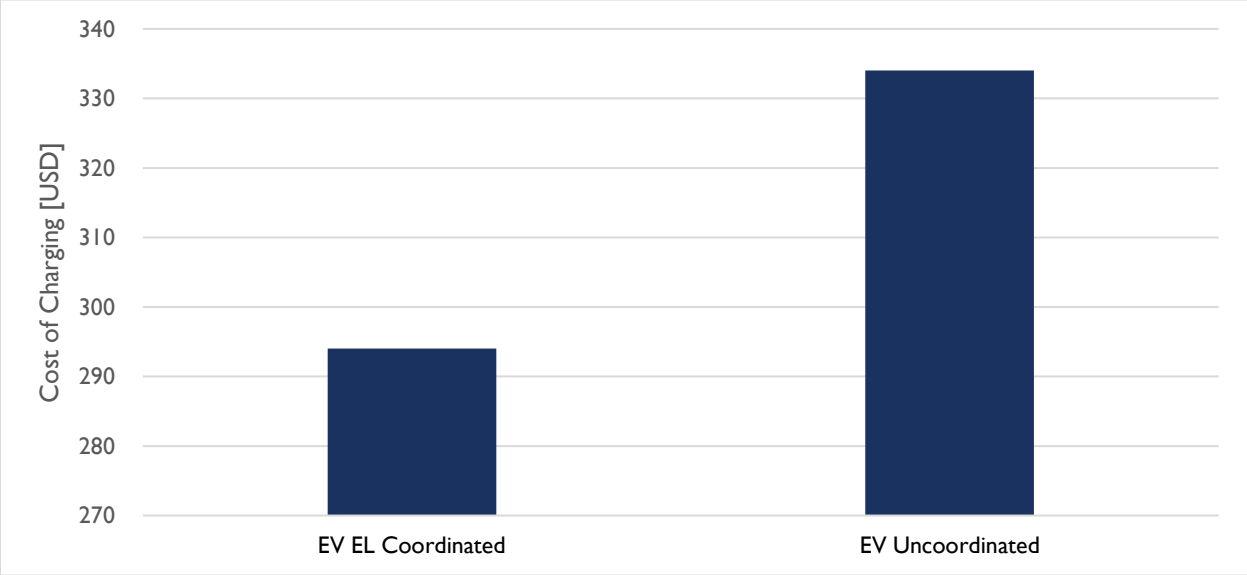

Figure 23. Comparison between the coordinated and uncoordinated cost in USD of EV charging for 1000 EVs .

1.9 Discussion

Figure 24 shows a graph of the system and the EV loads for the day of 2 February, the same day as is presented in the previous figures with the dispatch stacks. The system load is shown by the light-blue bars (refers to the left-hand scale), and the EV load in the red (coordinated) and yellow (uncoordinated) bars, both referring to the right-hand scale and having a much lower magnitude than the system load. Compared to the system load alone, the uncoordinated EV charging increased the system's peak load. In our particular simulation, 1000 EVs led to an increase in peak demand of 1 MW. Coordinated EV charging occurred during low-LMP hours and therefore did not increase the peak load.

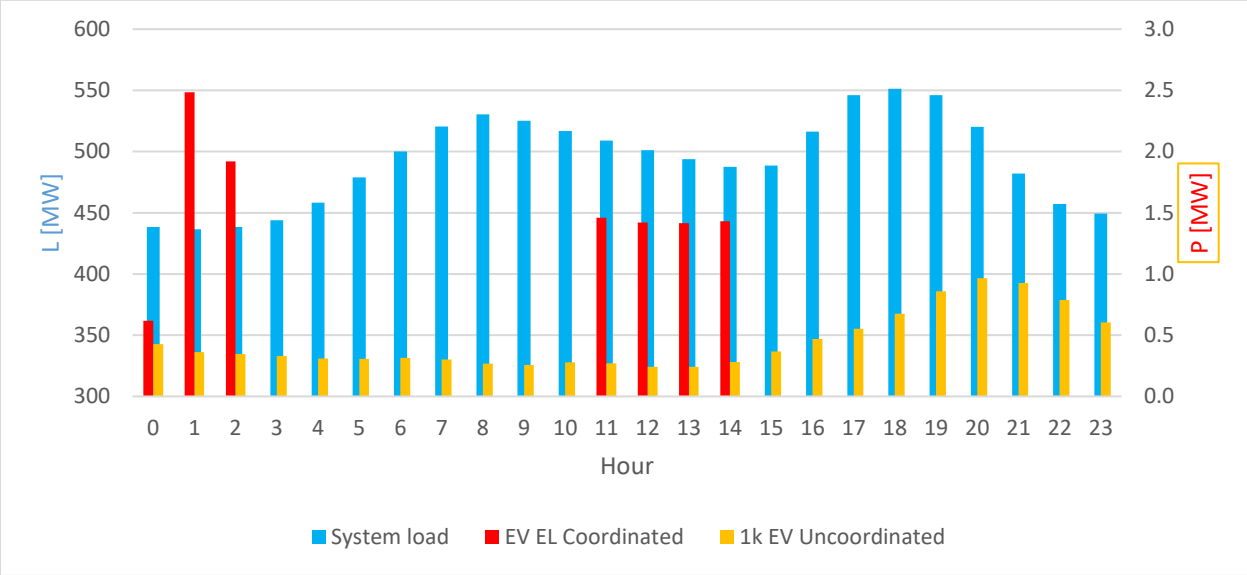

Figure 24. Comparison of the system load (L) in MW (left axis) against the EV coordinated and EV uncoordinated charging power (P) profiles (right axis) of 1000 EVs.

It is interesting to compare operating costs and LMPs for each of the cases. In

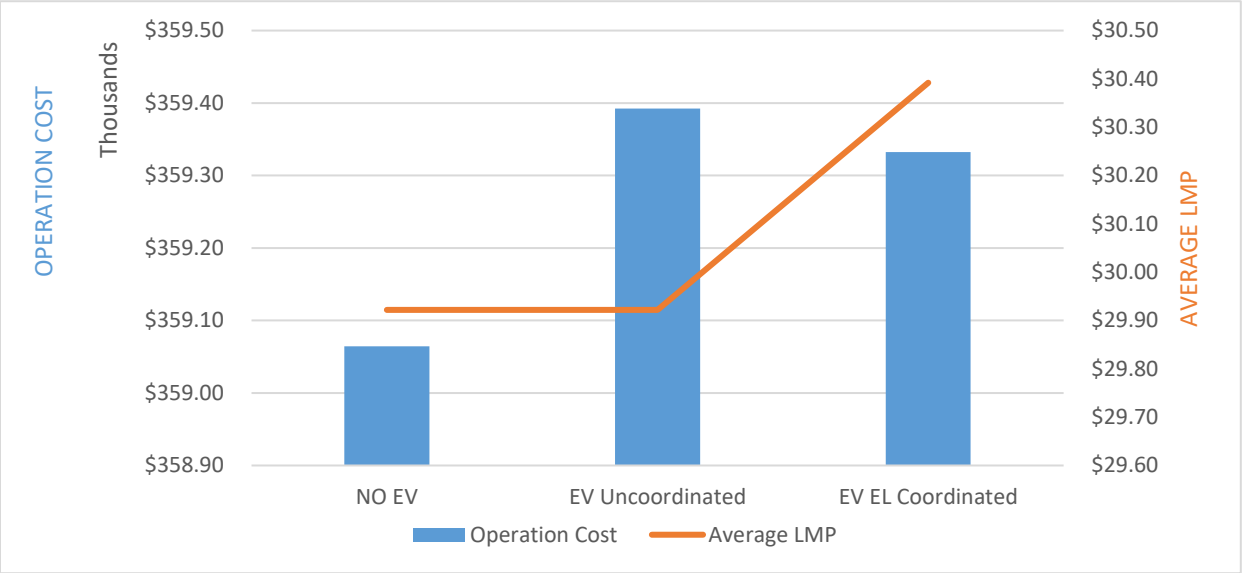

Figure *25*, the operation cost is shown in the blue columns associated with the primary *y* axis on the left. In addition, in

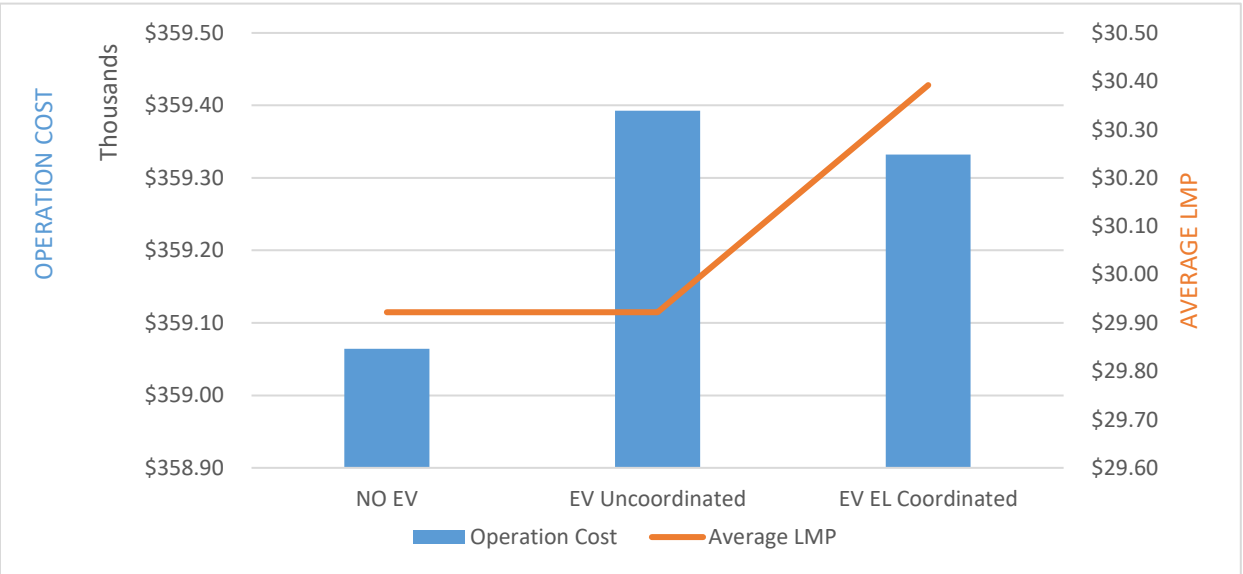

Figure *25*, the average LMP is shown by the orange line related to the secondary *y* axis on the right. In this figure, the left column is for the system operation with no EV with a cost of 359,060 USD, the central column is for the system operation with uncoordinated EV charging with a cost of 359,390 USD, and the

right column is for the system operation with coordinated EV charging with a cost of 359,330 USD. Thus, as shown by comparing the central and right columns with the left one, the addition of the EV load increased the system operation cost. However, the EV coordinated charging profile (right blue column) led to lower operating costs than the uncoordinated charging profile (central column). At the same time, the daily average LMP increased slightly (in 0.47 USD) with coordinated charging (right line). This is not uncommon in power system operation; average LMPs can increase while system operating costs decrease.

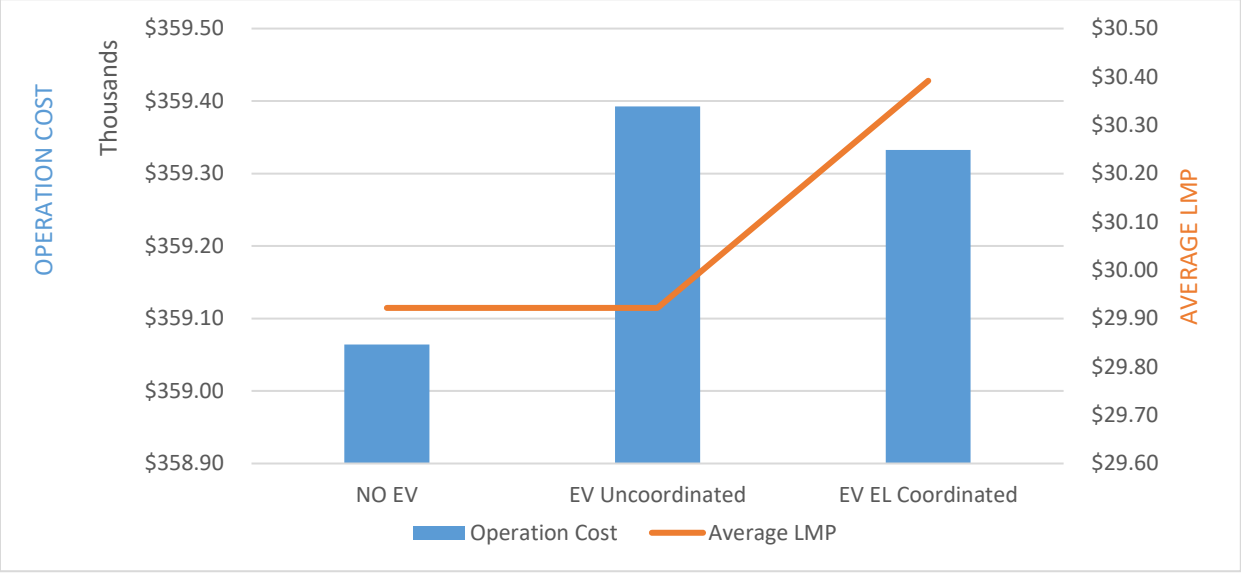

Figure 25. Summary of the system operation cost and LMP change with the introduction of EV charging, gross comparison against the system with no EVs.

1.10 Conclusions

The purpose of this work was to create statistical models for EV charging that were suitable for power system operation. Statistical models for EV charging were created using data from the EV Project. This modeling with the appropriate data resulted in reasonable and scalable EV charging load profiles. The

models recognized coordinated and uncoordinated charging loads. A production cost model could integrate the EV charging model and assess the EV effects on the power system cost and loads.

The modeling of uncoordinated and coordinated charging profiles required the battery size and charging level (power kW). In addition, the arrival time and planned energy consumption were necessary (i.e., the initial and final SoC). However, for coordinated charging, both the arrival and departure, or the equivalent availability, plus the energy or charging requirement (MWh) for the whole fleet were required.

Statistical modeling recreated the uncoordinated charging profile. A Monte Carlo simulation technique modeled the uncoordinated charging profile of each vehicle by sampling the initial SoC, final SoC, charging level, and arrival time as the start time of charging. The fleet charging profile was the sum of the individual charging profiles. The statistical analysis chi-square method was used to find the best fit distribution for the initial and final SoC. The best fit for the initial SoC was a beta distribution, and two beta distributions for the final SoC. The least-mean-square method provided the beta parameters to fit the data to beta distributions.

The authors developed an algorithm for modeling the uncoordinated charging and incorporated the result into the PCM model as a time series, similar to the load forecast or VRE forecast. However, coordinated charging modeling must be part of the PCM and modeled as a controllable load with the constraints imposed by the fleet characteristics, energy requirement (MWh), charging availability, and charging level (kW). Otherwise, the modeling will neglect the influence of the EV fleet on the electricity price.

The NAU 5-bus system, a simple 5-bus power system similar to the PJM 5-bus model but with time-series data from the RTS-GMLC model, was created to test the statistical models of the EVs. Polaris Systems Optimization's PSO was the PCM used for this demonstration, and it showed the potential effects of 1000 EVs (maximum demand of ~0.2% of the NAU 5-bus peak load) on power system operating costs, LMPs,

and dispatch stacks when implementing the two charging strategies mentioned above. The demonstration showed interesting results, and revealed the potential positive or negative effects of EVs on system operation. Coordinated charging exemplified the positive effects of accommodating EV charging coincident with VRE. However, uncoordinated charging demonstrated the negative effect of increasing the system peak load. With scalable statistical models of EVs, such as those presented here, it is possible to investigate the impact of charging strategies for the large-scale adoption of EVs on power system operations and costs.

Chapter Four: Power System Impacts of Electric Vehicle Charging Strategies

Preface

This chapter is under review for publication in the Electricity journal. In detail, this journal expands the EV modeling from the previous chapter in a power system with a larger footprint, three regions, a broader generation mix, and exceptionally high penetration of VRE.

Abstract

This article explores the potential impacts of integrating electric vehicles (EVs) and variable renewable energies (VRE) on power system operation. EV penetration scenarios of the light-duty vehicle fleet of 10%, 20%, and 30% are considered in the RTS-GMLC test system. RTS-GMLC is an updated version of the IEEE RTS-96 test system, allowing for modern inter-hour or real-time market modeling; it has a generation fleet with characteristics comparable to current power systems used in the western United States, and VRE penetration equal to 34% of annual energy consumption. The impacts of EVs are investigated during the annual peak in the summer and during four weeks of the year in which high VRE combined with low loads lead to overgeneration. Uncoordinated and coordinated EV charging scenarios are considered. In the uncoordinated scenario, charging is undertaken at the convenience of the EV owners, and this is modeled using data from the Idaho National Laboratory's EV Project. Coordinated charging is modeled using an "aggregator" model, wherein EV charging is scheduled to minimize operating costs while meeting the daily charging requirements subject to EV availability and charging constraints. To capture the impacts, the production cost model (PCM) Power System Optimizer (PSO), created by Polaris, is employed. The model uses load and VRE forecasts as part of a multiple-planning cycle rolling horizon approach to commit realistic generating units based on their start-up characteristics, while preserving the flexibility of units with short start-up times and EV charging. At each EV penetration level, the uncoordinated charging costs were higher than the coordinated ones. At 10% EV penetration, the uncoordinated charging cost per

vehicle was four times higher than with coordinated charging during a low load week in February. During a high-VRE, low-load week in April, with uncoordinated EV charging at 30% penetration (3% energy penetration), the peak load increased as much as 27%. Using coordinated EV charging, the EV load shifts to hours with low prices, coincident with either low load, high VRE, or both. Furthermore, coordinated charging reduces the curtailment of PV by as much as nine times during the winter operation season, and the curtailment of wind generation by more than half during the summer operation season, compared to the scenarios with no EVs and uncoordinated EV charging. Using multiple planning cycles, load and VRE forecasts, and a "look ahead" period during scheduling and dispatching, units were judged to be important in creating and utilizing the flexibility of coordinated EV charging.

1.11 Introduction

Climate change has driven many governments and organizations to set aggressive clean energy goals, seeking to achieve significant reductions in carbon emissions by 2035 and to achieve carbon neutrality by mid-century; e.g., Hawaii's 100% clean energy standard, California's standard [102], the European Union [103], and organizations such as Google[104], Walmart [105], Amazon [106], etc.. In the electrical supply system, decarbonization will be centered upon renewable energy resources, primarily wind and solar due to their low costs [107], but also nuclear power, energy storage, dynamic and controllable loads, and market innovations [108][109]. In 2020, the U.S. Energy Information Agency (EIA) reported that 36% percent of CO_2 emissions were due to the transportation sector [110]. Consequently, for decarbonization to occur, the transportation sector must decarbonize.

Potential paths to decarbonize transportation include carbon neutral biofuels, hydrogen fuel cells, and electric vehicles (EVs), among others. For vehicle transportation, EVs are the most likely path to decarbonization. According to the U.S. National Renewable Energy Laboratory (NREL), the levelized cost of driving (LCOD), with no tax credits or incentives, for some conventional vehicles and EVs have been the

same since 2021 [86]. For example, the estimated cost of driving after eight years is the same between a Tesla Model 3 Standard Range and a Toyota Camry XLE [88]. One of the most important drivers in the cost of a modern EV is the battery pack, which may account for up to 40% of the cost [111]. In 2020, on a per unit energy basis, battery packs cost USD 137/kWh, representing a reduction of 89% from 2010 to 2020 [65], and further decreases are expected. Thus, it is likely that EVs will represent a larger share of the car fleet soon. Sales continues on rise, in 2021 the EV sales worldwide doubles from 2020 numbers achieving more than 6% market share [112], while in USA the sales doubles from 2020 numbers but the market share was only 4% [113]. Some have projected that 75% of the sales of light-duty vehicles will be electric in 2050 [89].

Automakers have committed to transitioning their fleets from internal combustion vehicles to EVs over the coming decades [114]. Given that the electricity sector is on a path to decarbonize, EVs will eventually derive their energy from carbon-free resources. Because of their ability to use carbon-free energy and due to their good performance and low operating costs, wide-scale adoption of EVs is expected as they achieve first-cost price parity with conventional internal combustion vehicles, which is expected to occur later this decade [111][115].

The transition from internal combustion engines to electric drives in the transportation sector will lead to an increase in power demand in the electric sector [66]. In doing so, it is crucial to avoid increases in the peak load and to maintain affordable electricity [27]. For example, there is evidence that the uncoordinated charging of EVs can increase the peak load, or possibly introduce a second peak during off-peak hours [68]. However, if it is coordinated, EV charging can also enhance the penetration of variable renewable energy such as wind and solar power, [67].

Recent work on the topic of integrating EVs has analyzed the effects of EVs when their charging is included in day ahead (DA) market by using a production cost model (PCM) [116-118]. The work by Szinai et al. [116] performed monthly simulations of power system operations for a whole year. EV modeling comes from a bottom up analysis, in which a portion is flexible (coordinated) and the rest is inflexible (uncoordinated). Their model represents the U.S. Western Interconnection zonally and focuses on California in 2025 assuming an EV fleet ranging from 0.95 to 5 million cars. Their model neglects intraday commitments, i.e., models only the Day-Ahead (DA) market. In this simplified transmission system, EV flexible charging is modeled as an electric storage unit. The modeling assumes storage is full at the beginning of each month (horizon), and the model load is shifted by not charging at peak hours and charging at times with low electricity prices. The monthly energy requirement (battery size in MWh) value returns to its original SOC (full charged) at the beginning of each month. Their main conclusion is that charging of the EV fleet (flexible and inflexible) increases the total power system operation cost by up to 10% (690 million USD), but it also reduces the VRE curtailment up to 40% annually. The study also found that utilizing TOU rates instead of flexible charging led to a similar production cost but does not provide curtailment reductions. Mowry and Mallapragada [117] focused on highway fast charging which has a high power requirement and are modeled as an inflexible load (uncoordinated charging) along intercity highways in the ERCOT power system in 2033. The central case evaluated an EV fleet of 3 million LDVs, with low and high scenarios of 1.5 to 4.5 million LDVs. They used a grid operation model (PCM) but with major simplifications, neglecting the procurement of reserves, and no intraday reschedule of the thermal generation fleet in the power system. The DC fast charging station in the modeling assuming on site electric battery storage units (lithium batteries). Demand flexibility (coordinated charging) in their work was up to 20 percent of the charging load and within a narrow window of 1 h. They concluded that 3 million EVs will increase the annual power system operation cost by 8%, or the equivalent of 2 USD per MWh served. In addition, based on their assumption that the EV load is inflexible and at the best case can

be flexible only within an hour window, the use of a 4 h battery at the fast charging stations are effective in reducing the price spikes due to vehicle charging. Alvarez Guerrero et al. [118] considered how to model EV charging for use in a PCM of power system operation. This work modeled the EV load assuming uncoordinated and coordinated charging models subject to the constraints of EV availability for charging, state-of-charge, and energy charging requirements. Their model incorporated EV charging constraints directly into the PCM, thus accounting for EV charging flexibility, contrary to the work of [116] that used a storage device . Additionally, the model in [118] provides a single optimization inside the PCM for the sake of EV flexible charging without the iterative process between two optimization tools [117]. In addition, the work [118] considered all types of charging levels, employing no additional storage devices. Thus, in [118], cost savings associate with coordinated charging can be directly compared to the same fleet's uncoordinated charging cost.

This article will report use the modeling approach of [118], but expands the method to include multiple planning horizons from a week-ahead to real-time. Thus, the modeling includes commitment decisions of a real power system in which some thermal units have a start time greater than a day, and intraday reschedule of combined-cycle and fast resources like combustion turbines that deal with forecast errors of VRE in the real-time (RT) market. In the RT market, all the commitments are final. The system operator dispatches generators based on actual weather conditions; only then can it calculate all the expenses involved in running the power system. By including forecast errors, the model is able to capture the costs associated with handling such errors. The total costs in [116][117] are underestimated because their models do not compensate for the differences between the DA forecast and the actual RT conditions. Therefore, the modeling approach in this article simulates power system operation and total costs more realistically.

The purpose of the work presented in this article is to present a power system production cost model that incorporates the full range of timing for unit commitment decisions (from week ahead to RT), in a power system that integrates the high penetration of electric vehicles (EVs) and variable renewable energies (VRE). Thus, this work targets the following specific research questions:

- What are impacts of uncoordinated and coordinated EV charging strategies in power system operation, peak loads, and cost?
- What are the combined impacts of a high-penetration EVs and VRE on power system loads, operation, and cost, when considering both uncoordinated and coordinated EV charging models? How do the two models of EV charging influence the integration of high-penetration solar and wind power, for example as related to curtailment of VRE?

Specific results relevant to answering the research questions will include power system operation cost; electricity locational marginal price (LMP); EVs charging costs; changes to the generation stack and changes in the peak load; and curtailment of VRE. This work starts by describing the magnitude of EV penetration and electrical load to be studied. Following this, the modeling tool and power system to be tested are laid out. After that, a description of the cases to be examined is given, followed by the results, discussion and conclusions.

1.12 Penetration levels of EVs

In 2020, EV penetration into the light-duty vehicle fleet in the U.S. was 2%, equivalent to 1.7 million EVs [119]. This number is small; however, EV sales are experiencing continuous growth, and from 2011 to 2017, the average grew sales rate was 49% [120]. Sales growth rate was 80% in 2018[121]. In USA during 2021 the EV sales doubles from 2020 numbers achieving a LDV market share of 4% [113]. Subsequently, higher levels of penetration are expected. For example, in California, zero-emission vehicles (ZEV)

regulation requires a minimum number of EV sales, which should reach 22% of the LDV sales by 2025 [122] (a ZEV is a vehicle with no pollutant or greenhouse gas emissions). This mandate is established by the California Executive Order that requires up to 1.5 million ZEV by 2025 [123]. A study by the National Renewable Energy Laboratory (NREL) suggested that under a scenario of high policy support for consumer adoption, up to 84% of the light-duty vehicle (LDV) fleet can be made EV by 2050, and 20% LDV by 2030 [16]. Furthermore, the International Renewable Energy Association (IRENA) estimates that 30% of the worldwide vehicle fleet will be made electric by 2030 [4]. The International Energy Agency (IEA) suggested in its Global Energy Outlook that 10% of the vehicle fleet could be made electric by 2030 [124]. Based upon these forecasts, this work investigates the impacts of light-duty EV penetration scenarios of 10%, 20% and 30%.

1.13 Production Cost Model

A power system production cost model (PCM) seeks to simulate the planning and decisions made in power system operation, while minimizing the operation costs subject to physical and security constraints [31]. To do this requires a model of the power system's generation, transmission, and load characteristics and constraints, and an optimization program designed to mimic power system operation. The modeling tool used in this research is the PCM Power System Optimizer (PSO), created by Polaris [91]. PSO was selected for its following abilities:

- Multi-timescale modeling, enabling unit commitment (UC) decisions at several time intervals, beginning several days ahead (for slow-start generation units) with an hourly resolution, to real-time (RT) economic dispatch (ED) with a five-minute resolution;
- Capacity to represent power system operations and reserve procurement similar to actual power systems, from vertically integrated utilities to independent system operators;

- The ability to represent demand response and storage in order to assess resource value under different market and operation conditions.

PSO can replicate the decision cycles that utilities and ISOs employ for power systems and market operation with the high fidelity necessary to study the integration of EVs.

1.14 Description of RTS-GMLC Power System

To test the new methods and techniques used in system operation and control, the IEEE has provided power system reference models to evaluate reliability and system operation metrics, constituting a reliability test system (RTS). An RTS offers a full description (dataset or model) of the load, the generation fleet, and the transmission network layout [30], and thus enables the study of the economics of power systems while adhering to the transmission and operational constraints. Thus, by using a PCM in modeling the operation of an RTS, it is possible to investigate the impacts of different operational practices, forecasts, generation and transmission resources, load, reserve margins, etc., enabling the calculation of outputs such as the system operating cost and the locational marginal prices (LMPs) of the electricity (USD/MWh) [101]. The RTS-GMLC (Grid Modernization Laboratory Consortium) system was selected in addressing this study's research questions and will be described below.

The original RTS of the IEEE was introduced in 1979 (RTS-79), and consisted of 24 buses connected via a transmission layout [30]. The RTS-79 was modified in 1986 (RTS-86) with an upgrade of the generation data. In 1996, RTS-96 was created by modifying RTS-79 to include different types of generators and a more complex transmission layout. This update created a broader system that enabled multi-area analysis to simulate interregional transactions, such as those between utilities or balancing authorities. A recent update of the RTS-96 system was given by the U.S. National Renewable Energy Laboratory on behalf of a consortium of U.S. Department of Energy laboratories [100]. The updated model is named RTS-GMLC, with GMLC standing for “Grid Modernization Lab Consortium.” The GMLC version allows for modeling

modern inter-hour or real-time markets by increasing the time resolution from hourly to every 5 minutes, and by extending the data to cover a whole year. This new update considers additional transmission congestion caused by removing some transmission lines and reducing some of their rated capacities. Furthermore, the RTS-GMLC includes a new generation mix by replacing outdated oil and coal generators with natural gas combustion turbines (NG-CT) and natural gas combined cycles (NG-CC). The RTS-GMLC does not represent any actual transmission system, but does represent the characteristics of many real systems. In its basic setup, the RTS-GMLC was created to possess characteristics similar to those of the southwest U.S.; its power demand, VRE resources, and hydro profiles mirror those of this region. Thus, the RTS-GMLC with scaled data can be generally be interpreted to represent the characteristics of following three regions: Region 3 is the Los Angeles Department of Water and Power (LADWP), Region 2 is Nevada Energy (NEV), and Region 1 is Arizona Public Service (APS). The RTS-GMLC load data were drawn from a low-carbon grid study (LCGS), in which the day ahead (DA) forecast was hourly, and the real-time (RT) dispatch data had a five-minute resolution [48]. The VRE in the RTS-GMLC was derived from the Western Wind and Solar Integration Study Phase 2 (WWSIS-II) [125]. Both load and VRE datasets, plus all the parameters that define the RTS-GMLC, are publicly available in a repository [99]. The VRE penetration into RTS-GMLC is 34% of the annual energy demand and is thus relatively high. As a reference, we employed the existing Renewable Portfolio Standards (RPS's), which prescribe the minimum renewable energy generation for California, Nevada, and Arizona, at 33%, 25%, and 15%, respectively [126]. In the RTS-GMLC, the peak power is about 8.2 GW, and the total conventional generation fleet's capacity is close to 9.1 GW. Traditional generation is categorized by groups that aggregate units with the same capacity, fuel, and constraint characteristics. The VRE is composed of 1.55 GW of utility-scale solar photovoltaic (PV), 1.16 GW of rooftop solar photovoltaic (RTPV), and 2.51 GW wind. Figure 26 summarizes the generation capacity of the system, with a column for every region, and the height of each column illustrates the capacity in MW. In this figure, every column is composed of stacked sections representing

the penetration per technology, as indicated by the legend on the right of the figure, with the fuels and technologies stacked in the following order shown in the legend. Note that the proportion of generation is different in every region: Region 1 is the only one displaying nuclear generation; Region 2 shows no wind generation; and most of the VRE in Regions 1 and 3. The lower dashed line shows the peak demand per region, and the upper dashed line shows the total system peak demand. The constraint characteristics of the conventional generation fleet in this dataset include ramp rate (MW/min), start time (h), shutdown time (h), minimum up- and down-time (h), and start-up heat (MMBtu). Refer to Appendix III **Error! Reference source not found.**for a summary of the characteristics of the thermal generator in the RTS-GMLC dataset.

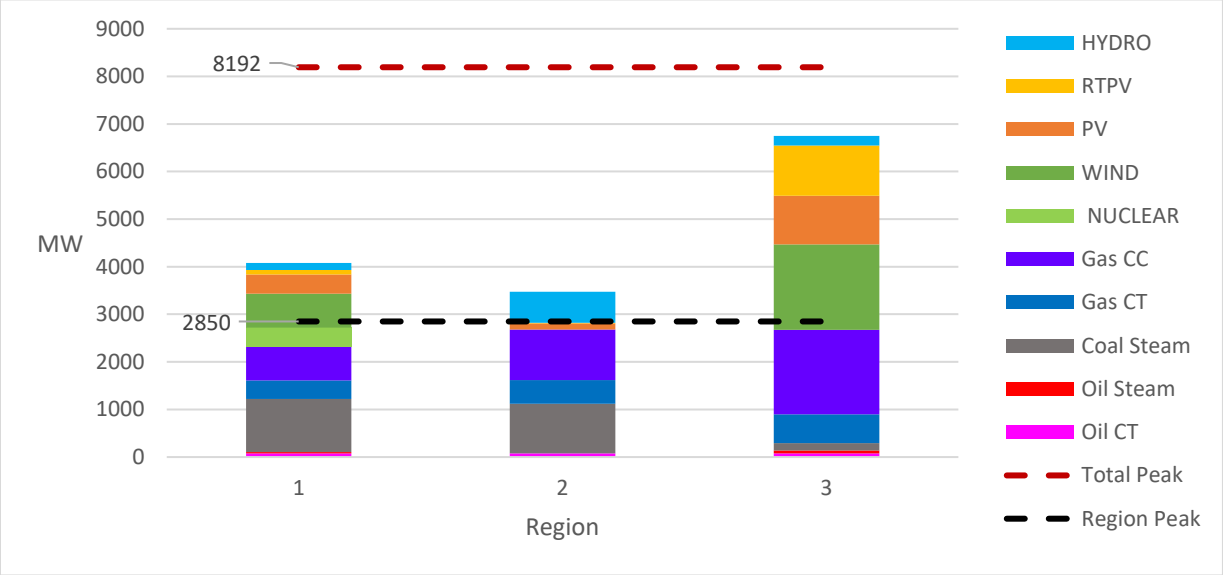

Figure 26. Installed capacity in MW per region in the RTS-GMLC. The peak load per region is the same at 2,850 MW and is shown by the lower dashed line, with a total peak load of 8.2 GW shown by the upper dashed line, with at total installed capacity of 14.3 GW.

1.14.1 Commitment Decisions and Multicycle Rolling Planning Horizons

The constraint parameters of conventional generation in the RTS-GMLC lead to the selection of the modeling cycles. The slow-start coal units have start-up times of 96 hours and 60 hours, and therefore fit into a weekly decision cycle, which we call week ahead (WA). The nuclear generator is always committed

in the WA since its startup time is very long and therefore it is always committed. Some coal and oil units have a 12 h start-up time, and consequently the units are committed in the day ahead (DA) cycle. Natural gas combined cycle units have a start-up time of 2 hours, and therefore fit into a four-hour ahead (4HA) decision cycle. Natural gas combustion turbines have a start-up time of 1 hour, and therefore are committed in the ahead (HA) cycle. Finally, hydro and VRE generators (PV, RTPV, and Wind groups) operate in the real time (RT) cycle which is the trading hour. Forecasts for load and VRE generation are used in each cycle's commitment optimization. Those units with short startup times are selected and planned for in each optimization cycle, but are not irrevocably committed until necessary.

The previous discussion of the commitment timeframe provides the basis for a multicycle rolling horizon model. In PSO, multiple decision horizons are used to mimic the multiple timeframes used to commit units. The first cycle is called a System Cycle (SC), or Security Analysis, and it approximates the transmission network's power flow and sets a preliminary commitment schedule that is sufficient to ensure reliability. The time resolution in the SC cycle is hourly on every day, and preliminary decisions are made 112 h (4.7 days) in advance. The next horizon is what will be hereafter called the week ahead (WA) cycle, in which slow coal units (start-up time longer than 12 h) are committed; decisions here are made using data with an hourly time resolution and are completed 109 h (4.54 days) in advance. The next cycle is the DA cycle, which uses hourly data and commits steam units with a start-up time of 12 hours. The next decision cycle is the 4HA cycle, which commits CC generators with a two-hour start-up time. Decisions are finalized for these units four hours in advance. The last decision cycle is the HA cycle, which commits CT units with a start-up time of one hour; decisions are finalized for these units one hour in advance. The final layer in the multi-cycle model is the RT cycle, in which the VRE in incorporated and the rest of the generators are dispatched. The schedule is finalized 15 minutes in advance, and RT decisions are made every 15 minutes.

Figure 27 presents the rolling horizon multicycle model described above and implemented in PSO. Each of the decision cycles mentioned are represented in the six sets of horizontal bars shown in the figure, starting with the longest lead-time cycles on the top and moving downwards toward RT. For example, the SA cycle is represented by the top set of two horizontal bars, which represent the SA decision cycle over two successive horizons. The gray segments of these bars represent a look-ahead period of six additional days for which the predicted load is taken into consideration by PSO when committing units. Thus, commitment of long-start units takes into account predicted future conditions. The green segments on the left end of these lines are broken into 24 hourly periods which are represented by the smaller green blocks indicating the hourly resolution of the data and forecasted load in the SA commitment. The look-ahead for each cycle ensures that each planning horizon's decisions take into consideration the conditions expected in the following time periods. For example, if the load forecast indicates a large change in load at the beginning of the next period, then the units committed must be able to meet that load change. The WA, DA and 4HA cycles each use hourly resolution data, with look-ahead periods of 6 days, 1 day, and 12 hours, respectively (see Figure 27). The HA cycle employs a time resolution of 15 min with a 4-hour look-ahead period. Finally, the RT cycle has data with a resolution of 5 minutes with a 45-minute look-ahead period; thus the dispatch takes in to consideration the conditions expected in the following 45 minutes.

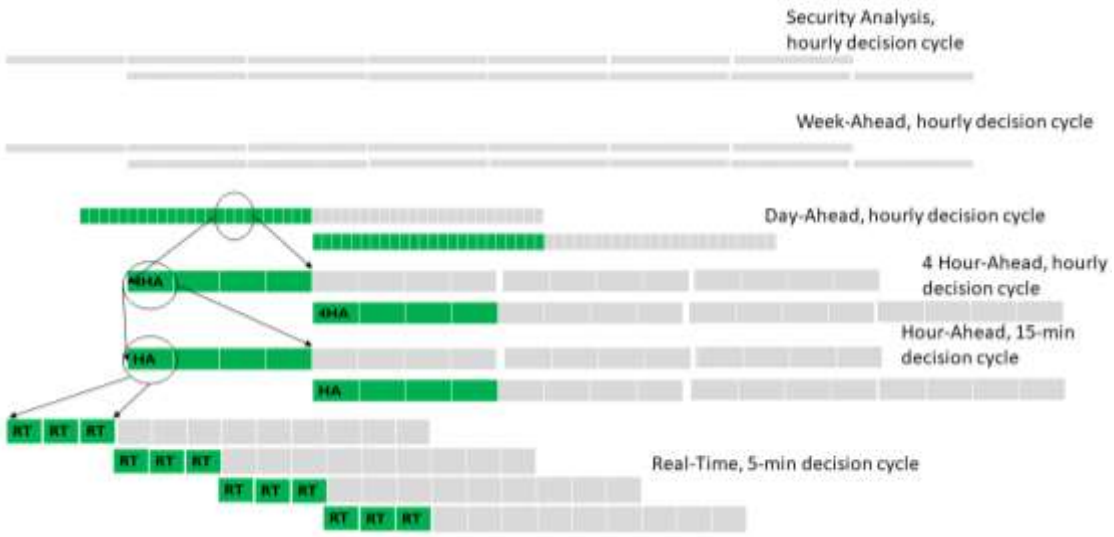

Figure 27. Multicycle rolling horizon modeling implemented in this study.

In its current formulation, the RTS-GMLC employs hourly time resolution data for any planning cycle prior to the day of operation, like the DA cycle, and 5-minute data for cycles within the day of operation, like the HA and the RT cycles. Hourly resolution forecast data for the load and VRE were used in the SA, WA, and DA decision cycles, and the actual conditions (RT) were used when committing units in the 4HA, HA, and RT cycles. In PSO, this collection of different cycles is referred to as a multicycle rolling horizon model. For example, the SA cycle is run to define an initial commitment schedule that is sufficient to ensure reliability. For the RTS-GMLC the SA cycle confirms the Nuclear generation is committed and ensures there is sufficient generation available to guarantee reliability. Next, the WA cycle commits slow start units (greater than 12 h start time), followed by the DA cycle where units requiring greater than 2 and less than 12 h are committed. Next, the 4HA cycle commits CC units with 2-hour start-up times, and then the HA cycle for the 1 hour start-up CTs. Each of these commitment cycles is executed with the look-ahead periods mentioned previously, to ensure awareness of the upcoming load conditions that must be met, so that generation is able to ramp and met load changes from one horizon to the next. As the model proceeds with simulating system operation over a specific time period (one-week periods were used in

this work, but it could apply to a full year or longer), each of these decision horizons is considered in sequence.

1.14.2 EV modeling

One way in which our model is different from the original RTS-GMLC is the introduction of EVs. EV penetration is defined here as the percentage of EVs in the LDV fleet. Because the character of the three regions in the RTS-GMLC is based upon generators in LADWP, NEV, and APS, the number of EVs per region and the EV load per region is derived from an estimation of the vehicles in the LADWP, NEV, and APS balancing areas. Projecting 10%, 20% and 30% of LDVs in each region are EVs, the estimated number of EVs is presented in Table 9. These penetration levels of EVs correspond very nearly to 1%, 2%, and 3% of the energy served in each region, as shown in the first (left-most) column of Table 9. The number of vehicles in each region, in thousands, is shown in columns 2 to 4 of the table, and the total number of vehicles is shown in the column on the right.

Table 9. EV penetration in thousands of vehicles as a percent of LDVs and of the annual system load, and the number of vehicles assumed in each region.

EV penetration LDV (% energy)	Region 1	Region 2	Region 3	Total
10% (1%)	96.9	76.2	197	~400
20% (2%)	193.8	152.4	394	~700
30% (3%)	290.7	228.6	591	~1,000

The procedure of assigning EVs into each regional nodes in the RTS-GMLC transmission topology involves splitting the number of EVs based on nodal peak load participation. Thus, nodes with higher load consumption are assumed to have a higher number of EVs. Table 10 illustrates the EV distribution by node at 10% for Region 1, which has a total of 96.9 thousand vehicles. In Table 10, the first column represents

the nodes in Region 1, the second column is the load during peak operation, and the third column is the number of EVs in that node. In this table, the color scale facilitates visualization— red is high and green is low. For example, node 118 shows a larger portion of load consumption and therefore a greater number of EVs, illustrated by the darker red color. Thus, the higher the load participation factor, the higher the number of EVs.

Table 10. EV nodal distribution at 10% penetration of LDV in RTS-GMLC Region 1 based on the nodal peak load participation.

Node	Load (MW)	EV
101	108	3,672
102	97	3,298
103	180	6,120
104	74	2,516
105	71	2,414
106	136	4,624
107	125	4,250
108	171	5,814
109	175	5,950
110	195	6,630
113	265	9,010
114	194	6,596
115	317	10,778
116	100	3,400
118	333	11,322
119	181	6,154
120	128	4,352

EV charging data from the EV Project reported by Idaho National Laboratory [68][127][97] were fundamental to the creation of the statistical models of uncoordinated and coordinated EV charging, which are scalable and suitable for implementation in a PCM [118]. In the uncoordinated scenario, charging occurs at the convenience of EV owners. The load due to uncoordinated charging is implemented with a Monte Carlo technique that uses the charger type, battery capacity, availability for charging, and battery beginning and ending states-of-charge in the EV fleet. Coordinated charging is modeled using an "aggregator", wherein EV charging is scheduled to minimize operating costs while meeting the daily charging requirements, as subject to battery capacity and charging constraints due to EV availability and states-of-charge. When modeling coordinated charging, to include the effects of the EV load on the electricity price, it was shown that the EVs should be represented as a controllable load, with constraints, with the PCM; refer to [118] for a detailed description of these models.

Coordinated EV charging is represented as an energy-limited (EL) resource in PSO. To meet the expected charging load, PSO allocates the EV's charging energy (MWh) in the DA cycle, within a time window of 24 h. This process is constrained within a time series with the maximum energy dispatch allowed for the next day, which is a function of the number of vehicles plugged in and their charger capacity per time (vehicle charging availability derived from EV Project). To expand the EV charging plan into consecutive intraday cycles, the ones with a solution time smaller than the time window of 24 h, such as DA and 4HA, must be used to hold the dispatch of the DA cycle, which process is equivalent to a non-recourse decision, but for dispatch purposes. The PCM cannot allocate charging cycles with an optimization window of less than 24 h. Thus, the PSO can include EV charging as part of the system plan in all the cycles (SA, WA, DA, 4HA, HA, and RT), dispatching the EV that minimizes the system’s operation cost.

1.14.3 Weeks of Analysis

Stress during power system operation, i.e., high LMPs and low reserve margins, depends on several factors including the number of conventional generators online and the load profile, both of which vary throughout the year. This study explores the impact of EVs during some key weeks of the year when stress is expected—some during the winter and spring (off-peak seasons) when VRE is high but load is not, and some during the summer (on-peak season). The weeks selected were based on overgeneration during the off-peak season, whereas during the on-peak season they included the days of maximum annual peak load the day with the most significant ramp. Figure 28 shows the monthly distribution of hourly net load (the net load is defined as the load minus VRE) in the RTS-GMLC using a boxplot, representing the 5th and 95th quantiles in the bounds and the 25th, 50th and 75th quantiles in the boxes. In this figure, the only two months without an hourly net load falling below zero are July and August. Figure 29 illustrates the daily average load and net load for each day of the year. The difference between the lines on this plot indicate the daily average VRE. These figures show that the net load is lower in the winter months and higher in the summer months due to the peak loads being driving by cooling loads in the summer.

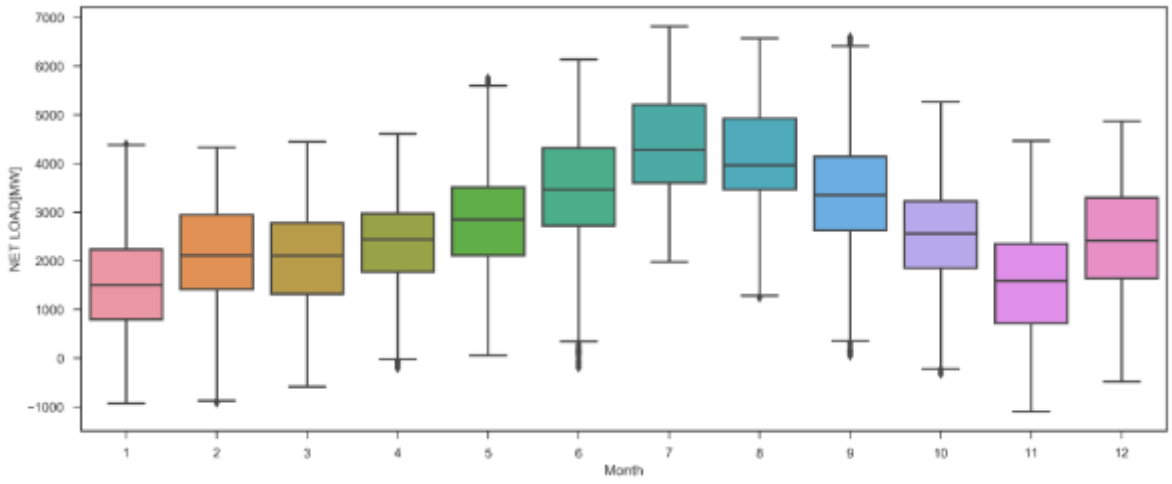

Figure 28. Net load distribution per month in the RTS-GMLC.

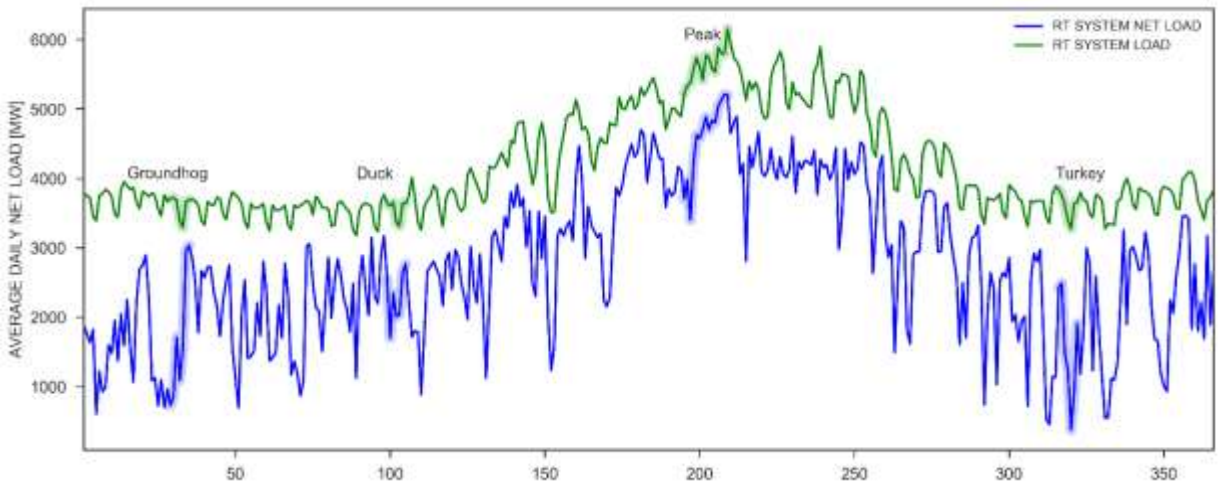

Figure 29. Average net load per day of the year occurring in the RTS-GMLC.

The weeks analyzed during the low-load months are:

- Wednesday 01-29-2020 to Tuesday 02-04-2020 (Referred to as "Groundhog week" since Groundhog day in the U.S. is on Sunday 02-02-2020);
- Wednesday 04-08-2020 to Tuesday 04-14-2020 (Referred to as "Duck week" since the load and VRE generation produce a net load curve that is often called the "duck curve", and is of significance in the western U.S.);
- Wednesday 11-11-2020 to Tuesday 11-17-2020 (called "Turkey week" since it is near the Thanksgiving holiday in the U.S.).

The weeks analyzed during the summer operation are:

- Monday 07-13-2020 to Sunday 07-19-2020 (the most significant daily ramp is on Thursday 07-16-2020 with value of 4600 MW);
- Wednesday 07-22-2020 to Tuesday 07-28-2020 (peak load is on Monday 07-27-2020).

Due to the proximity in the summer weeks, the model is run for two consecutive weeks from Monday 07-13-2020 to Tuesday 07-28-2020.

Figure 30 shows the load (solid green), net load (solid blue), and minimum dispatch (dotted red) of nuclear generation (vertical-axis in MW) during Duck week. Notice the two red boxes highlighting two days (2020-04-09 and 2020-04-11) on which the high penetration of VRE pushes the net load below the minimum

dispatch of nuclear, and even into negative values. The expectation is that a net load below the minimum dispatch of nuclear power will result in curtailment of VRE.

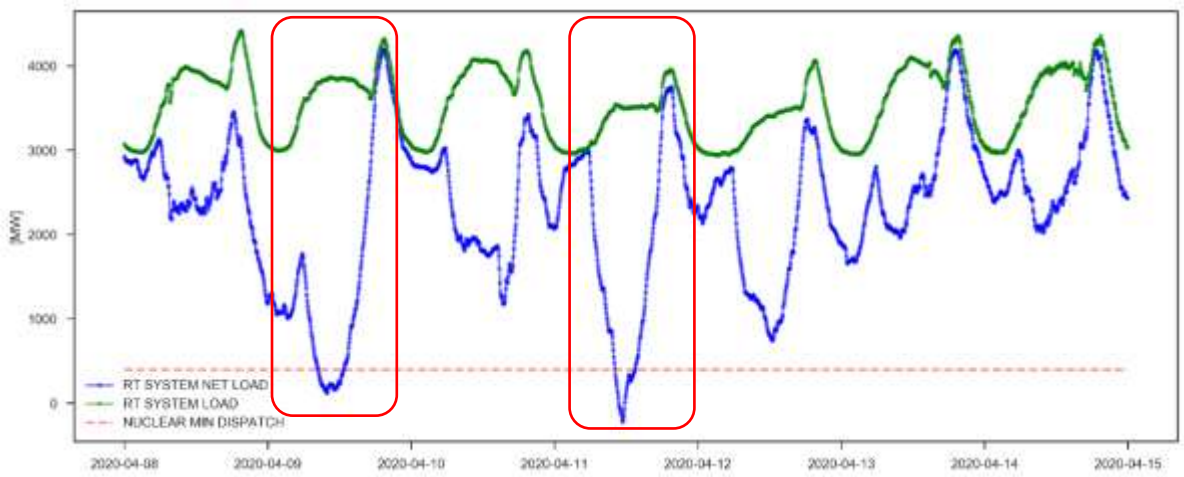

Figure 30. The load, net load, and minimum dispatch of nuclear power generation occurring in the RTS-GMLC during Duck week.

1.15 PCM Results and Metrics

Before describing the base case scenario and cases with EVs, it is necessary to describe the PCM results regarding system operation cost, marginal electricity cost and aggregated generation dispatch stack to serve the demand, as well as key reliability metrics. The system operation cost is the sum of the expenditures and fuel costs related to running the RTS-GMLC system's generators. The fuel cost has different components: the fuel expended during the startup, the fuel used to keep the machine running regardless of the level of generation, and the variable fuel cost derived from the incremental heat rate curve, which changes according to the production of the machines. The other variable costs are small compared with the fuel expenditures and are neglected. To keep the operation cost as low as possible, it is necessary to use the most fuel-efficient power plant first, and only operate the least efficient if it is strictly needed. The different levels of EVs allow us to explore changes in this system with a new load, the influence of which changes according to the size of the EV fleet.

The marginal electricity cost is the price paid for the last unit energy purchased. Since transmission constraints can exist between different areas within a power system, including the areas in the RTS-GMLC, the marginal cost of electricity can vary by location, and is thus call the locational marginal price. The marginal generator, which supplies the next energy unit, sets this electricity cost. Therefore, if the marginal generator does not use fuel to generate electricity, that is, uses only solar or wind, the LMP is zero. Each generator's revenue is the product of the electricity cost (LMP) times the energy produced by the generator. The cost of charging the EVs is the difference between the production cost with a given penetration of EVs minus the production cost of running the system with no EVs .

Additionally, we explore the operational curtailment, power not delivered from VRE due to constraints in the conventional fleet, and demand and reserves not served as reliability metrics. These reliability metrics determine the system's flexibility in the face of changes in the net load, resulting from either changes in the load or instantaneous VRE penetration.

1.16 Cases Examined

A total of 28 cases were examined through use of the PCM for the weeks described earlier. For each week, EV penetration levels of 0 (base case), 10%, 20%, and 30% were considered. When EVs loads were introduced in the RTS-GMLC, they were analyzed twice: once assuming uncoordinated charging and once with coordinated charging. A summary of the case examined are presented in Table 11. The lefthand column describes the week, and the numbers in the subsequent columns show the EV penetration level in percent of the LDV fleet. Recall that these EV penetration levels correspond very nearly to 1%, 2% and 3% of the overall system total load.

Table 11 Enumeration of the cases considered in the analysis of the effects of EV Charging in the RTS-GMLC.

		Charging Strategy	
Week	**Base Case**	**Uncoordinated**	**Coordinated**
Jan 29 - Feb 4 (Groundhog)	0%	10, 20, 30%	10, 20, 30%
Apr 8 - 14 (Duck)	0%	10, 20, 30%	10, 20, 30%
Jul 13 - 28 (Peak)	0%	10, 20, 30%	10, 20, 30%
Nov 11 - 27 (Turkey)	0%	10, 20, 30%	10, 20, 30%

The base case scenarios provide results for operating the RTS-GMLC with no EVs and typical electricity prices. These results are useful to gain insight into normal operation of the RTS-GMLC and to ensure the PCM is producing a rational solution for commitment and dispatch (i.e., under normal conditions load should be met by generation without violating reserve margins). The four different weeks, three EV penetration scenarios, two charging strategies, and four base scenarios with no EV, led to a total of 28 runs of the PCM. Comparing the results of the different EV penetration scenarios allow us to analyze the effects on system operation under different system conditions during times of the annual peak load and off-peak weeks during which the load is low and VRE is high (overgeneration). In the section to follow, the most relevant results from these cases will be presented.

1.17 Results

In this section, we present results for all the cases analyzed, with a focus on the results for Duck week (April) and the Peak (summer) weeks to determine differences in production costs, LMPs, the generation stacks, VRE curtailment, and reliability metrics of unserved energy (load shed) and reserve shortages. Results for the base case without EVs will be presented first, followed by the cases with EVs.

1.17.1 RTS-GMLC model results without EVs

This section shows the production costs, electricity prices, generation mix, and reliability metrics for the RTS-GMLC base case without EVs. The production costs will be presented first along with some reliability

indicators, followed by exploring the generation mix required to serve the demand, followed by the electricity prices and VRE curtailments.

1.17.1.1 Production Costs and Reliability Metrics

The average production costs for the RTS-GMLC base case are shown in the second column of Table 12 for the weeks of analysis listed in the first column. Notice that the average production cost is more than double in the peak season than in the other weeks of study, while the peak load is about double that of the rest of the year. The reliability metrics of interest are the unserved energy (load shed) and reserve shortages. If there are problems in the unit commitment and economic dispatch solutions of the PCM, and the load cannot be met with generation, the result is unserved energy. The PCM seeks to minimize the operation cost. In doing so, the PCM is setup to avoid load shed by assigning a high cost, i.e, a penalty, if load is shed. Thus, in minimizing the production cost, it is advantageous to avoid high penalties for unserved energy. As can be seen in Table 12, for the base case setup with no EVs, there is no load shed, and consequently the production costs result from the costs for generation unit startup and marginal costs of operation. Reserve shortages are used to indicate when the PCM solution is not able to maintain the necessary reserve margin. The reserve margin used in the RTS-GMLC model is 3% of load served during any hour for spinning reserve, and in average 2% of the load for non-spinning reserves, and flex reserves. When the reserves allocated in the RTS-GMLC fall below what is required, then the shortfall is reported as a shortfall in the capacity in MW. As shown in Table 12, there are not reserve shortages in the base case. Together, these reliability metrics show that the RTS-GMLC base case with no EVs results in a rational dispatch, and that the load can be met with existing generation and reserve margins.

Table 12. Summary of production costs and reliability metrics for the RTS-GMLC base case with no EVs.

Week	Average Daily Production	Peak Load (MW)	Unserved Energy (MWh)	Reserve Shortages (MW)

	Cost (Million USD)			
Groundhog	0.709	4468	0	0
Duck	0.744	4484	0	0
Peak	1.963	8036	0	0
Turkey	0.548	4780	0	0

1.17.1.2 Generation Stack

1.17.1.2.1 Generation Stack during the April Week (Duck curve)

A generation stack illustrates the generation resource used to serve the demand. For the RTS-GMLC base case with no EVs, the "generation stack" for the duck week (April) is shown in Figure 31. The vertical axis on this plot shows the generation and load in MW, and the horizontal axis the days of the week. Shown on the plot is the load (magenta dashed line), net load (white dashed line), and generation used to meet the load. Note the "net load" is defined here as the load minus VRE. The generation plotted in the stack is identified in the legend. Starting at the bottom, the legend shows the EV load in navy blue; note that there are no EVs shown in the stack for this base case (EV load will be shown as a negative). Next in the generation stack is nuclear generation, here illustrated in green, with a dispatch that does not vary with time. Above nuclear in the stack are three types of coal steam units: 350 MW units (black), a 155 MW units (gray) and 76 MW units (silver). The next two in the stack are a natural gas combined cycle, NG-CC (indigo), and a natural gas combustion turbine, NG-CT (blue), with capacities of 355 MW and 55 MW, respectively. Next on the stack is a 50 MW hydropower unit (cyan), which is topped by the VRE generation: wind (green), utility-scale PV (orange) and roof-top PV, RTPV (gold). Looking at the generation stack across this week in April, there are days in which VRE plus hydro supplies most of the power during daylight hours, for example on April9, 11, and 12. As can be seen, during the middle of the day when VRE generation is high, their production flattens out as the resources are curtailed to permit the nuclear

generation to maintain its steady output (in the RTS-GMLC, the nuclear generation is not allowed to ramp). During each day shown, in the late afternoon when RTPV and PV generation drops, and the fossil generators (natural gas and coal) must increase their output (ramp) to supply the daily peak demand in the evening hours and much of the overnight load. During this week, which is representative of weeks in the spring in the Southwest U.S., the flexible CC and CT units are crucial in following the net load, and what flexibility that does exist in the smaller coal units is also utilized.

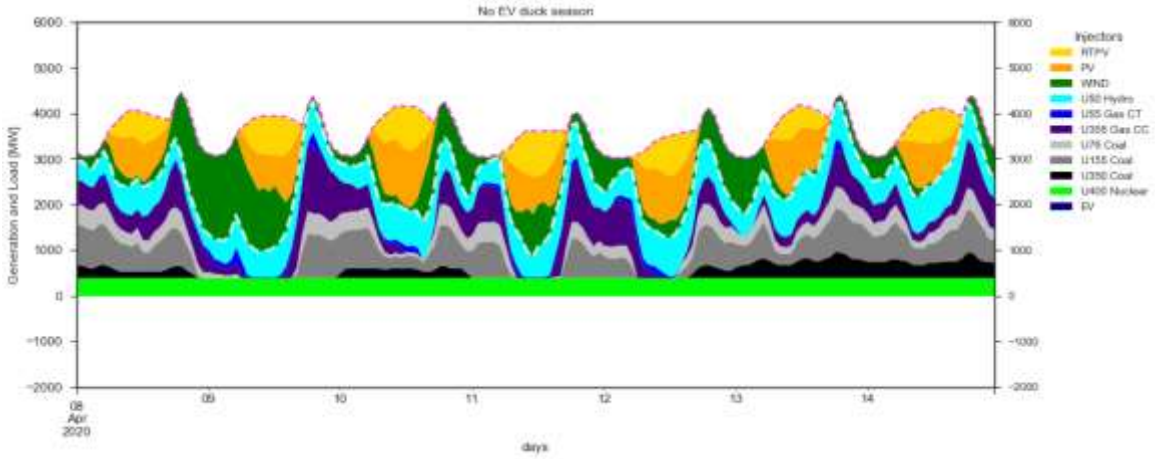

Figure 31. The generation stack for Duck week in April, assuming no EV charging.

1.17.1.2.2 Generation stack during the July Weeks (Peak)

Figure 32 shows the generation stack during the peak weeks in July. The daily peak load occurs during the afternoon (2 PM) on July 27. RTPV and PV generators are available at the peak, thus reducing the peak net load (white dashed line) substantially to 6524 MW. In July, the coal steam units (black to silver) tend to fluctuate less from day to day than the other weeks analyzed. Focusing on July 15, we can see a large contribution from the wind resource further reducing the peak net load, but that is not common during these weeks in July (this is consistent with wind resources in the Southwest U.S.). On each of the days analyze, the flexibility of the natural gas generators (CC and CT) is used to fill the gap between the net load and the less-flexible coal and nuclear generators by ramping up and down each day. On days with

significant solar and wind generation (July 13-15), the flexibility of the CC and CT units are key to meeting the net load variations. Compared to the spring “duck” week, the commitment and dispatch is much more consistent, and more like that in systems with low VRE penetration.

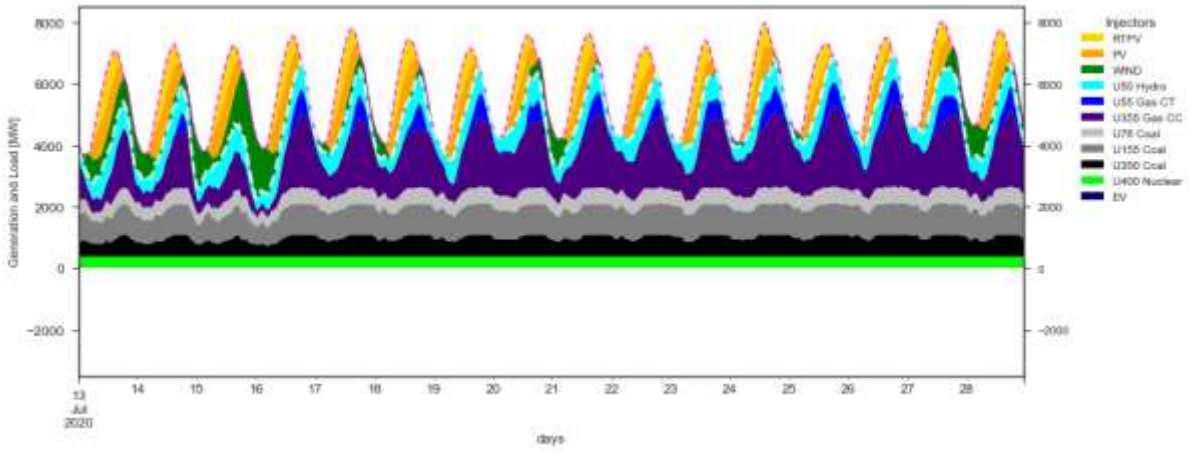

Figure 32. The generation stack for the peak weeks in July, assuming no EV charging.

1.17.1.3 Locational Marginal Price (LMP)

This section describes the average LMP in the system as the load-weighted LMP for the whole network.

Table 13 presents the weekly average LMP in each week considered. The LMP was tabulated as the average load-weighted LMP on each node in the RTS-GMLC system. Note that the highest LMP occurs during the peak season when the load is the highest. The LMP during the peak weeks is about 60% than the off-peak weeks.

Table 13. Load-Weighted Average LMP (USD/MWh) over all nodes in the RTS-GMLC without EVs.

Week	Average LMP (USD/MWh)	Average Load (MW)
Groundhog	14.85	3682
Duck	17.86	3641
Peak	25.12	5821
Turkey	15.09	3684

An example of the LMP variation during a typical day (April 11) during the Duck week without any EVs is shown in Figure 33. The system 5-minute net load in MW is indicated by the solid line and refers to the scale on the left, and the system load-averaged LMP at a 5-minute resolution is indicated by the dashed red line and refers to the scale on the right in USD/MWh. The LMP follows the trend of the net load since the price of the marginal generator declines as the net load declines.

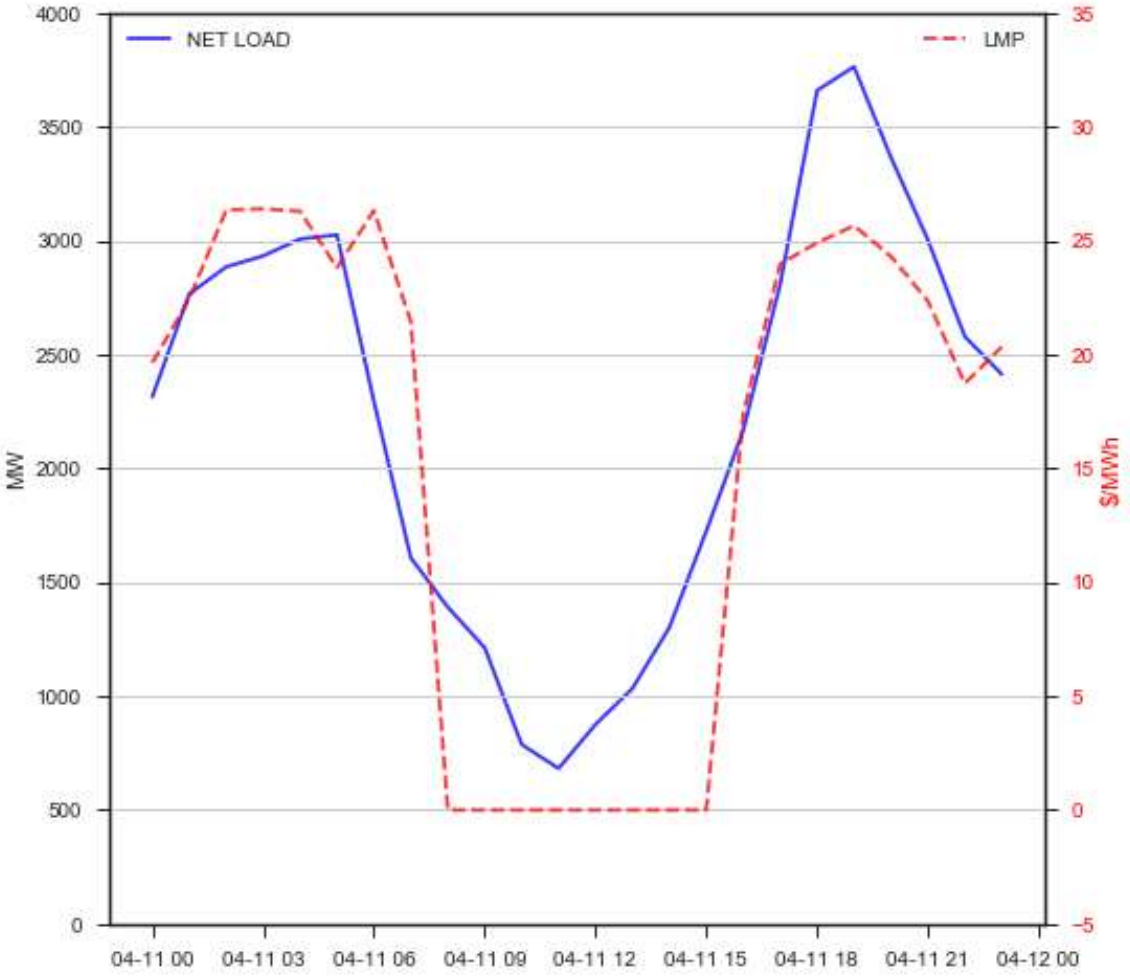

Figure 33. Net load after VRE curtailment and LMP for one day during Duck week (April) for the RTS-GMLC model without EVs.

The net load curve in Figure 33 shows a large dip in the middle of the day, and steep ramps in the morning and evening, which are characteristic of the Duck curve. Running the PCM PSO for the Duck week leads to an LMP that hovers between USD 20 and 25 per MWh in the nighttime hours, and drops to zero during the day when the net load is very low. During zero-LMP hours, solar generation is the main marginal resource. These results are consistent with operational experience during periods of high VRE and overgeneration.

1.17.2 VRE Curtailments

Because the net load can at times fall below the minimum dispatch level it may be necessary to curtail the VRE. Referring to Figure 30, during midday on April 11, the minimum net load falls below the minimum dispatch of nuclear generation (see the blue net load line, and the horizontal red dashed line). After honoring the system constraints, including generator minimum dispatch level, the net load on April 11 after VRE curtailment is shown by the blue line in Figure 33.. Figure 34 shows a zoomed-in view of the bottom of the generation stack, below 1400 MW, for April 11 between 4:00 to 18:00 from Figure 31. The coal and CC units are cycled off, subject to their minimum time-off fulfillments (commitment parameter) of eight hours (U155 Coal (gray)), four hours (U76 Coal (silver)), and four and a half hours (U355 Gas CC (indigo)). Additionally, in Figure 34 between 10:00 and 13:00, a CT unit is shown as running at its minimum dispatch of 22 MW. The nuclear generation remains constant, while the hydro and natural gas CT generation operate at their minimum dispatch levels until later in the afternoon when the PV decreases. During the window of time from 9:00 to 17:00, there is VRE curtailment of 4042

MWh.

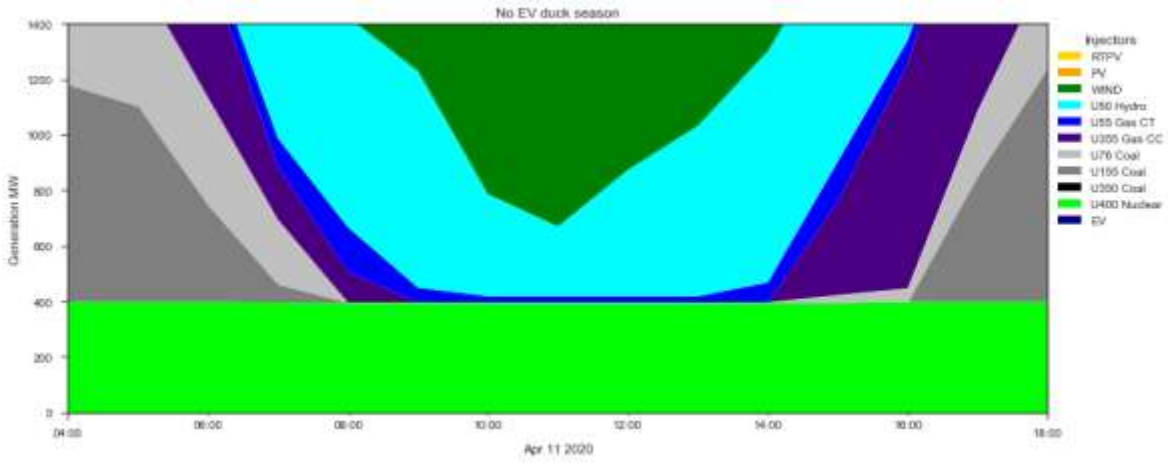

Figure 34. Zoomed-in view of the generation stack on April 11 (Duck curve) with no EVs.

Table 14 summarizes the total curtailment during each of the weeks analyzed for the base case with no EVs. The percentage of VRE curtailment reported is the amount of energy produced by VRE that is not used. Focusing on the Duck week where VRE curtailments are the moderate during the off-peak season, the RTPV curtailment is the smallest, at less than 1%; wind curtailment is less than 4%, and the PV curtailment is largest at 12%. During the peak weeks analyzed with no EV, the curtailment of PV and RTP was zero, while it was approximately 1% for wind. Curtailment is more during the off-peak weeks because the load is relatively lower while VRE production can be high.

Table 14. VRE curtailments expressed as a percentage of total weekly VRE production for each of the weeks analyzed for the base case with no EVs.

	VRE Curtailment		
Week	**Wind**	**PV**	**RTPV**
Groundhog	9%	18%	5%
Duck	4%	12%	1%
Peak	1%	0%	0%
Turkey	7%	14%	2%

1.18 Results for Cases with EVs

This section presents the results from running the PCM for the weeks of interest when employing either uncoordinated or coordinated charging strategies for EVs. These results will be compared with the base case RTS-GMLC and between themselves.

1.18.1 System Operation Cost

Figure 35 presents the daily average operation cost, in millions of USD, for all weeks analyzed and for all scenarios. The four-column groupings along the horizontal axis represent the levels of EV penetration and charging approach, from no EVs on the left up to 30% on the right. Inside each group of columns, the colors (order) represent the different weeks of analysis, starting from early in the year (leftmost column)

to late in the year (rightmost column). The operating cost (start-up and operational fuel costs) is proportional to the net load served for the conventional generation fleet, and ranges from 0.5M USD to nearly 2.5M USD. In the RTS-GMLC, the net load is highest in the summer peak load months (annual peak in July; see **Error! Reference source not found.**) and lowest in the off-peak winter months (lowest monthly p eak in November; see Table 12). Therefore, as shown in Figure 35, the operating cost is higher during the summer (third—orange columns) than in the non-peak seasons, more than three times higher if one compares days in July (peak) and November (turkey) at every penetration level. Regardless of the level of EV penetration or week, coordinated charging results in a lower operating cost than uncoordinated. The savings achieved in operating cost when using coordinated charging are consistently 1% during the summer peak weeks. The savings, however, ranged from 4% to 8% during the other weeks. The percent savings are more significant at 10% EV penetration than 20% or 30% EV penetration, due to less fuel expenditure and less generation being committed to cover the additional power consumption due to EVs. In summer, EV represents a smaller proportion of the net load, and the savings are lower.

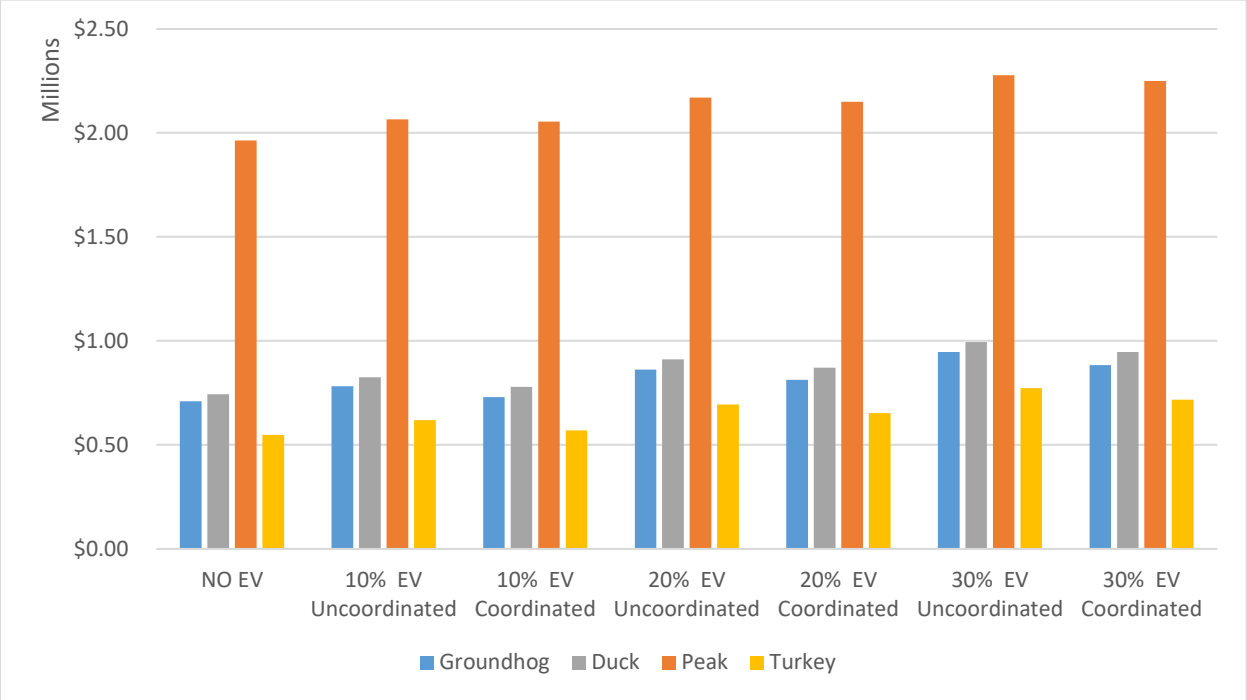

Figure 35. Average daily system operation cost for all the scenarios considered.

1.18.2 Cost to Charge EVs

The cost due to EV charging is determined by taking the difference between the production cost with a given penetration of EVs minus the production cost of running the system with no EVs. Figure 36 presents the average daily EV charging cost per vehicle for each of the scenarios. In Figure 36, the charging cost is shown on the vertical axis, while the horizontal axis illustrates the levels of EV penetration and charging approach, following the convention of Figure 35. Note the charging costs range from 0.05 USD to 0.25 USD per day, which is consistent with energy requirement for the battery size and charging requirements of the LDVs assumed in this model (equivalent to a daily usage of about ~10 kWh per vehicle, equivalent to ~30 miles a day). No transmission use payments are considered, nor are the costs of distribution to end-users or any other costs. For the peak week, when comparing coordinated and uncoordinated charging costs for all three penetration levels, the cost goes down by 10% percent. This happens because the coordinated charging approach accommodates EV charging when VRE is available. For the Duck week,

the cost reduction elicited by coordinated charging varies from 45% to 24% as the EV penetration increases. The jump in charging cost for coordinated charging from 10% to 20% and 30% EVs is due to the number of fossil generators that must be used to provide power, an additional generating unit is committed. Overall, the cost of charging EVs is substantially lower when using coordinated charging versus uncoordinated.

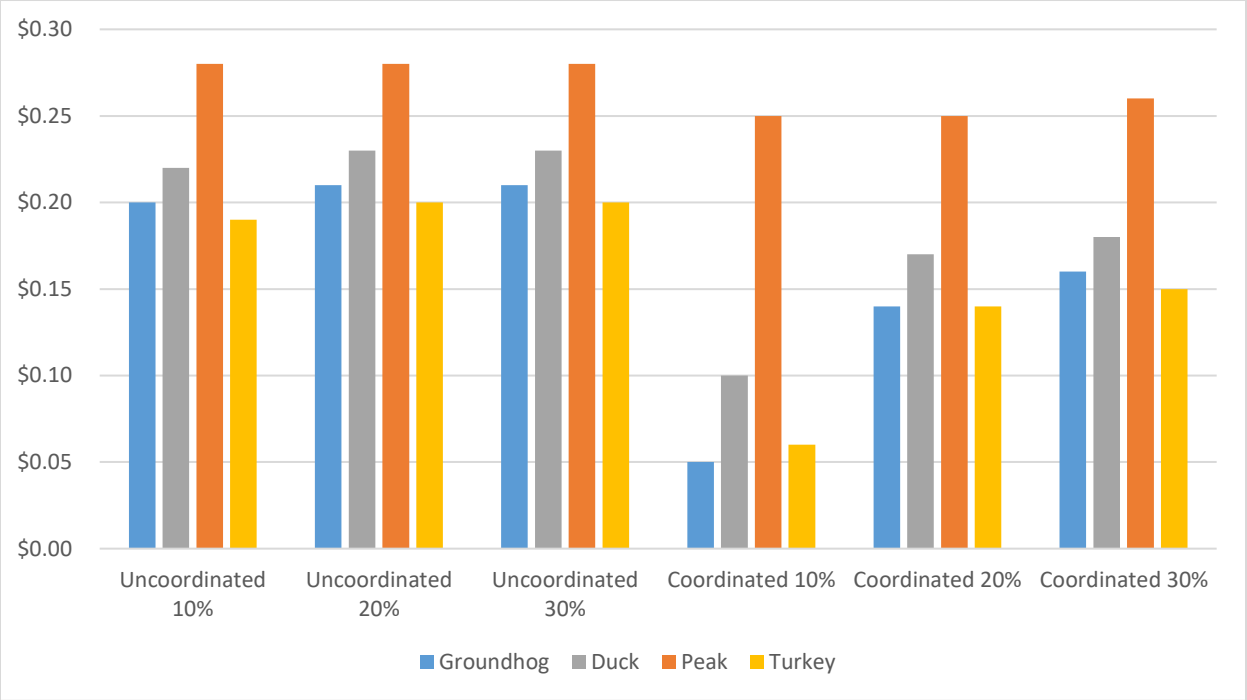

Figure 36. The average daily cost to charge an EV per scenario.

1.18.3 Locational Marginal Price (LMP)

Table 15 shows the weekly average LMP in the RTS-GMLC system for all scenarios. The first column lists the scenarios, followed by columns for every analysis week, ordered from lowest to highest LMP (Groundhog, Turkey, Duck, and Peak). Note that the first row provides the same data as

Table 13 and shows the lowest LMP because it has the lowest total demand (no EV charging). The highest LMPs arises at 30% EV penetration due to the higher overall load. For example, at 30% penetration of coordinated EV charging, the average LMP increases by 4% compared to a system with no EV charging. Comparing the LMP of the various scenarios, the uncoordinated cases often have a lower LMP than their coordinated counterparts. Though production costs are lower with coordinated charging, It is not uncommon for the LMP to be higher because the load shifts to times with lower prices, often increasing the low prices during those periods leading to an overall increase in LMP.

Table 15. Weekly average LMP (USD/MWh) occurring over the entire system (RTS-GMLC).

Scenario	Groundhog **(USD/MWh)**	Turkey **(USD/MWh)**	Duck **(USD/MWh)**	Peak **(USD/MWh)**
NO EV	14.85	15.09	17.86	25.12
10% EV Uncoordinated	16.17	17.34	18.42	25.57
10% EV Coordinated	16.71	16.12	20.48	25.44
20% EV Uncoordinated	16.75	16.35	19.12	25.85
20% EV Coordinated	17.75	17.98	20.48	25.76
30% EV Uncoordinated	17.63	17.86	19.53	26.14
30% EV Coordinated	19.73	18.41	21.10	26.23

1.18.4 Generation Stack

This section presents the cumulative generation dispatch for the system, comparing uncoordinated and coordinated charging. The generation stack figures are similar to those shown in Figure 31 and Figure 32. The results shown below refer to an EV penetration rate of 30% of LDVs, corresponding to 1% of the annual energy load.

1.18.4.1 Generation Stack April Week (Duck curve) Uncoordinated EV Charging

Figure 37 shows the generation resources used to supply the demand for the case of 30% uncoordinated EV charging. Note that there are two primary differences in this generation stack and the stack shown in

Figure 31 for the system with no EVs: 1) the uncoordinated EV charging load is plotted on the negative side of the generation scale (navy blue); and, 2) the generation stack includes the generation needed to serve the EV load, so is higher on a daily basis. Shown on the plot in Figure 37 is the load without EVs (magenta dashed line), the net load with EVs (white dashed line), and the generation used to meet the load. Because the EV load for uncoordinated charging peaks every day in the evening, the peak net load exceeds the peak load without EVs on five of the seven days analyzed, with no change on the other two days. Consequently, on some days the dispatch of fossil generation increases during the peak conditions. For example, on April 9 and April 13, the peak net load exceeds 5,000 MW, representing a large increase of 1,200 MW (27%) relative to the case with no EVs. Especially on the days when there is nor VRE during the peak hours after sunset, the fossil generation increases output to meet the increased net load.

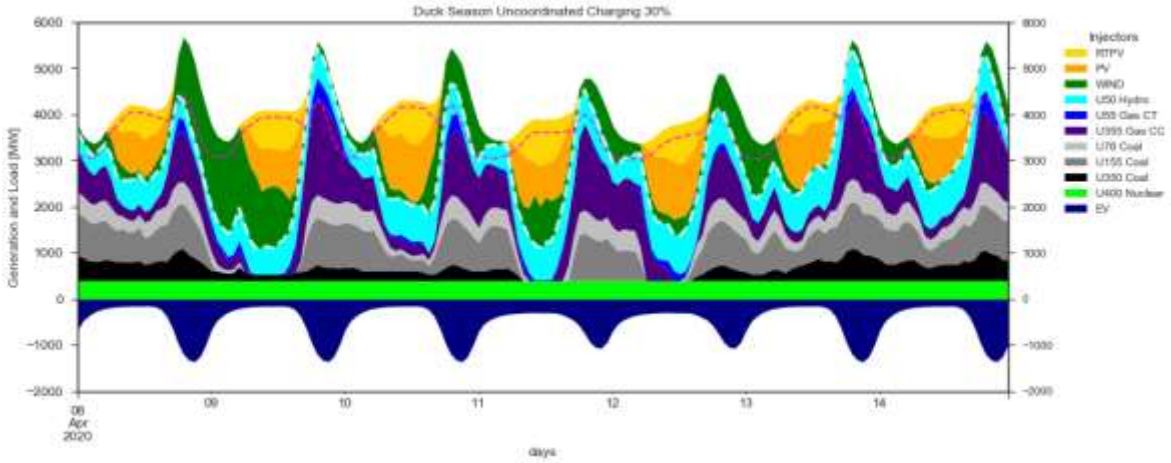

Figure 37. The generation stack for Duck week in April, assuming 30% EV penetration and uncoordinated EV charging.

1.18.4.2 Generation Stack April Week (Duck curve) Coordinated EV Charging

Figure 38 presents the case of 30% EV penetration employing coordinated charging. Notice how, in contrast with the previous scenario, coordinated charging shifts this EV load (navy blue on the negative side of the stack) to the middle of the day and takes advantage of the low LMPs resulting from the high VRE or light load during the night. Note the net load tends to show a morning and evening peak each day

(white dashed line). Within the constraints of meeting the daily EV charging load, subject to constraints of availability for charging and charging requirement, the EV charging aligns with solar power in the middle of the day and wind power during the evening hours. Overall, the peak of the net load served each day is lower than the corresponding peak load without EVs, due to coordinated EV charging aligning better with the VRE. Comparing the shape of the generation stacks in Figure 37 and Figure 38, with coordinated charging, the fossil generators are used less and cycled more to meet the net load.

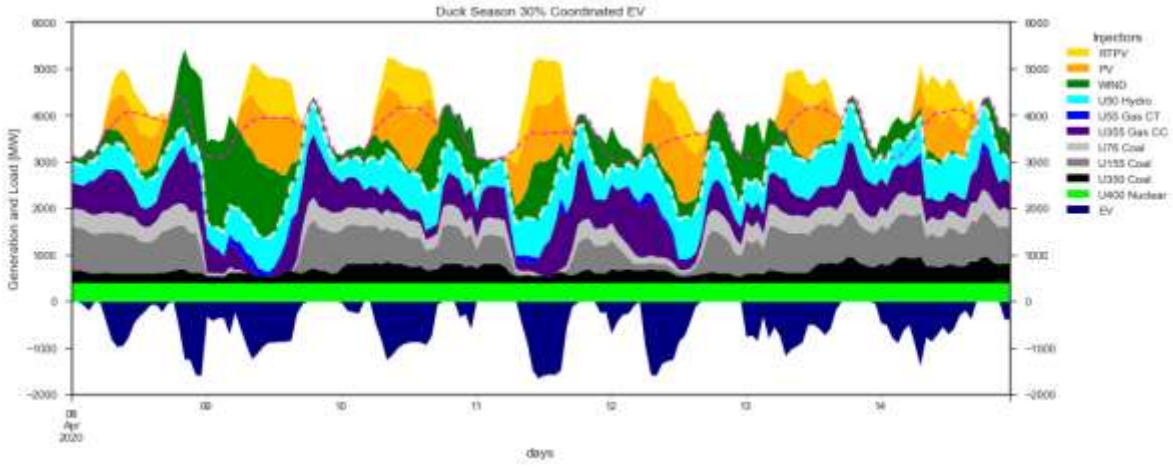

Figure 38. The generation stack for Duck week in April, assuming 30% EV penetration and coordinated EV charging.

1.18.4.3 Generation stack July Weeks (Peak) Uncoordinated EV Charging

Figure 39 shows the case of 30% uncoordinated EV charging during the peak weeks in July. On two of the days, July 16 and 21, the peak net load (dashed white line) increases by about 3.8% (300 MW) above the peak load without EVs shown by the magenta dashed line. On the remaining days, the peak in the net load is equal to or less than the peak load without EVs. On every day, the EV load shifts the peak net load two hours later into the early evening (7 PM). Relative to the off-peak weeks, the magnitude of impact on peak load is less during the summer peak weeks since the peak load is significantly higher.

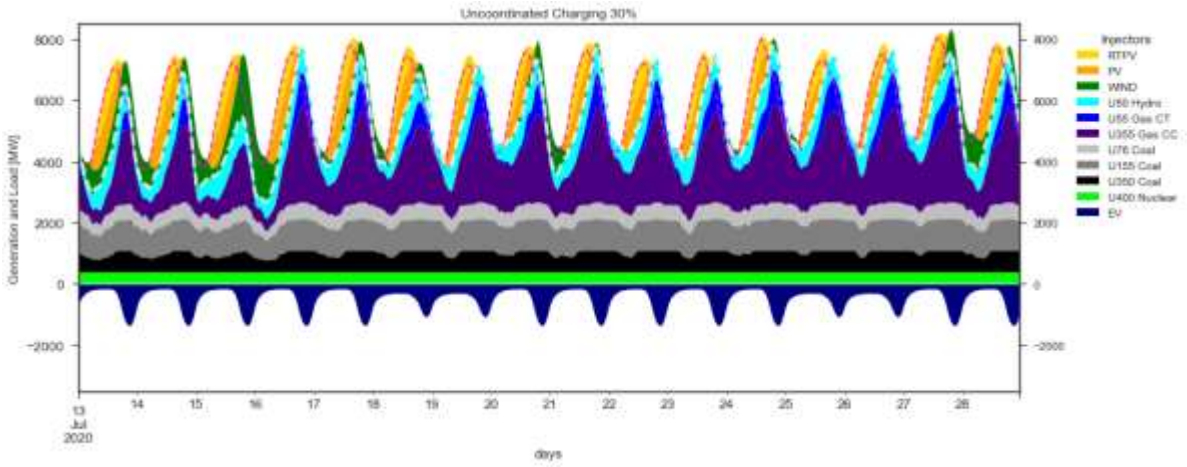

Figure 39. The generation stack for peak weeks in July, assuming 30% EV penetration and uncoordinated EV charging.

1.18.4.4 Generation stack July Weeks (Peak) Coordinated EV Charging

In Figure 40 is shown the case of 30% coordinated EV charging. Similar to the Duck week (Figure 39), coordinated charging shifts this EV load to the middle of the day, and takes advantage of the low LMPs due to VRE, primarily solar. With coordinated charging, the daily peak net load (white dashed line) is shifted two hours later into the evening relative to the peak load without EVs (magenta dashed line). More importantly, the peak net load is always less than the peak load with uncoordinated charging, and sometimes substantially so. Similar to the Duck week results, the output of the fossil units changes more frequently than with uncoordinated charging.

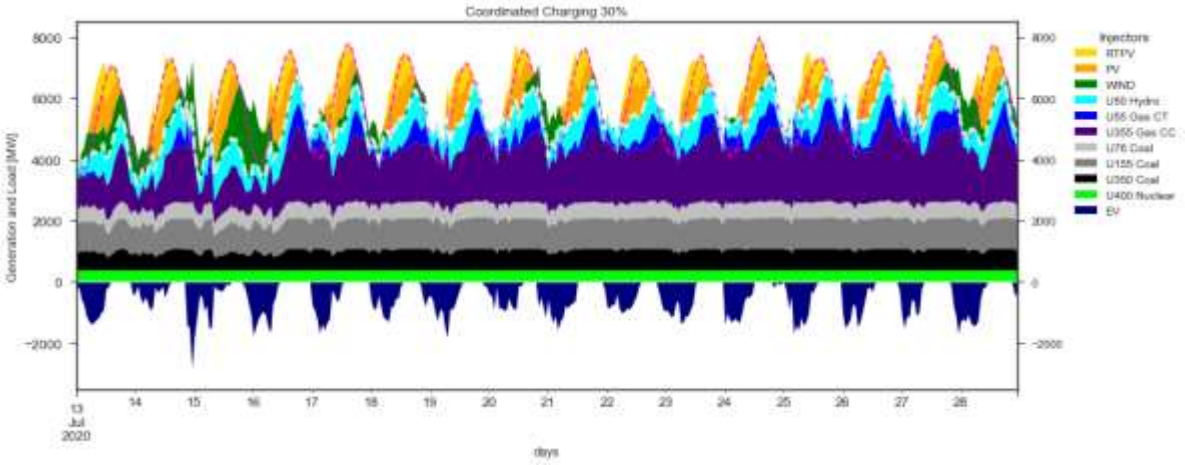

Figure 40. The generation stack for peak weeks in July, assuming 30% EV penetration and coordinated EV charging.

1.18.5 VRE Curtailments

We will next look at curtailments of VRE at all penetration levels considered for both charging strategies, and as compared to the case of no EVs. As stated previously (sec. 1.17.2), VRE curtailments are often necessary to keep conventional generation online during low "net load" periods in the middle of the day (to honor generator constraints) and/or to maintain sufficient operating reserves. In the no EV base case, curtailments of VRE are higher during April because of high VRE production and low load (see Table 14).

1.18.5.1 April week (Duck) curtailments

The curtailment of VRE (Wind, PV, RTPV) for the Duck week is shown in Figure 41. The curtailment percentage is shown on the vertical axis, and the groupings of bars show the magnitude of curtailment for each scenario. The first group of columns regards the case without EV charging (NO EV), followed by the uncoordinated charging scenarios (U10%, U20%, and U30%), and the last three for the coordinated charging scenarios (C10%, C20%, and C30%). This ordering shows that the curtailment is highest in the case without EV charging. Adding EVs in the uncoordinated cases reduces curtailment relative to the base case, due to the additional load. Comparing the three uncoordinated penetration levels, as the EV penetration increases, the curtailment of PV and RTPV decreases. This is due to additional EV load added

during hours of PV generation. Wind curtailment, however, increases across the uncoordinated cases because as the EV load increases, additional thermal generation is committed that requires wind production to decrease during hours where not much charging occurs. For the coordinated charging cases shown in the rightmost set of columns, it is evident that the magnitude of curtailment is lower than for no EVs and for uncoordinated charging. Both wind and solar curtailment decreases with increased EV penetration because the EV load can be scheduled (within availability and charging requirement constraints) to occur during low LMP hours of high VRE production.

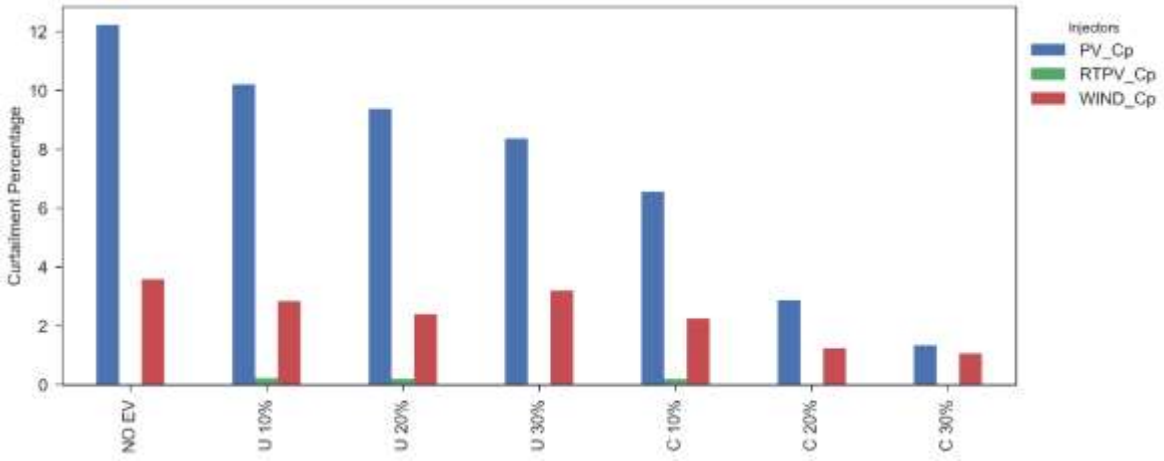

Figure 41 VRE curtailments during the Duck week in April for all scenarios and charging strategies.

1.18.5.2 July weeks (Peak) curtailments

Figure 42 shows the VRE curtailments during the peak weeks in July. Note the vertical scale in this figure is 1/10 of that in Figure 41, and the level of curtailment is smaller in all scenarios as compared to the Duck week. In all cases, the curtailment of PV and RTPV is zero, and the curtailment of wind is lower than 1.3%. The curtailment of WIND starts at 1.0% (NO EV) and increases with uncoordinated charging (U10%, U20%, and U30%). Similar to the Duck week, the increase occurs because additional thermal generation is committed to meet the additional load due to EVs during the on-peak hours, causing wind to be curtailed away from the peak. For the coordinated charging cases (C10%, C20%, and C30%), the wind curtailment

decreases with increasing EV penetration, once again because of the ability to move some of the EV charging load to low LMP, high VRE hours. Therefore, coordinated charging reduces wind energy curtailment in July.

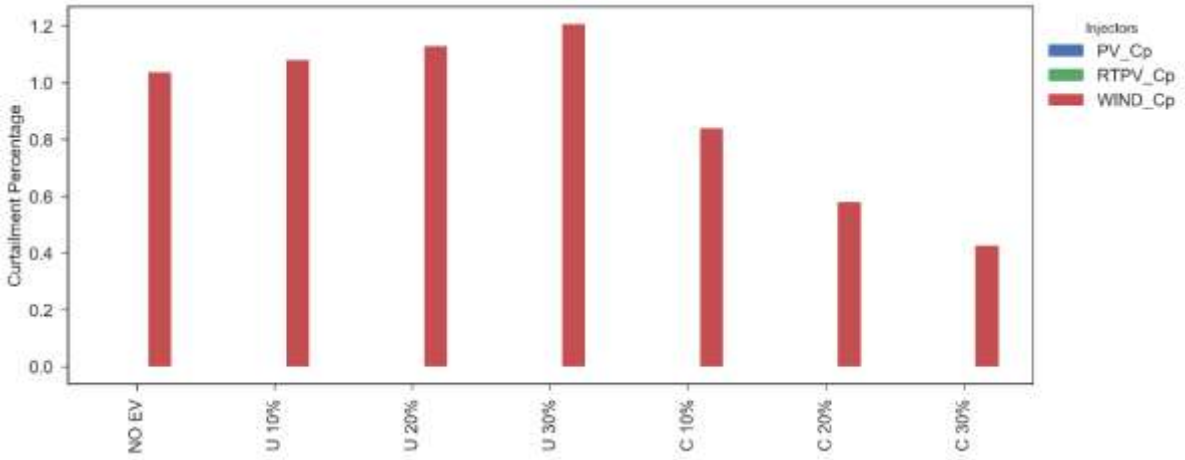

Figure 42. The percent curtailments during peak weeks in July for all EV penetration scenarios and charging strategies.

1.19 Discussion

The uncoordinated charging scenarios were established to explore the effects of charging at the convenience of EV users, based upon actual charging habits recorded part of the EV Project [97], which led to increases in the peak load. Figure 43 shows the uncoordinated EV charging load for 30% EV penetration and LMP for the same day as in Figure 33 (April 11, Duck week). In Figure 43, the uncoordinated charging load is presented with the solid blue line, referring to the vertical axis on the left. The system's LMP values are depicted in the dashed red line, and refer to the secondary axis on the right, in USD/MWh. Figure 43 shows EV charging peaks in the evening, reaching a value greater than 1000 MW during the time when the LMP is high. Consequently, the cost of EV charging is relatively high and the operation cost is higher.

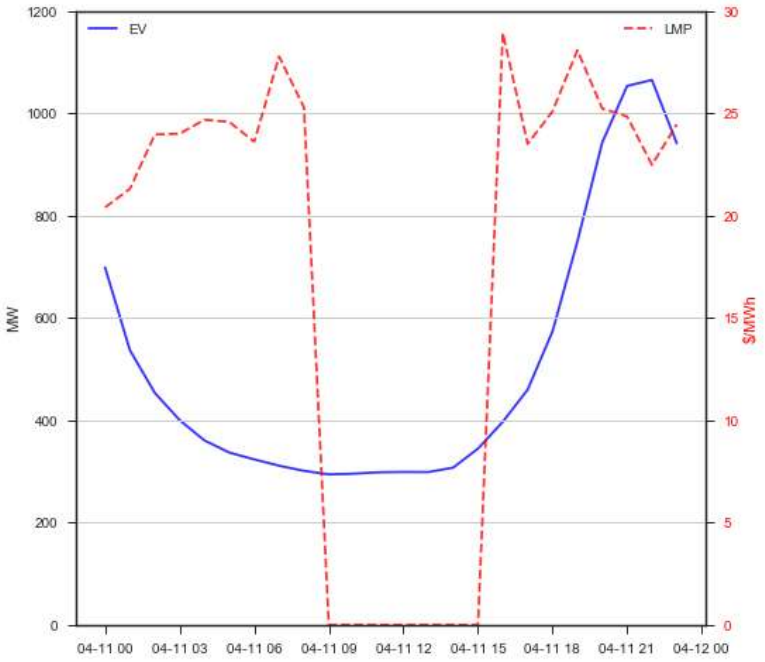

Figure 43. EV load and LMP results for one day during Duck week, including 30% EVs implemented with uncoordinated charging.

The results for coordinated charging confirm that when EV charging is scheduled to coincide with low electricity prices, within the constraints of EV availability and charging requirements, that the charging costs and system operation cost will be lower. Figure 44 shows the EV charging load profile and LMP for the same day in April as the previous figure. Note that the EV charging is scheduled to occur during the low LMP hours, and that LMPs change in response to additional load being served relative to the no EV and uncoordinated charging cases.

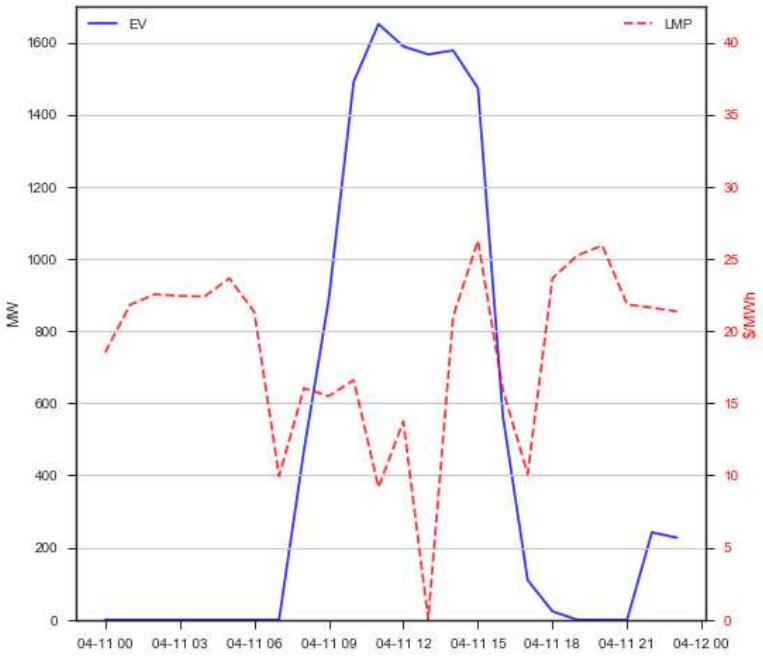

Figure 44. LMP and EV load profiles when employing coordinated EV charging, on a day during Duck week.

1.20 Conclusion

This article presented the impacts of EV charging on operation of the RTS-GMLC power system using the PCM PSO. In the base case, the RTS-GMLC model included no EVs. Modeling of EVs considered two charging strategies, uncoordinated and coordinated, and three EV penetration levels: 10%, 20%, and 30% of the light-duty vehicles (equal to 1%, 2% and 3% penetration of the annual energy load). To understand the impacts, the model was applied weeks during representative on-peak and off-peak weeks during the year. The findings are presented in terms of power system loads, operation cost, LMPs, EV charging cost, and VRE curtailment, and the impact of the two charging strategies. With regard to the reliability metrics of unserved energy and maintaining reserve margins, the EV charging scenarios led to no increase in unserved energy, and no violation of the reserve margins.

The integration of electric transportation increases the power system load, operation cost, and electricity prices, but the magnitude and character of the effects depend upon the charging strategy. The overall system operation cost under uncoordinated charging is higher, regardless of the level of EV penetration, when compared to coordinated charging. The operation cost is proportional to the net load served by the conventional fleet, and consequently much higher during the peak load weeks in the summer. During the summer weeks, the savings in production costs between coordinated charging and uncoordinated charging are consistently 1% for all three EV penetration scenarios tested. However, during the off-peak weeks when load is lower and VRE production is high, the savings in production costs range from 4% to 8% when using coordinate charging.

EV charging cost was computed by taking the production cost for a scenario with a given EV penetration level and subtracting the cost of running the system with no EVs. The average charging cost per EV follows the same trends as the system operation cost—higher on summer days and lower on winter days, due to the higher LMP, but there are significant differences when considering the charging strategy. At 10% EV penetration (1% in energy penetration) during February (Duck week), the uncoordinated charging cost per vehicle is four times higher than the coordinated charging cost. The lowest savings in charging cost occurred for 30% EVs during the peak weeks in July, because electricity prices are generally high due to high load and LMPs during those weeks.

Regarding the daily system peak load, during off-peak weeks under uncoordinated charging, the peak net load increases with an increase in EV penetration, because peak load and EV charging are coincidental. During a week in April (Duck week), operating under uncoordinated EV charging, the peak load increases as much as 27% at 30% penetration of EVs (3% in energy penetration). However, coordinated EV charging shifts the EV charging load to off-peak hours as much as is possible, within the constraints of the charging requirement and the availability for charging. The result is an increase in the charging during off-peak

hours, which is coincident with PV, RTPV, and wind. The net load profile during the day changes under coordinated charging but the peak load does not increase.

Related to the LMP, the shift of charging to off-peak hours due to coordinated charging increases the LMP simply because the EV load increases during those off-peak hours, and consequently the LMP increases during those hours. During the Peak weeks (July), with 30% penetration of coordinated EV charging, the average LMP increases by 4.4% compared to the system with no EV charging. However, it increases by 33% during a winter week in early February. Note, although the LMP increases, both the operation costs and EV charging costs decrease with coordinated charging versus uncoordinated charging.

Regarding VRE curtailment, coordinated charging reduces the curtailment of PV (by as much as nine times during off-peak season operation for 30% EV penetration) and wind (more than half during the summer operation season for 30% EV penetration) compared to the scenario with no EVs or uncoordinated EV charging. Coordinated charging reduces the curtailment of VRE, mainly because charging can be scheduled at hours of peak PV generation when the LMP is low, which addresses the problem of overgeneration (Duck curve). Therefore, coordinated charging is beneficial to the integration of VRE. To realize this potential for scheduling the charging during low LMP, high VRE hours of operation, it is necessary to have an accurate model of EV availability for charging and charging requirements.

Conclusions

This chapter recapitulates the overall goal and the successive methodology steps. It highlights the main results and conclusions of every chapter. Then, the research questions are put back into context and answered with specific findings.

The main objective of this research is to determine the impacts of electric vehicles on power system operation and costs under high penetration of EV and VRE (wind and solar power). The approach is broken down into two steps.

The first step was to develop the methodology to model and integrate EVs into power system operation using a production cost model (PCM). This work presented statistical models for EV charging that were suitable for power system operation. Statistical models for EV charging were created using data from the EV Project. This modeling with the appropriate data resulted in reasonable and scalable EV charging load profiles. The models recognized coordinated and uncoordinated charging loads. The dissertation provided an algorithm for modeling the uncoordinated charging and incorporated the result into the PCM model as a time series, similar to the load forecast or VRE forecast. However, coordinated charging modeling must be part of the PCM and modeled as a controllable load with the constraints imposed by the fleet characteristics, energy requirement (MWh), charging availability, and charging level (kW). Otherwise, the modeling will neglect the influence of the EV fleet on the electricity price. A production cost model could integrate the EV charging model and assess the EV effects on the power system cost and loads.

The second step of the process integrates the model into full range of planning stages or markets, from the week-ahead (WA) to the intraday real-time (RT). Here, this dissertation presented the impacts of EV charging on operation of the RTS-GMLC power system using the PCM PSO. In the base case, the RTS-GMLC model included no EVs. Modeling of EVs considered two charging strategies, uncoordinated and

coordinated, and three EV penetration levels: 10%, 20%, and 30% of the light-duty vehicles (equal to 1%, 2% and 3% penetration of the annual energy load). To understand the impacts, the model was applied weeks during representative on-peak and off-peak weeks during the year. The findings are presented in terms of power system loads, operation cost, LMPs, EV charging cost, and VRE curtailment, and the impact of the two charging strategies. With regard to the reliability metrics of unserved energy and maintaining reserve margins, the EV charging scenarios led to no increase in unserved energy, and no violation of the reserve margins.

Research questions

Following the recapitulation of the main objective and the methodology, this part enumerates the research questions. The answers present a brief of the process involved to elucidate the pieces of evidence and conclusions related.

- What are impacts of uncoordinated and coordinated EV charging strategies in power system operation, peak loads, and cost?
- What are the combined impacts of a high-penetration EVs and VRE on power system loads, operation, and cost, when considering both uncoordinated and coordinated EV charging models? How do the two models of EV charging influence the integration of high-penetration solar and wind power, for example as related to curtailment of VRE?

The integration of electric transportation increases the power system load, operation cost, and electricity prices, but the magnitude and character of the effects depend upon the charging strategy. The overall system operation cost under uncoordinated charging is higher, regardless of the level of EV penetration, when compared to coordinated charging. The operation cost is proportional to the net load served by the

conventional fleet, and consequently much higher during the peak load weeks in the summer. During the summer weeks, the savings in production costs between coordinated charging and uncoordinated charging are consistently 1% for all three EV penetration scenarios tested. However, during the off-peak weeks when load is lower and VRE production is high, the savings in production costs range from 4% to 8% when using coordinate charging.

EV charging cost was computed by taking the production cost for a scenario with a given EV penetration level and subtracting the cost of running the system with no EVs. The average charging cost per EV follows the same trends as the system operation cost—higher on summer days and lower on winter days, due to the higher LMP, but there are significant differences when considering the charging strategy. At 10% EV penetration (1% in energy penetration) during February (Duck week), the uncoordinated charging cost per vehicle is four times higher than the coordinated charging cost. The lowest savings in charging cost occurred for 30% EVs during the peak weeks in July, because electricity prices are generally high due to high load and LMPs during those weeks.

Regarding the daily system peak load, during off-peak weeks under uncoordinated charging, the peak net load increases with an increase in EV penetration, because peak load and EV charging are coincidental. During a week in April (Duck week), operating under uncoordinated EV charging, the peak load increases as much as 27% at 30% penetration of EVs (3% in energy penetration). However, coordinated EV charging shifts the EV charging load to off-peak hours as much as is possible, within the constraints of the charging requirement and the availability for charging. The result is an increase in the charging during off-peak hours, which is coincident with PV, RTPV, and wind. The net load profile during the day changes under coordinated charging but the peak load does not increase.

Related to the LMP, the shift of charging to off-peak hours due to coordinated charging increases the LMP simply because the EV load increases during those off-peak hours, and consequently the LMP increases during those hours. During the Peak weeks (July), with 30% penetration of coordinated EV charging, the average LMP increases by 4.4% compared to the system with no EV charging. However, it increases by 33% during a winter week in early February. Note, although the LMP increases, both the operation costs and EV charging costs decrease with coordinated charging versus uncoordinated charging.

Regarding VRE curtailment, coordinated charging reduces the curtailment of PV (by as much as nine times during off-peak season operation for 30% EV penetration) and wind (more than half during the summer operation season for 30% EV penetration) compared to the scenario with no EVs or uncoordinated EV charging. Coordinated charging reduces the curtailment of VRE, mainly because charging can be scheduled at hours of peak PV generation when the LMP is low, which addresses the problem of overgeneration (Duck curve). Therefore, coordinated charging is beneficial to the integration of VRE. To realize this potential for scheduling the charging during low LMP, high VRE hours of operation, it is necessary to have an accurate model of EV availability for charging and charging requirements.

Future Work

The model does not include other DSM resources like TOU or emergency power curtailment (light, pump, and air conditioning). Also, the model does not have different load-shifting technologies like batteries, hydro pump storage, or thermal storage. Moreover, the model is flexible enough to accommodate the coordinated EV charging in intraday cycles with horizons of four hours and one hour.

Another item for future work is finding the EV penetration limits of the system. In other words, how much EV penetration can the system take before it needs to change physically. Physical changes can include transmission and power generation additions. Furthermore, additional policies (constraints) can influence

the power system operation. The present model does not have emission constraints, which can favor natural gas power generation and reduce coal generation.

References

[1] NREL, “Plug-In Electric Vehicle Handbook for Public Charging Station Hosts,” NREL, Golden, CO, NREL/BR-7A30-51227, Apr. 2012, doi: 10.2172/1042497

[2] M. Smith, J. Castellano, “Costs Associated With Non-Residential Electric Vehicle Supply Equipment Factors to consider in the implementation of electric vehicle charging stations,” Prepared by New West Technol. LLC for DOE, Englewood, CO, DOE/EE-1289, Nov. 2015. [Online]. Available: https://afdc.energy.gov/files/u/publication/evse_cost_report_2015.pdf

[3] DOE/EERE, “Alternative Fueling Station Locator.” Alternative Fuels Data Center. https://www.afdc.energy.gov/stations/#/find/nearest?fuel=ELEC (Accessed: Aug. 18, 2018).

[4] L.M. Fulton, A. Seleem, F. Boshell, A. Salgado, and D. Saygin, “Electric Vehicles Technology Brief,” IRENA, Abu Dhabi, UAE, Feb. 26, 2017. Accessed: Aug. 19, 2019. [Online]. Available: http://www.irena.org/-/media/Files/IRENA/Agency/Publication/2017/IRENA_Electric_Vehicles_2017.pdf

[5] E. Wood, C. Rames, M. Muratori, S. Raghavan, and M. Melaina, “National Plug-In Electric Vehicle Infrastructure Analysis,” Sep. 15, 2017. Accessed: Aug. 19, 2019. [Online]. Available: https://www.energy.gov/sites/default/files/2017/09/f36/NationalPlugInElectricVehicleInfrastructureAnalysis_Sept2017.pdf

[6] EPRI “Consumer Guide to Electric Vehicle Charging,” EPRI, Palo Alto, CA, Rep. 3002016961, Nov. 4, 2019. [Online]. Available: http://mydocs.epri.com/docs/public/3002016961_Print.pdf

E. Wood, C. Rames, M. Muratori, S. Raghavan, and M. Melaina, “National Plug-In Electric Vehicle Infrastructure Analysis,” Sep. 15, 2017. Accessed: Aug. 19, 2019. [Online]. Available: https://www.energy.gov/sites/default/files/2017/09/f36/NationalPlugInElectricVehicleInfrastructureAnalysis_Sept2017.pdf

[7] DOE/EERE, “Developing Infrastructure to Charge Plug-In Electric Vehicles.” Alternative Fuels Data Center. https://www.afdc.energy.gov/fuels/electricity_infrastructure.html (Accessed: Aug. 18, 2018).

[8] P. B. Jones, J. Levy, J. Bosco, J. Howat, and J. W. Van Alst, “The Future of Transportation Electrification: Utility, Industry and Consumer Perspectives,” Ed. Schwartz, Lisa C., LBNL, Berkeley, CA, Vol. FEUR Report No. 10, Aug. 13, 2018. [Online]. Available: http://eta-publications.lbl.gov/sites/default/files/feur_10_transportation_electrification_final_20180813.pdf

[9] P. B. Jones, J. Levy, J. Bosco, J. Howat, and J. W. Van Alst, “The Future of Transportation Electrification: Utility, Industry and Consumer Perspectives,” Ed. Schwartz, Lisa C., LBNL, Berkeley, CA, Vol. FEUR Report No. 10, Sep. 13, 2018. [Online]. Available: https://eta-publications.lbl.gov/sites/default/files/feur_10_webinar_transportation_electrification_20180913.pdf

[10] M. Muratori, “Impact of uncoordinated plug-in electric vehicle charging on residential power demand,” *Nat. Energy*, vol. 3, pp. 193-201, Jan. 2018, doi:10.1038/s41560-017-0074-z.

[11] F. C. Graves, “A Primer on Electric Power Flow for Economists and Utility Planners,” EPRI, Palo Alto, CA, Rep. TR-104604, Mar. 1995. [Online]. Available: https://www.epri.com/research/products/TR-104604

[12] Gellings, C. “Estimating the Costs and Benefits of the Smart Grid,” EPRI, Palo Alto, CA, Rep. 1022519, Mar. 2011. [Online]. Available: https://www.epri.com/research/products/000000000001022519

[13] A. J. Wood and B. F. Wollenberg, “Economic Dispatch of Thermal Units and Methods of Solution” in Power Generation, Operation, and Control, 3rd ed. New York, NY, USA: Wiley, 2013, Ch. 3, pp. 63-146.

[14] M. Kintner-Meyer, K. Schneider, and R. Pratt, “Impacts Assessment of Plug-in Hybrid Vehicles on electric utilities and regional U.S. Pow er Grids,” PNNL, Richland, WA, Jan. 8, 2007. [Online]. Available: https://energyenvironment.pnnl.gov/ei/pdf/PHEV_Feasibility_Analysis_Part1.pdf

[15] California ISO, “What the duck curve tells us about managing a green grid,” CAISO, Folsom, CA, Nov. 2016. [Online]. Available: http://www.caiso.com/Documents/FlexibleResourcesHelpRenewables_FastFacts.pdf#search=%2FFlexibleResourcesHelpRenewables_FastFacts.pdf

[16] T. Mai et al., “Electrification Futures Study: Scenarios of Electric Technology Adoption and Power Consumption for the United States,” NREL, Golden, CO, NREL/TP-6A20-71500, Jun. 2018. [Online]. Available: https://www.nrel.gov/docs/fy18osti/70485.pdf

[17] B. J. Kirby, “Frequency Regulation Basics and Trends,” ORNL, Oak Ridge, TN, ORNL/TM-2004/291, May 2005. [Online]. Available: https://doi.org/10.2172/885974

[18] Z. Zhou, T. Levin, and G. Conzelmann, “Survey of U.S. Ancillary Services Markets,” ANL, Argonne, IL, ANL/ESD-16/1 Rev 1, Jun. 2016. [Online]. Available: https://doi.org/10.2172/1327815

[19] E. Ela, M. Milligan, and B. Kirby, “Operating Reserves and Variable Generation,” NREL, Golden, CO, NREL/TP-5500-51978, Aug. 2011. [Online]. Available: https://doi.org/10.2172/1023095

[20] T. B. Group, S. & C. Freeman, and L. Global Energy Partners, “A National Assessment of Demand Response Potential,” FERC, Washington, DC, Jun. 2009. [Online]. Available: https://www.ferc.gov/sites/default/files/2020-05/06-09-demand-response.pdf

[21] DOE “Demand Response.” Office of Electricity. Available: https://www.energy.gov/oe/activities/technology-development/grid-modernization-and-smart-grid/demand-response (Accessed: Nov. 16, 2018).

[22] M. Ahmadi, N. Mithulananthan, and R. Sharma, “Dynamic load control at a bidirectional DC fast charging station for PEVs in weak AC grids,” in *2015 IEEE PES Asia-Pacific Power and Energy Eng. Conf. (APPEEC)*, Nov. 2015, pp. 1-5, doi: 10.1109/APPEEC.2015.7380948.

[23] S. A. El Batawy, M. K. Gray, and W. G. Morsi, “Multi-objective optimization of energy storage and wind DGs for self-adequacy of microgrid equipped with fast DC charging station,” in *2017 IEEE Power & Energy Society Innovative Smart Grid Technologies Conference (ISGT)*, Apr. 2017, pp. 1–5, doi: 10.1109/ISGT.2017.8085960.

[24] P. H. Andersen, J. A. Mathews, and M. Rask, “Integrating private transport into renewable energy policy: The strategy of creating intelligent recharging grids for electric vehicles,” *Energy Policy*, vol. 37, no. 7, pp. 2481–2486, Apr. 2009, doi: 10.1016/j.enpol.2009.03.032.

[25] P. Denholm, E. Ela, B. Kirby, and M. Milligan, “The Role of Energy Storage with Renewable Electricity Generation,” NREL, Golden, CO, NREL/TP-6A2-47187, Jan. 2010. [Online]. Available: https://doi.org/10.2172/972169

[26] ISO/RTO Council, “Assessment of Plug-in Electric Vehicle Integration with ISO/RTO Systems,” prepared by Taratec Corp. for IRC, Columbus, OH, Mar. 2010. [Online]. Available: http://www.ercot.com/content/news/presentations/2011/IRC_Report_Assessment_of_Plug-in_Electric_Vehicle_Integratio.pdf

[27] Z. Luo, Z. Hu, Y. Song, Z. Xu, and H. Lu, “Optimal coordination of plug-in electric vehicles in power grids with cost-benefit analysis - Part I: Enabling techniques,” *IEEE Trans. Power Syst.*, Nov. 2013, doi: 10.1109/TPWRS.2013.2262318.

[28] Z. Luo, Z. Hu, Y. Song, Z. Xu, and H. Lu, “Optimal coordination of plug-in electric vehicles in power grids with cost-benefit analysis - Part II: A case study in China,” *IEEE Trans. Power Syst.*, Nov. 2013, doi: 10.1109/TPWRS.2013.2252028.

[29] K. Clement-Nyns, E. Haesen, and J. Driesen, “The Impact of Charging Plug-In Hybrid Electric Vehicles on a Residential Distribution Grid,” *IEEE Trans. Power Syst.*, vol. 25, no. 1, pp. 371–380, Feb. 2010, doi: 10.1109/TPWRS.2009.2036481.

[30] Probability Methods Subcommittee/IEEE, “IEEE Reliability Test System,” *IEEE Trans. Power Appar. Syst.*, vol. PAS-98, no. 6, pp. 2047–2054, Nov. 1979, doi: 10.1109/TPAS.1979.319398.

[31] E. Boyd, “Power Sector Modeling 101,” US Dep. Energy DOE´s Tech. Assist., Washington, DC, Feb. 2016 [Online]. Available: https://www.energy.gov/sites/default/files/2016/02/f30/EPSA_Power_Sector_Modeling_FINAL_021816_0.pdf

[32] W. Short et al., “Regional Energy Deployment System (ReEDS),” NREL, Golden, CO, NREL/TP-6A20-46534, Nov. 2011. [Online]. Available: https://doi.org/10.2172/1031955

[33] J. Logan, P. Sullivan, W. Short et al, "Evaluating a Proposed 20% National Renewable Portfolio Standard," NREL, Golden, CO, NREL/TP-6A2-45161, Feb. 2009. [Online]. Available: https://doi.org/10.2172/948750

[34] L. Bird, C. Chapman, J. Logan, J. Sumner, and W. Short, "Evaluating renewable portfolio standards and carbon cap scenarios in the U.S. electric sector," *Energy Policy*, vol. 39, no. 5, pp. 2573–2585, May 2011, doi: 10.1016/j.enpol.2011.02.025.

[35] J. Macknick, S. Cohen, R. Newmark, A. Martinez, P. Sullivan, and V. Tidwell, "Water Constraints in an Electric Sector Capacity Expansion Model," NREL, Golden, CO, NREL/TP-6A20-64270, Jul. 2015. [Online]. Available: https://doi.org/10.2172/1215271

[36] J. Logan, A. Lopez, T. Mai, C. Davidson, M. Bazilian, and D. Arent, "Natural gas scenarios in the U.S. power sector," *Energy Econ.*, vol. 40, pp. 183–195, Nov. 2013, doi: 10.1016/j.eneco.2013.06.008.

[37] R. Wiser et al., "Assessing the costs and benefits of US renewable portfolio standards," Environ. Res. Lett., vol. 12, no. 9, p. 094023, Sep. 2017, doi: 10.1088/1748-9326/aa87bd.

[38] N. Blair et al., "Electricity Capacity Expansion Modeling, Analysis, and Visualization: A Summary of High-Renewable Modeling Experience for China," NREL, Golden, CO, NREL/TP-6A20-64270, Oct. 2015. [Online]. Available: https://doi.org/10.2172/1225943

[39] V. Diakov et al., "Improving Power System Modeling : A Tool to Link Capacity Expansion and Production Cost Models," NREL, Golden, CO, NREL/TP-6A20-64905, Nov. 2015. [Online]. Available: https://doi.org/10.2172/1233204

[40] C. Barrows, "Latest Computational and Mathematical Tools for Transmission Expansion Operations," in *IEEE PES T&D Meeting*, Apr. 2014. [Online]. Available: https://www.ieee-pes.org/presentations/td2014/td2014p-000644.pdf

[41] C. Barrows, M. Hummon, W. Jones, and E. Hale, "Time Domain Partitioning of Electricity Production Cost Simulations," NREL, Golden, CO, NREL/TP-6A20-60969, Jan. 2014. [Online]. Available: https://doi.org/10.2172/1123223

[42] P. Denholm and W. Short, "Preliminary assessment of plug-in hybrid electric vehicles on wind energy markets," NREL, Golden, CO, NREL/TP-6A20-39729, Apr. 2006. [Online]. Available: https://doi.org/10.2172/881921

[43] Hand, M. M., Baldwin, S., DeMeo, E., et al., "Renewable Electricity Futures Study. Volume 1. Exploration of High-Penetration Renewable Electricity Futures," NREL, Golden, CO, NREL/TP-6A20-52409-1, Jun. 2012. [Online]. Available: https://doi.org/10.2172/1219711

[44] D. Hostick, D. Belzer, S. Hadley, et al., "Renewable Electricity Futures Study. Volume 3. End-Use Electricity Demand," NREL, Golden, CO, NREL/TP-6A20-52409-3, Jun. 2012. [Online]. Available: https://doi.org/10.2172/1219713

[45] U.S. EIA, "Annual Energy Outlook 2019 with projections to 2050," DOE/EIA, Washington, DC, Jan. 2019. [Online]. Available: https://www.eia.gov/outlooks/archive/aeo19/pdf/aeo2019.pdf

[46] P. Sullivan, W. Cole, and N. Blair, "2015 Standard Scenarios Annual Report: U.S. Electric Sector Scenario Exploration," NREL, Golden, CO, NREL/TP-6A20-64072, Jul. 2015. [Online]. Available: https://doi.org/10.2172/1215209

[47] C. Wesley, W. Frazier, P. Donohoo-Vallett, T. Mai, and P. Das, "2018 Standard Scenarios Report : A U.S. Electricity Sector Outlook," NREL, Golden, CO, NREL/TP-6A20-71913, Nov. 2018. [Online]. Available: https://doi.org/10.2172/1481848

[48] G. Brinkman, J. Jorgenson, A. Ehlen, and J. H. Caldwell, "Low Carbon Grid Study: Analysis of a 50% Emission Reduction in California," NREL, Golden, CO, NREL/TP-6A20-64884, Jan. 2016. [Online]. Available: https://doi.org/10.2172/1235548

[49] E3, "California Transportation Electrification Assessment Phase 2: Grid Impacts," Energy and Environmental Economics, Inc., San Francisco, CA, Oct. 2014. [Online]. Available: https://caletc.com/assets/files/CalETC_TEA_Phase_2_Final_10-23-14.pdf

[50] J. Hargreaves, E. K. Hart, R. Jones, and A. Olson, "REFLEX: An Adapted Production Simulation Methodology for Flexible Capacity Planning," *IEEE Trans. Power Syst*., vol. 30, no. 3, pp. 1306–1315, May 2015, doi: 10.1109/TPWRS.2014.2351235.

[51] D. Bain and T. Acker, "Hydropower Impacts on Electrical System Production Costs in the Southwest United States," *Energies*, vol. 11, no. 2, Art. no. 368, Feb. 2018, doi: 10.3390/en11020368.

[52] M. Milligan et al., "Review and Status of Wind Integration and Transmission in the United States : Key Issues and Lessons Learned," NREL, Golden, CO, NREL/TP-5D00-61911, Mar. 2015. [Online]. Available: https://doi.org/10.2172/1214995

[53] D. J. Olsen et al., "Grid Integration of Aggregated Demand Response , Part 1 : Load Availability Profiles and Constraints for the Western Interconnection," LBNL, Berkeley, CA, LBNL-6417E, Sep. 2013. [Online]. Available: https://doi.org/10.2172/1165113

[54] M. Hummon et al., "Grid Integration of Aggregated Demand Response, Part 2: Modeling Demand Response in a Production Cost Model," NREL, Golden, CO, NREL/TP-6A20-58492, Dec. 2013. [Online]. Available: https://doi.org/10.2172/1260332

[55] T. Acker, "IEA Wind Task 24 Integration of Wind and Hydropower Systems; Volume 2: Participant Case Studies," NREL, Golden, CO, NREL/TP-5000-50182, Dec. 2011. [Online]. Available: https://doi.org/10.2172/1033024

[56] R. Piwko, K. Clark, L. Freeman et al., "Western Wind and Solar Integration Study : Executive Summary," NREL, Golden, CO, NREL/SR-550-47781, May 2010. [Online]. Available: https://doi.org/10.2172/979815

[57] EnerNex Corporation, "Eastern Wind Integration and Transmission Study," NREL, Golden, CO, NREL/SR-5500-47078, Feb. 2011. [Online]. Available: https://doi.org/10.2172/1009271

[58] GE-Energy, "New England Wind Integration Study Executive Summary," Prepared by GE for ISO-NE, Schenectady, NY Dec. 2010. [Online]. Available: https://www.nrcm.org/documents/ISO_NE_integration_report_execsummary.pdf

[59] GE Energy, "Analysis of Wind Generation Impact on ERCOT Ancillary Services Requirements Electric Reliability Council of Texas," Prepared by GE for ERCOT, Schenectady, NY, Mar. 2008. [Online]. Available: https://www.nrc.gov/docs/ML0914/ML091420463.pdf

[60] A. Bloom et al., "Eastern Renewable Generation Integration Study: Executive Summary," NREL, Golden, CO, NREL/TP-6A20-64472-ES, Aug. 2016. [Online]. Available: https://www.nrel.gov/docs/fy16osti/64472-ES.pdf

[61] E. Ela, M. Milligan, B. Parsons, D. Lew, and D. Corbus, "The evolution of wind power integration studies: Past, present, and future," in *2009 IEEE Power Energy Soc. Gen. Meet. PES '09*, Jul. 2009, pp. 1–8, doi: 10.1109/PES.2009.5275981.

[62] C. McKerracher, "Electric Vehicle Outlook 2017," Blomberg Finance L.P., Jul. 3, 2017. Accessed: Aug. 19, 2019. [Online]. Available: https://data.bloomberglp.com/bnef/sites/14/2017/07/BNEF_EVO_2017_ExecutiveSummary.pdf

[63] Enerdata "Up to 50% of the global car fleet could be electric* in 2050 Executive Brief," Feb. 28, 2018. [Online]. Accessed: Aug. 19, 2019. Available: https://www.enerdata.net/publications/executive-briefing/half-vehicles-cars-will-be-electrical-2050.pdf

[64] M. Chediak, "The Latest Bull Case for Electric Cars: the Cheapest Batteries Ever - Bloomberg," 2017. https://www.bloomberg.com/news/articles/2017-12-05/latest-bull-case-for-electric-cars-the-cheapest-batteries-ever (Accessed: Sep. 14, 2018).

[65] V. Henze, "Battery Pack Prices Cited Below $100/kWh for the First Time in 2020, While Market Average Sits at $137/kWh," BloombergNEF Press, 2020. Available: https://about.bnef.com/blog/battery-pack-prices-cited-below-100-kwh-for-the-first-time-in-2020-while-market-average-sits-at-137-kwh/ (Accessed: Apr. 18, 2021).

[66] M. Muratori, M. J. Moran, E. Serra, and G. Rizzoni, "Highly-resolved modeling of personal transportation energy consumption in the United States," *Energy*, vol. 58, pp. 168–177, Sept. 2013, doi: 10.1016/j.energy.2013.02.055.

[67] F. Tuffner and M. Kintner-Meyer, "Using Electric Vehicles to Meet Balancing Requirements Associated with Wind Power," PNNL, Richland, WA, PNNL-20501, Jul. 9, 2011.

[68] S. Schey, D. Scoffield, and J. Smart, “A First Look at the Impact of Electric Vehicle Charging on the Electric Grid in The EV Project,” World Electr. Veh. J, vol. 5, no. 3, pp. 667-668, Sept. 28, 2012, doi: 10.3390/wevj5030667.

[69] P. Sokorai, A. Fleischhacker, G. Lettner, and H. Auer, “Stochastic modeling of the charging behavior of electromobility,” *World Electr. Veh. J*., vol. 9, no. 3, Art. no. 44, Oct. 2018, doi: 10.3390/wevj9030044.

[70] Y. Wang and D. Infield, “Markov Chain Monte Carlo simulation of electric vehicle use for network integration studies,” *Int. J. Electr. Power Energy Syst.*, vol. 99, pp. 85–94, Jul. 2018, doi: 10.1016/j.ijepes.2018.01.008.

[71] A. Ul-Haq, M. Azhar, Y. Mahmoud, A. Perwaiz, and E. A. Al-Ammar, “Probabilistic modeling of electric vehicle charging pattern associated with residential load for voltage unbalance assessment,” *Energies*, vol. 10, no. 9, pp. 1–18, Sep. 2017, doi: 10.3390/en10091351.

[72] P. Grahn, “Electric vehicle charging modeling,” Ph.D. dissertation, School of Elect. Eng., Royal Institute of Technol., Stockholm, Sweden, Oct. 2013. [Online]. Available: http://news.hydroquebec.com/media/filer_private/2013/11/28/fiche_dinformation_recharge_vfinaleang.pdf

[73] Y. W. Chung, B. Khaki, T. Li, C. Chu, and R. Gadh, “Ensemble machine learning-based algorithm for electric vehicle user behavior prediction,” *Appl. Energy*, vol. 254, Art. no. 113732, Nov. 2019, doi: 10.1016/j.apenergy.2019.113732.

[74] M. Lahariya, D. F. Benoit, and C. Develder, “Synthetic Data Generator for Electric Vehicle Charging Sessions: Modeling and Evaluation Using Real-World Data,” *Energies*, vol. 13, no. 16, Art. no. 4211, Aug. 2020, doi: 10.3390/EN13164211.

[75] H. Lin, Y. Liu, Q. Sun, R. Xiong, H. Li, and R. Wennersten, “The impact of electric vehicle penetration and charging patterns on the management of energy hub – A multi-agent system simulation,” *Appl. Energy*, vol. 230, pp. 189–206, Nov. 2018, doi: 10.1016/j.apenergy.2018.08.083.

[76] P. Olivella-Rosell, R. Villafafila-Robles, A. Sumper, and J. Bergas-Jané, “Probabilistic agent-based model of electric vehicle charging demand to analyse the impact on distribution networks,” *Energies*, vol. 8, no. 5, pp. 4160–4187, May 2015, doi: 10.3390/en8054160.

[77] C. Sheppard, R. Waraich, A. R. Gopal, A. Campbell, and A. Pozdnukov, “Modeling plug-in electric vehicle charging demand with BEAM, the framework for behavior energy autonomy mobility,” LBNL, Berkeley, CA, LBNL-2001018, May, 2017. [Online]. Available: https://eta-publications.lbl.gov/sites/default/files/lbnl-2001018.pdf

[78] H. Lin, K. Fu, Y. Liu et al., “Modeling charging demand of electric vehicles in multi-locations using agent-based method,” *Energy Procedia*, vol. 152, pp. 599-605, 2018, doi: 10.1016/j.egypro.2018.09.217.

[79] N. S. Lopez, A. Allana, and J. B. M. Biona, “Modeling Electric Vehicle Charging Demand with the Effect of Increasing EVSEs: A Discrete Event Simulation-Based Model,” *Energies*, vol. 14, no. 13, Art. no. 3734, Jun. 2021, doi: 10.3390/EN14133734.

[80] M. Værbak, Z. Ma, Y. Demazeau, and B. N. Jørgensen, “A generic agent-based framework for modeling business ecosystems: a case study of electric vehicle home charging,” *Energy Informatics*, vol. 4, no. 2, Art. no. 28, Sep. 2021, doi: 10.1186/S42162-021-00158-4.

[81] K. Nguyen and R. Schumann, “A socio-psychological modal choice approach to modelling mobility and energy demand for electric vehicles,” *Energy Informatics 2020*, vol. 3, no. 1, Art. no 20, Oct. 2020, doi: 10.1186/S42162-020-00123-7.

[82] R. Lee, S. Yazbeck, and S. Brown, “Validation and application of agent-based electric vehicle charging model,” *Energy Reports*, vol. 6, no. 5, pp. 53–62, May 2020, doi: 10.1016/j.egyr.2020.02.027.

[83] V. Heinisch, L. Göransson, R. Erlandsson, H. Hodel, F. Johnsson, and M. Odenberger, “Smart electric vehicle charging strategies for sectoral coupling in a city energy system,” *Appl. Energy*, vol. 288, Art. no. 116640, Apr. 2021, doi: 10.1016/j.apenergy.2021.116640.

[84] J. Stiasny, T. Zufferey, G. Pareschi, D. Toffanin, G. Hug, and K. Boulouchos, “Sensitivity analysis of electric vehicle impact on low-voltage distribution grids,” *Electr. Power Syst. Res.*, vol. 191, Art. no. 106696, Feb. 2021, doi: 10.1016/j.epsr.2020.106696.

[85] J. H. Moon, H. N. Gwon, G. R. Jo, W. Y. Choi, and K. S. Kook, “Stochastic Modeling Method of Plug-in Electric Vehicle Charging Demand for Korean Transmission System Planning,” Energies 2020, Vol. 13, Page 4404, vol. 13, no. 17, p. 4404, Aug. 2020, doi: 10.3390/EN13174404.

[86] P. Jadun, C. McMillan, D. Steinberg, M. Muratori, L. Vimmerstedt, and T. Mai, “Electrification Futures Study : End-Use Electric Technology Cost and Performance Projections through 2050,” NREL, Golden, CO, NREL/TP-6A20-70485, Jan. 2017. [Online]. Available: https://www.nrel.gov/docs/fy18osti/70485.pdf

[87] M. Davis, “Total Cost of Ownership for Current Plug-in Electric Vehicles, Update to Model 2013 and 2014 Model Year Vehicles,” EPRI, Palo Alto, CA, Rep. 3002004054, May 10, 2014. [Online]. Available: https://www.epri.com/research/products/000000003002004054

[88] U. S. D. of Energy, “Alternative Fuels Data Center: Vehicle Cost Calculator.” https://afdc.energy.gov/calc/ (Accessed: Jul. 12, 2021).

[89] J. Rissman, “THE FUTURE OF ELECTRIC VEHICLES IN THE U.S.,” Energy Innov. Policy & Technol. LLC, San Francisco, CA, Sept. 13, 2017. [Online]. Available: http://energyinnovation.org/wp-content/uploads/2017/09/2017-09-13

[90] J. D. Guy, “SECURITY CONSTRAINED UNIT COMMITMENT,” *IEEE Trans. Power Appar. Syst.*, vol. PAS-90, no. 3, pp. 1385–1390, May 1971, doi: 10.1109/TPAS.1971.292942.

[91] Polaris, “Power System Optimizer (PSO).” [Online]. Available: http://psopt.com/pso/ (Accessed: Sep. 10 2018)

[92] R. Shrestha, “Uncoordinated and Price Incentive Based Load Profiles due to Electric Vehicle Charging,” M.S. thesis, Dept. Mech. Eng, Northern Arizona Univ., Flagstaff, AZ, 2019. [Online]. Available: https://www.proquest.com/docview/2369458122/fulltextPDF/48EE3FB51EE44BCEPQ/1?accountid=12706

[93] B. Bhattarai, “Aggregator Based Charging Management of Electric Vehicles,” M.S. thesis, Dept. Mech. Eng, Northern Arizona Univ., Flagstaff, AZ, 2019. [Online]. Available: https://www.proquest.com/docview/2377906639?pq-origsite=primo

[94] J. Dunckley, “Electric Vehicle Driving , Charging , and Load Shape Analysis: A Deep Dive Into Where, When, and How Much Salt River Project (SRP) Electric Vehicle Customers Charge,” EPRI, Palo Alto, CA, Rep. 3002013754, Jul. 2018. [Online]. Available: https://www.epri.com/research/products/000000003002013754

[95] E. W. Weisstein, “Beta Distribution,” *MathWorld*. https://mathworld.wolfram.com/BetaDistribution.html (Accessed: Nov. 20, 2019).

[96] J. Smart and S. Schey, “Battery Electric Vehicle Driving and Charging Behavior Observed Early in The EV Project,” in *SAE Int. J. Altern. Powertrains*, Apr. 2012, pp. 27–33. [Online]. Available: https://doi.org/10.4271/2012-01-0199

[97] INL, “EV Project Electric Vehicle Charging Infrastructure Summary Report period: January - December 2013,” Idaho Natl. Labratory, Idoha Falls, ID, INL/MIS-10-19479, Oct. 2014. [Online]. Available: https://avt.inl.gov/sites/default/files/pdf/EVProj/EVProject Infrastructure ReportJan13Dec13.pdf

[98] J. L. Vujic, “Monte Carlo Sampling Methods,” UCB Dept. of Nucl. Eng., Berkeley, CA, 2004. [Online]. Available: http://web.tecnico.ulisboa.pt/~mcasquilho/acad/theo/simul/Vujic.pdf

[99] C. Barrows, “Reliability Test System of the Grid Modernization Laboratory Consortium (RTS-GMLC),” NREL, Golden, CO, Jul. 2018. [Online]. Available: https://github.com/GridMod/RTS-GMLC/blob/master/RTS-GMLC.pdf

[100] C. Barrows et al., “The IEEE Reliability Test System: A Proposed 2019 Update,” *IEEE Trans. Power Syst.*, vol. 35, no. 1, pp. 119–127, 2020, doi: 10.1109/TPWRS.2019.2925557

[101] Fangxing Li and Rui Bo, “Small test systems for power system economic studies,” in *IEEE PES General Meeting*, Jul. 2010, pp. 1–4, doi: 10.1109/PES.2010.5589973.

[102] National Conference of State Legislature, “State Renewable Portfolio Standards and Goals,” NCSL 2021. Available: https://www.ncsl.org/research/energy/renewable-portfolio-standards.aspx (Accessed: Mar. 18, 2022).

[103] E. Commission, "Climate strategies & targets," EU, 2021. Available: https://ec.europa.eu/clima/eu-action/climate-strategies-targets_en (Accessed: Mar. 18, 2022).

[104] Google, "Our Commitment to Sustainability | Google Sustainability," Google, 2022. Available: https://sustainability.google/commitments/ (Accessed: Mar. 18, 2022).

[105] Walmart Inc., "Climate Change," Walmart, 2022. Available: https://corporate.walmart.com/planet/climate-change (Accessed: Mar. 18, 2022).

[106] Amazon.com Inc., "Amazon Sustainability," Amazon, 2022. Available: https://sustainability.aboutamazon.com/ (Accessed: Mar. 18, 2022).

[107] Lazard, "Lazard's levelized cost of energy analysis-version 15.0," New York, NY, 2021. [Online]. Available: https://www.lazard.com/media/451881/lazards-levelized-cost-of-energy-version-150-vf.pdf (Accessed: Mar. 18, 2022).

[108] NextEra, "Environmental, Social and Governance," Juno Beach, FL, 2021. [Online]. Available: https://www.nexteraenergy.com/content/dam/nee/us/en/pdf/2021_NEE_ESG_Report_Final.pdf (Accessed: Mar. 18, 2022).

[109] Breakthrough, "Electricity Policies from the Climate Policy Playbook," Kirkland, WA, 2021. [Online]. Available: https://www.breakthroughenergy.org/api/playbookbuilder/downloadplaybook?playbookId=6f7599f0-4695-4beb-a1b8-761ca5836254 (Accessed: Mar. 18, 2022).

[110] U.S. EIA, "Annual Energy Outlook 2022 with projections to 2050," 2022. [Online]. Available: https://www.eia.gov/outlooks/aeo/index.php (Accessed: Mar. 18, 2022).

[111] N. Lutsey and M. Nicholas, "Update on electric vehicle costs in the United States through 2030," Washington, DC, 2019. [Online]. Available: https://theicct.org/sites/default/files/publications/EV_cost_2020_2030_20190401.pdf (Accessed: Mar. 18, 2022).

[112] L. Paoli and T. Gul, "Electric cars fend off supply challenges to more than double global sales – Analysis - IEA," 2022. Available: https://www.iea.org/commentaries/electric-cars-fend-off-supply-challenges-to-more-than-double-global-sales (Accessed: Mar. 20, 2022).

[113] V. T. Office (DOE), "FOTW #1227, February 28, 2022: Light-Duty Plug-in Electric Vehicle Sales in the United States Nearly Doubled from 2020 to 2021 | Department of Energy." Available: https://www.energy.gov/eere/vehicles/articles/fotw-1227-february-28-2022-light-duty-plug-electric-vehicle-sales-united (Accessed: Mar. 20, 2022).

[114] J. Motavalli, "Every Automaker's EV Plans Through 2035 And Beyond - Forbes Wheels," Forbes, 2021. Available: https://www.forbes.com/wheels/news/automaker-ev-plans/ (Accessed: Mar. 19, 2022).

[115] EVADOPTION LLC, "EV Sales Forecasts – EVAdoption," 2022. Available: https://evadoption.com/ev-sales/ev-sales-forecasts/ (Accessed: Mar. 19, 2022).

[116] J. K. Szinai, C. J. R. Sheppard, N. Abhyankar, and A. R. Gopal, "Reduced grid operating costs and renewable energy curtailment with electric vehicle charge management," *Energy Policy*, vol. 136, Art. no. 111051, 2020, doi: 10.1016/j.enpol.2019.111051.

[117] A. M. Mowry and D. S. Mallapragada, "Grid impacts of highway electric vehicle charging and role for mitigation via energy storage," *Energy Policy*, vol. 157, Art. no. 112508, 2021, doi: 10.1016/j.enpol.2021.112508.

[118] J. D. Alvarez Guerrero, B. Bhattarai, R. Shrestha, T. L. Acker, and R. Castro, "Integrating Electric Vehicles into Power System Operation Production Cost Models," *World Electr. Veh. J.*, vol. 12, no. 4, Art. no. 263, 2021, doi: 10.3390/wevj12040263.

[119] Y. Zhou, "Light Duty Electric Drive Vehicles Monthly Sales Updates," *Argonne National Laboratory*. [Online]. Available: https://www.anl.gov/es/light-duty-electric-drive-vehicles-monthly-sales-updates (Accessed: Feb. 01, 2021).

[120] D. Gohlke and Y. Zhou, "Impacts of Electrification of Light-Duty Vehicles in The United States, 2010 – 2017," ANL, Argonne, IL, ANL/ESD-18/1, Jan. 2018. [Online]. Available: https://doi.org/10.2172/1418278 (Accessed: Nov. 29, 2018).

[121] J. Ryser and G. Gentile, "US EV sales tumble in 2020, but EV load increases with more charging stations," *S&P Global Platts*, 2021. Available: https://www.spglobal.com/platts/en/market-insights/latest-news/electric-power/012821-us-ev-sales-tumble-in-2020-but-ev-load-increases-with-more-charging-stations (Accessed: Aug. 01, 2021).

[122] California Air Resources Board (CARB), "Zero-emission vehicle standards for 2018 and subsequent passenger cars, light-duty trucks, and medium-duty vehciles," CARB, Mar. 2012. [Online]. Available: https://ww3.arb.ca.gov/regact/2012/zev2012/fro2rev.pdf (Accessed: Dec. 04, 2018).

[123] Governor's Interagency Working Group on Zero-emission Vehicles, "ZEV Action Plan," Sacramento, CA, 2013. [Online]. Available: https://opr.ca.gov/docs/Governors_Office_ZEV_Action_Plan_(02-13).pdf (Accessed: Dec. 04, 2018).

[124] IEA, "Global EV Outlook 2020," IEA, Paris, France, 2020. [Online]. Available: https://www.iea.org/reports/globalev-outlook-2020 (Accessed: Aug. 01, 2021).

[125] D. Lew, et. al, "The Western Wind and Solar Integration Study Phase 2," NREL, Golden, CO, NREL/TP-5500-55588, Sep. 2013. [Online]. Available: https://doi.org/10.2172/1095399 (Accessed: Jul. 26, 2018)

[126] C. P. P. D. U.S. Environmental Protection Agency, "Energy and Environment Guide to Action: Chapter 5 Renewable Portfolio Standards," EPA, May 2015. [Online]. Available:

https://www.epa.gov/sites/production/files/2015-08/documents/guide_action_chapter5.pdf (Accessed: Dec. 4, 2018)

[127] J. Smart and S. Schey, “Battery Electric Vehicle Driving and Charging Behavior Observed Early in The EV Project,” in *SAE Int. J. Altern. Powertrains*, Apr. 2012, pp. 27–33. [Online]. Available: https://doi.org/10.4271/2012-01-0199

Appendix I

Cost Curves NAU-5 Bus System

Dispatch or cost curves of the committable generators presented in the NAU-5 Bus System, showing the variable cost of producing a unit of energy with respect of the power output these generators: (a) 121_NUCLEAR_1; (b) 101_STEAM_3 Coal; (c) 113_CT_1, 2, 3, 4 NG; (d) 102_CT_1 Oil; (e) 118_CC_1; (f) 117_CC_1; (g) 213_CC_3.

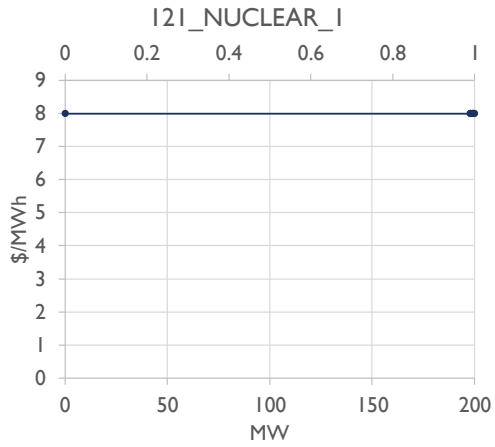

(a)

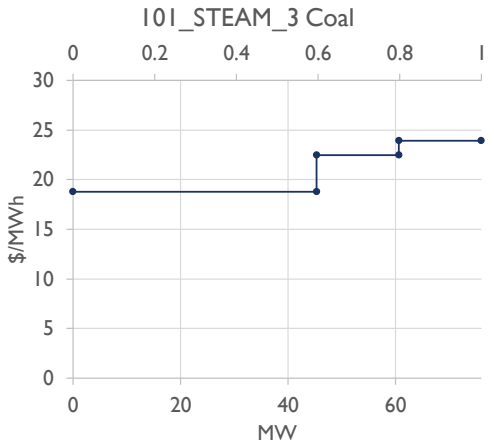

(b)

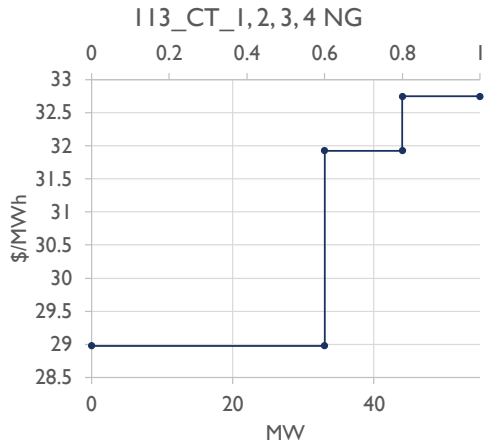

(c)

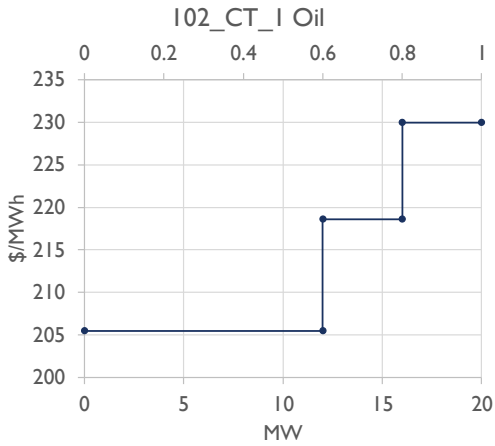

(d)

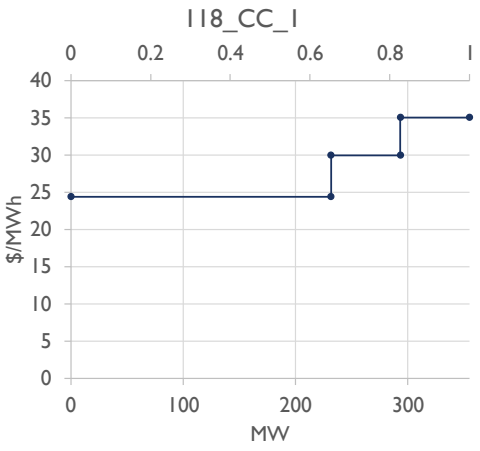
118_CC_1
0
0.2
0.4
0.6
0.8
1
40
35
30
25
20
15
10
5
0
$/MWh
0
100
200
300
MW

(e)

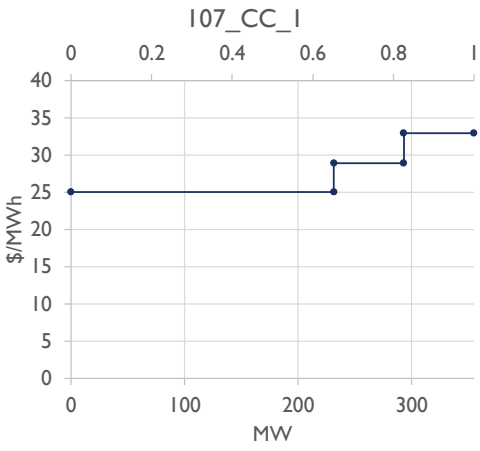
107_CC_1
0
0.2
0.4
0.6
0.8
1
40
35
30
25
20
15
10
5
0
$/MWh
0
100
200
300
MW

(f)

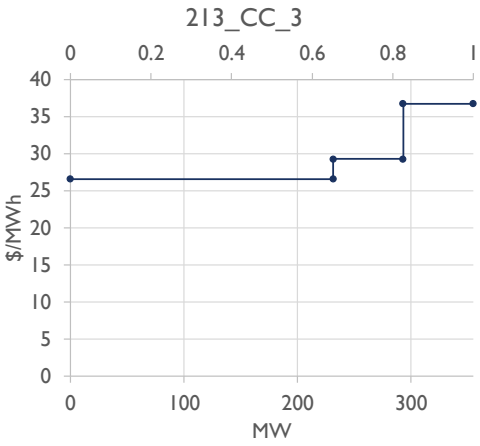
213_CC_3
0
0.2
0.4
0.6
0.8
1
40
35
30
25
20
15
10
5
0
$/MWh
0
100
200
300
MW

(g)

Appendix II

PSO inputs

The models in PSO use data defined per libraries and inputs as data tables. This appendix provides a brief description of each of the input files of the model in the PSO 2.6.3 version. There are three variants (scenarios): the base scenario, the uncoordinated charging, and the coordinated charging.

Model Setup (MS)

This input provides a quick list of setups that will be in use in the libraries defining the model.

- DateFormat defines the date format in the time series data. This format ensures data is readable by AIMMS.
- SlackBusName (PN) defines the slack bus or reference bus in the system.
- NoCaseFile (PC) states that the model does not store core topology.
- MipGap (MC) specifies the convergence tolerance for the optimization problem.
- UserSeed (TS) ensures replicability by given a seed to the random number generator. This seed applies if the model creates data (random schedules) used in a given scenario, not the case here but specified if further modeling is added.
- NoLoadShed (ED) ensures violation of unserved energy (load shed) should be removed from the solution of the model.

Table 16 Model Setup (MS) input parameters provide a quick list of parameters that defines the PSO model.

//OptionName	OptionValue
DisplayCount	1
DateFormat	%c%y.%m.%d %H:%M
MipGap	1.00E-04
UserSeed	9
SlackBusName	D
NoCaseFile	1
NoLoadShed	1

Model Definition (MDL_ID)

This input table specifies the time unit in the model and dates consider for solving the model. Note table is transposed to fit the page. The original input file provides the field (rows) as columns. The name of the model changes according to the scenario.

Table 17 Model Definition (MDL_ID) specifies the unit of time and temporal length covered in the model

//Name	NAU 5 BUS Groundhog EV Uncoordinated Charging 7days
MajorRelease	2
MinorRelease	6
BranchRelease	3
TimeUnit	minute
IntervalLength	1
MaxInterval	0
StartInterval	0
StopInterval	0
MinDate	2020.01.01 00:00
MaxDate	2020.12.31 00:00
StartDate	2020.01.29 00:00
StopDate	2020.02.04 23:00

Model Configuration (MC)

This library defines the data for the rolling-horizon model, the cycles, periods, and look ahead of each horizon.

Cycle ID (CYC_ID)

Note table is transposed to fit the page. The original input file provides the field (rows) as columns. The model has a single cycle DA. DeltaTime defines the solution time of each horizon in the cycle, 1440 minutes for a day.

Table 18 Cycle ID (CYC_ID) defines the solution time of the horizons contemplated in the cycle.

//Cycle	DA
Name	
DeltaTime	1440
LeadTime	0
DecisionTime	0
OrderTime	0
MipGap	0
MaxSolveTime	0
MaxIterations	0

Cycle Period ID (CYC_PRD_ID)

The DA cycle has 24 periods of 60 minutes that define the solution time (1440 minutes), plus the look ahead of 12 periods with a coarser length of 120 minutes (1440 minutes).

Table 19 Cycle Period ID (CYC_PRD_ID) defines the resolution of horizons and their look ahead.

//Cycle	Period	Length
DA	1	60
DA	2	60
DA	3	60
DA	4	60
DA	5	60
DA	6	60
DA	7	60
DA	8	60
DA	9	60
DA	10	60
DA	11	60
DA	12	60
DA	13	60
DA	14	60
DA	15	60
DA	16	60
DA	17	60
DA	18	60
DA	19	60
DA	20	60
DA	21	60
DA	22	60
DA	23	60
DA	24	60
DA	25	120
DA	26	120
DA	27	120
DA	28	120
DA	29	120
DA	30	120
DA	31	120
DA	32	120
DA	33	120
DA	34	120
DA	35	120
DA	36	120

Scenario Cycle (SCN_CYC)

Every Cycle requires at least a scenario to associate the Time Series Data.

Table 20 Scenario Cycle (SCN_CYC) specifies the scenario of the PSO model.

//Scenario	Cycle	Weight	Reference
ScnDA	DA	0	0

Time Series Data (TS)

This library identifies the schedule data, like the forecast for load and VRE energies. Moreover, schedules define availability and limits for generation and load resources.

Schedule Attributes (SCH_ATT)

This table specifies that the time series data repeat every week, like a simplification to model with a small fraction of data.

Table 21 Schedule Attributes (SCH_ATT) provides characteristics of the model's Time Series Data (TS).

Schedule	RepeatTime	StepChange	Cycle	Periodic	UseMin	UseMax	UseFirst	UseLast
AvgLoad	10080	0		0	0	0	0	0
Evload	10080	0		0	0	0	0	0
WIND	10080	0		0	0	0	0	0
PV	10080	0		0	0	0	0	0
RTPV	10080	0		0	0	0	0	0

Schedule Time-point (SCH_TMP)

This table provides the time series data. Instead of giving the whole data, the first ten items provide insight into the input structure.

Table 22 Schedule Time-point (SCH_TMP) provides the time series data in the model.

//Schedule	Time	Value	Enforce
AvgLoad	2020.01.29 00:00	9.00E+02	1
AvgLoad	2020.01.29 01:00	9.01E+02	1
AvgLoad	2020.01.29 02:00	9.15E+02	1
AvgLoad	2020.01.29 03:00	9.57E+02	1

AvgLoad	2020.01.29 04:00	1.07E+03	1
AvgLoad	2020.01.29 05:00	1.22E+03	1
AvgLoad	2020.01.29 06:00	1.27E+03	1
AvgLoad	2020.01.29 07:00	1.22E+03	1
AvgLoad	2020.01.29 08:00	1.15E+03	1
AvgLoad	2020.01.29 09:00	1.10E+03	1

Economic Dispatch (ED)

This library is the minimum to use for modeling power systems

Scenario Area Load (SCN_ARA_LOD)

There is a single data set for load, and the scenario “zero” implies common data to all scenarios. Scale factor adjusts the data set to fit the model capacity.

Table 23 Scenario Area Load (SCN_ARA_LOD) specifies the data the model uses as system load.

//Scenario	Area	Load	Enforce	ScaleFactor	Schedule	Sequence
0	0	0	0	0.52	AvgLoad	

Injector ID (INJ_ID)

This table defines the economic dispatch parameters of the injectors. Injectors are generators or loads and are located in a single location. This table is transposed to fit the page. This table exemplifies a couple of the injectors. This table constrains the max MW and identifies if an injector is a load. See EV. The EV fleet is assumed very flexible and can go to max power or down to zero in just a minute.

Table 24 Injector ID (INJ_ID) defines the economic dispatch parameters of the injectors (generation or load resources) in the model.

//Injector	118_CC_1	113_CT_2	102_CT_1	101_STEAM_3	121_NUCLEAR_1	EV
Name	118_CC_1	113_CT_2	102_CT_1	101_STEAM_3	121_NUCLEAR_1	
Area						
LoadFlag	0	0	0	0	0	1
Link	0	0	0	0	0	0

MaxMw	355	55	20	76	200	160
MinMw	0	0	0	0	0	0
RaiseRR	0	0	0	0	0	160
LowerRR	0	0	0	0	0	160
RampCapOnly	0	0	0	0	0	0
EnergyCost	0	0	0	0	0	0
CostAdder	0	0	0	0	0	0
RampUpCost	0	0	0	0	0	0
RampDnCost	0	0	0	0	0	0

Injector in Service (INJ_INS)

This table allows disabling injectors. The EV injector is not in service for the base case with no EV in the table below. For the uncoordinated charging scenario, the Unavailable value is zero.

Table 25 Injector in Service (INJ_INS) specifies the injectors disabled in the base model.

//Injector	Unavailable	InstallDate	RetireDate
EV	1		

Scenario Injector Dispatch (SCN_INJ_DSP)

This table informs PSO to follow a schedule for a giving injector at a specified scenario. The table below provides the expected uncoordinated EV charging. Thus this table is not part of the input for the coordinated charging scenario.

Table 26 Scenario Injector Dispatch (SCN_INJ_DSP) defines fixed schedules for a given set of injectors.

//Scenario	Injector	Dispatch	Enforce	ScaleFactor	Schedule	Sequence
ScnDA	EV	0	0	1	Evload	

Scenario Injector Max-MW (SCN_INJ_MAX)

In the particular case of the base scenario, this table provides maximum limits for the VRE dispatch passed as time series. Thus, PSO can withdraw that level or less. Moreover, it allows scaling the VRE resource to fit the target penetration of the NAU-5 Bus System.

Table 27 Scenario Injector Max-MW (SCN_INJ_MAX) specifies the maximum power limits of a set of injectors passed as a time series.

//Scenario	Injector	MaxMw	Enforce	ScaleFactor	Schedule	Sequence
ScnDA	WIND	0	0	0.04	WIND	
ScnDA	PV	0	0	0.19	PV	
ScnDA	RTPV	0	0	0.72	RTPV	

Unit Commitment (UC)

This library provides information for the commitment constraints and commitment scenario for the conventional fleet.

Injector Commit (INJ_CMT)

This table provides the commitment constraints for the injectors. At least a minimum dispatch should be offered here to enforce the constraints. This table is transposed to fit the page and exemplifies a couple of the injectors.

Table 28 Injector Commit (INJ_CMT) provides the commitment constraints for the model's injectors.

//Injector	118_CC_1	113_CT_2	102_CT_1	101_STEAM_3	121_NUCLEAR_1
MinDispatch	170	22	8	30	198
MinOn	0	0	0	0	0
MinOff	0	0	0	0	0
BaseCost	0	0	0	0	0
HotStartCost	0	0	0	0	0
WarmStartCost	0	0	0	0	0
ColdStartCost	30303	6121	120	8600	31600
TimeToWarm	0	0	0	0	0
TimeToCold	0	0	0	0	0
HotUpTime	0	0	0	0	0
WarmUpTime	0	0	0	0	0
ColdUpTime	0	0	0	0	0

Cycle System Commitment (CYC_SYS_CMT)

This table informs PSO to solve the commitment in all the periods of a cycle if solve has a value of one.

Table 29 Cycle System Commitment (CYC_SYS_CMT) specifies to solve the commitment in a given cycle.

//Cycle	Solve	HoldCycle	PricingCycle	IgnoreBaseCost	EnforceStartCost
0	1		0	0	0
DA	1		0	0	0

Power Network (PN)

This library allows defining the power network and its constraints.

Branch ID (BRN_ID)

This table defines the branches or transmission lines of the power network. Also, this table provides the power flow constraints of the power lines.

Table 30 Branch ID (BRN_ID) defines the parameters of the transmission lines in the model.

//Branch	AB	AD	AE	BC	CD	DE

Name						
FrEnode	A	A	A	B	C	D
ToEnode	B	D	E	C	D	E
Circuit						
Voltage	0	0	0	0	0	0
Resistance	0.00281	0.00304	0.00064	0.00108	0.00297	0.00297
Reactance	0.0281	0.0304	0.0064	0.0108	0.0297	0.0297
NormalLimit	400	0	0	0	0	240
CtgLimit	0	0	0	0	0	0
Solve	0	0	0	0	0	0
Enforce	1	0	0	0	0	1
Monitor	0	0	0	0	0	0
Switchable	0	0	0	0	0	0
Penalty	0	0	0	0	0	0
AngleLimit	0	0	0	0	0	0
Hvdc	0	0	0	0	0	0
CID						

Electrical Node ID (NDE_ID)

This table provides the Busbar or Substation name of the nodes in the power network.

Table 31 Electrical Node ID (NDE_ID) specifies the nodes (substations) in the power network.

//Enode	Name	Busbar	Substation	ReportNode
A1		A		0
A2		A		0
BL		B		0
CL		C		0
DL		D		0

Injector Network (INJ_NET)

This table identifies the physical (node) location of the injectors to the transmission network.

Table 32 Injector Network (INJ_NET) identifies the nodal location of each injector.

//Injector	Node	PhysicalArea	LossFactor	IgnoreLoss
107_CC_1	E		0.00E+00	0

118_CC_1	E	0.00E+00	0
213_CC_3	C	0.00E+00	0
113_CT_1	D	0.00E+00	0
113_CT_2	D	0.00E+00	0
113_CT_3	C	0.00E+00	0
113_CT_4	C	0.00E+00	0
102_CT_1	A1	0.00E+00	0
101_STEAM_3	A1	0.00E+00	0
121_NUCLEAR_1	A2	0.00E+00	0
EV	B	0.00E+00	0
WIND	E	0.00E+00	0
PV	A1	0.00E+00	0
RTPV	D	0.00E+00	0

Power Flow States (PF)

This library provides power flow data from an external source like state estimator data.

State Electrical Node MW (STE_NDE)

In the particular model of the NAU-5 Bus System, this table provides the load distribution factors (LoadMW).

Table 33 State Electrical Node MW (STE_NDE) provides the load distribution factors for the model.

//State	Enode	GenMw	LoadMw	GenNode	LoadNode
0	BL	0	0.9	0	0
0	CL	0	0.9	0	0
0	DL	0	1.2	0	0

Power Constraints (PC)

For this library, the only option is the no case file from the MS. Therefore, all the transmission constraints are enforced.

Heat Dispatch (HD)

This library allows modeling the conventional fleet based on their thermal characteristics.

Injector Heat (INJ_HEA)

This input table is for modeling the nuclear injector, which runs as baseload. Therefore, a simplified representation is enough because the unit is not cycling. The table provides the base heat and the incremental heat of the nuclear injector.

Table 34 Injector Heat (INJ_HEA) provides a simplified heat representation for modeling the baseload nuclear generator.

//Injector	HeatCost	IncHeat	BaseHeat	HotStartHeat	WarmStartHeat	ColdStartHeat
121_NUCLEAR_1	0.8	10	1980	0	0	0

Heat Curve Attribute (HCV_ATT)

This table provides the Base Heat of the coal, natural gas, and oil generators. Base heat is MMBtu/h at 0 MW, the intercept of with Y-axis of the input-output curve.

Table 35 Heat Curve Attribute (HCV_ATT) provides the Base Heat for the model's dispatchable generators.

//HeatCurve	TotalHeat	BaseHeat	NonConvex
101_STEAM_3	0	398.1	0
102_CT_1	0	117.112	0
107_CC_1	0	1227.74	0
113_CT_1	0	288.75	0
113_CT_2	0	288.75	0
113_CT_3	0	288.75	0
113_CT_4	0	288.75	0
118_CC_1	0	1233.69	0
213_CC_3	0	1330.08	0

Heat Curve Points (HCV_PNT)

This table provides the definitions of the incremental-heat rates of the fossil-fueled units in the model.

Table 36 Heat Curve Points (HCV_PNT) provides the incremental heat rate curve for the model's dispatchable generators.

//HeatCurve	Point	X	Y
101_STEAM_3	1	45.333	6.713
101_STEAM_3	2	60.667	8.028
101_STEAM_3	3	76	8.549
102_CT_1	1	12	8.597
102_CT_1	2	16	9.147
102_CT_1	3	20	9.622
107_CC_1	1	231.667	5.97
107_CC_1	2	293.333	6.892
107_CC_1	3	355	7.854
113_CT_1	1	33	6.899
113_CT_1	2	44	7.602
113_CT_1	3	55	7.797
113_CT_2	1	33	6.899
113_CT_2	2	44	7.602
113_CT_2	3	55	7.797
113_CT_3	1	33	6.899
113_CT_3	2	44	7.602
113_CT_3	3	55	7.797
113_CT_4	1	33	6.899
113_CT_4	2	44	7.602
113_CT_4	3	55	7.797
118_CC_1	1	231.667	5.808
118_CC_1	2	293.333	7.14
118_CC_1	3	355	8.351
213_CC_3	1	231.667	6.334
213_CC_3	2	293.333	6.979
213_CC_3	3	355	8.749

Injector Heat Curve (INJ_HCV)

This table relates the heat curve with the injector.

Table 37 Injector Heat Curve (INJ_HCV) associates the heat curves with the model's injectors

//Injector	HeatCurve
107_CC_1	107_CC_1
118_CC_1	118_CC_1
213_CC_3	213_CC_3
113_CT_1	113_CT_1
113_CT_2	113_CT_2
113_CT_3	113_CT_3
113_CT_4	113_CT_4
102_CT_1	102_CT_1
101_STEAM_3	101_STEAM_3

Fuel Dispatch (FD)

This library provides the fuel definition in the model

Fuel ID (FUE_ID)

This table defines the thermal units and cost of the generator's fuels.

Table 38 Fuel ID (FUE_ID) defines the thermal units and cost of the generator's fuels.

//FuelType	Name	Quantity	Heat	Cost
Coal		MMBtu	1	2.8
NG		MMBtu	1	4.2
Oil		MMBtu	1	23.9

Fuel Thermal Unit (FUE_UTH)

This table links the fuel with the injectors.

Table 39 Fuel Thermal Unit (FUE_UTH) associates the fuel with the injectors.

//FuelType	ThermalUnit	FuelFactor	Cost	CostAdder
Coal	101_STEAM_3	1	0	0
NG	107_CC_1	1	0	0
NG	118_CC_1	1	0	0
NG	213_CC_3	1	0	0
NG	113_CT_1	1	0	0
NG	113_CT_2	1	0	0
NG	113_CT_3	1	0	0
NG	113_CT_4	1	0	0
Oil	102_CT_1	1	0	0

Specialized Injector Energy Limited (EL)

Energy Limited (EL) resources are part of the PSO specialized injectors library. This library defines the parameters for modeling the coordinated EV charging as a limited energy resource. An EL resource has a limited capacity of withdrawing or injecting power in a given time window. Therefore, the model for coordinated charging does not use the table INJ_DSP. Instead, the schedule Evload set the charging requirement for 24 h, constrained with the maximum charging availability Evloadmax schedule.

Injector Energy Limits (INJ_ELM)

This table provides the time window for the EL injector, the coordinated EV charging. Thus, this table is part only of the coordinated EV charging scenario. AvgMax should be less than the MaxMW, and AvgMin defines the minimum energy requirement, in this case, minimum charging in 24 h (1440 minutes).

Table 40 Injector Energy Limits (INJ_ELM) provides the time window for accomplishing the coordinated EV charging.

//Injector	TimeWindow	AvgMax	AvgMin
EV	1440	5	1.95

Scenario Injector Min-Energy (SCN_INJ_EMN)

This table is associated with INJ_ELM. It identifies the AvgMin in the Day-Ahead Scenario. Thus, the Evload schedule defines the daily charging requirement in MWh for the EV injector.

Table 41 Scenario Injector Min-Energy (SCN_INJ_EMN) defines the schedule for determining the EV charging requirement.

//Scenario	Injector	AvgMin	Enforce	ScaleFactor	Schedule
ScnDA	EV	0	0	1	Evload

Scenario Injector Max-MW (SCN_INJ_MAX)

This version of the SCN_INJ_MAX applies only for coordinated EV charging. The schedule Evloadmax (first data row of the table) defines the maximum charging availability per hour in the DA scenario (ScnDA) for the EV injector.

Table 42 Variant of the Scenario Injector Max-MW (SCN_INJ_MAX) defines the maximum charging availability for the coordinated EV charging.

//Scenario	Injector	MaxMw	Enforce	ScaleFactor	Schedule	Sequence
ScnDA	EV	0	0	1	Evloadmax	
ScnDA	WIND	0	0	0.04	WIND	
ScnDA	PV	0	0	0.19	PV	
ScnDA	RTPV	0	0	0.72	RTPV	

Appendix III

Generator Data

Group	Max (MW)	Min Dispatch (MW)	Min On (h)	Min Off (h)	Hot Up Time (h)	Warm Up Time (h)	Cold Up Time (h)	Hot Start Heat (MMBtu)	Warm Start Heat (MMBtu)	Cold Start Heat (MMBtu)	Raise Ramp Rate (MW / min)	Lower Ramp Rate (MW / min)
U20 Oil CT	20	8	2.2	2.2	0.25	0.75	1	0.005	0.005	0.005	3	3
U76 Coal	76	30	8	4	3	10	12	3.379	4.861	5.285	2	2
U355 Gas CC	355	170	8	4.5	0.5	1	2	3.197	4.536	7.215	4.14	4.14
U55 Gas CT	55	22	1	1	0	0	1	0.038	0.044	0.068	3.7	3.7
U12 Oil ST	12	5	4	2	2	4	12	0.453	1.123	1.457	1	1
U155 Coal	155	62	8	8	3	11	60	6.892	7.438	10.778	3	3
U400 Nuclear	400	396	24	48	9999*	9999*	9999*	9.999*	0	78.978	20	20
U350 Coal	350	140	24	48	8	12	96	9.768	10.114	17.384	4	4

*the number 9999 flags the Nuclear generator as always ON and dispatching at or near install capacity limits.